DEVELOPMENT OF NEW STEAM METHANE REFORMING MOBILE PLANT WITH MICRO-SCALE CATALYTIC CHANNELS

RAIS HANIZAM BIN MADON

A thesis submitted in fulfillment of the requirement for the award of the
Doctor of Philosophy of Mechanical Engineering

Faculty of Mechanical and Manufacturing Engineering
Universiti Tun Hussein Onn Malaysia

FEBRUARY 2019

DEDICATION

Special Dedication to

Supiah Jamil@Jamin my beloved mother, you are everything to me,

Madon Jais my late beloved father, you are my inspiration,

Meine Leibe, I believe in you and me,

My family members that always love me,

My friends that always care for me,

Thanks you for always giving me encouragement to complete this study.

ACKNOWLEDGEMENT

In the Name of Allah, the Most Gracious, the Most Merciful. I am so thankful to Allah S.W.T for giving me enough time, good health, spirit, and patience in order to complete this PhD's project. With the mercifulness of Allah, I am able to produce a lot of useful idea for this project.

I would like thank my supervisor, Assoc. Prof. Dr. Mas Fawzi bin Mohd Ali, for his continuous professional advices, useful guidance, inspiration, patience, financial aspects and enormous support in the effort to complete this project. Also, I would like to thank my co-supervisor, Prof. Dato' Ir. Dr. Abdul Wahab bin Mohammad for his advice and support during my study. I am would like to express my thankfulness to my beloved family, especially my beloved mother, Mrs. Supiah Jamil@Jamin, my beloved wife Mrs Nor Nadiah Harun, my daughter Ms Iffah Damia, my sons Rais Irfan Daniyal and Rais Iman Daaim for their prayers, support, patience, and motivation during my study. I am also grateful to both examiners for their brilliant ideas, advices and guidance to me

I am indebted to the Faculty of Mechanical and Manufacturing Engineering, Universiti Tun Hussein Onn Malaysia (UTHM) for their facilities, opportunity as well as financial aid provided in pursuing my research. I would like to thank the Ministry of Education Malaysia for supporting my scholarship under SLAB scheme and also for supporting this research project under the Fundamental Research Grant Scheme (FRGS) Vot 1421. I would like to dedicate my appreciation to all the lecturers and associates of the Faculty of Mechanical and Manufacturing Engineering, which involved in this project with their invaluable time, guidance and advice. Without their cooperation and sacrifices, this research would not be able to be completed and published. Especially to Mr. Muhamad Khairul Ilman bin Sarwani, Mr. Mzahar bin Abd. Jalal, Mr Asrul bin Bosiran and Dr. Shahrul Azmir bin Osman.

ABSTRACT

The search for clean alternative energy sources is vital to feed the ever-increasing world energy consumption. It is widely accepted that hydrogen is the cleanest and abundant energy source of the future. Currently, more than 90% of world hydrogen production is made via catalytic steam methane reforming (SMR). A performing catalyst favors thermodynamic equilibrium that ensures good hydrogen selectivity. This research explores the potential of SMR yield intensification using experimental micro reactor and active noble metal catalyst (Rhodium aluminide and Ruthenium aluminide). For that purpose, a laboratory scale SMR test rig bench was designed, fabricated and developed. A new micro channel reactor with interchangeable catalyst modules for methane conversion process was set up and tested. The rig is able to provide evaluation of SMR experimental tests, such as catalyst performance, conversion rate and products at output stream, with controlled reactants steam to carbon ratio up to 5:1 and reaction temperature up to 700°C. The developed conventional and noble metal catalyst for this research, affirmed and proved that the combination of test rig bench and micro reactor managed to generate methane conversion according to the theory related to material catalyst. From this work, reaction temperature 650°C and steam to carbon ratio of 3:1 were found to yield the optimum methane conversion and hydrogen formation for the developed catalyst. Using such setup, the use of noble metal catalyst was able to reform methane to hydrogen within 1 minute from the start of reaction as compared to 60 minutes using conventional catalyst. It was found that the rate of reaction (methane disappearing rate) of $-r'_{CH_4}$ (mol CH_4 / g catalyst.s), for Rhodium aluminide yield the highest of 181.58, followed by Ruthenium aluminide with 154.39 and lastly Nickel aluminide of 1.32. The outcomes of this work has the potential to be scaled up for hydrogen production supply chain system of future fuel-cell electric vehicle transportation sector especially in any region with affordable natural gas price.

ABSTRAK

Peningkatan terhadap penggunaan sumber tenaga dunia telah mewujudkan keinginan untuk mencari sumber tenaga baharu sebagai langkah untuk menangani fenomena tersebut. Tenaga dari sumber hidrogen dipercayai menjadi calon utama tenaga masa hadapan. Lebih 90% penghasilan hidrogen ialah melalui proses tindak balas kimia *Steam Methane Reforming* (SMR). Sesebuah pemangkin membantu fasa keseimbangan termodinamik bagi SMR dan meningkatkan pengeluaran hidrogen. Kajian ini meneroka kebolehupayaan peningkatan hasil SMR dengan menggunakan reaktor skala mikro dan pemangkin *noble metal (Rhodium aluminide* dan *Ruthenium alumninide)*. Oleh itu, sebuah pelantar ujian proses SMR berskala makmal telah direka, dibina dan dibangunkan. Reaktor pada skala mikro dibina dan diuji dengan mempunyai ciri kebolehupayan menggunakan pelbagai jenis pemangkin. Pelantar ujian tersebut, menghasilkan data SMR seperti prestasi pemangkin, penukaran bahan tindak balas, produk terhasil dan dikawal pada nisbah mol bahan tindak balas sehingga 5:1 dan suhu tindak balas sehingga 700°C. Pemangkin dalam kajian ini, telah menunjukkan kesetaraan menurut teori asas SMR tatkala menggunakan pelantar ujian proses SMR dan reaktor skala mikro. Hasil kajian ini menunjukan bahawa suhu tindak balas 650°C dan nisbah mol bahan tindak balas 3:1 menghasilkan penukaran metana dan pembentukan hidrogen yang optimum. Berdasarkan tetapan berkenaan, penggunaan *noble metal* telah menunjukkan masa tindak balas penukaran metana kepada hidrogen seawal 1 minit pertama, berbanding pemangkin konvensional pada 60 minit yang pertama. Kadar tindak balas penukaran metana bagi setiap berat pemangkin dan masa, *Rhodium aluminide* telah menunjukkan nilai tertinggi iaini 181.58, diikuti *Ruthenium aluminide* dengan nilai 154.39 dan *Nickel aluminide* pada nilai 1.32. Hasil kajian berupaya menjadi platform fasa peningkatan kepada skala besar penghasilan hidrogen dimasa hadapan, terutama di dalam sektor pengangkutan khususnya bagi sistem rantaian pembekalan untuk kenderaan *fuel-cell* di kawasan yang mempunyai sumber gas semulajadi pada kadar harga mampu milik.

CONTENTS

LIST OF TABLES

LIST OF FIGURES

LIST OF SYMBOLS AND ABBREVIATIONS

Al	Aluminum
AIGA	Asian Industrial Gas Association
Al_2O_3	Alumina oxide
C	Char
CH_4	Methane
CO	Carbon monoxide
CoGe	Cobalt Germanium
CO_2	Carbon dioxide
C-101	Condenser (101 = referring number of unit)
D-101	Dryer (101 = referring number of unit)
DME	Dimethyl ester
dV	Differential of reactor volume
dW	Differential of embedded catalyst weight inside reactor
dX	Differential of reaction conversion
Eqn.	Equation
$F^{o}_{CH_4}$	Molar flow rate of methane in feed
F_{CH_4}	Molar flow rate of methane at output
FIC 101	Flow Indicator Controller (101 = referring number of unit)
FT	Fischer Tropsch
F-101	Furnace (101 = referring number of unit)
H_2	Hydrogen
H-101	Steam generator (101 = referring number of unit)
ICE	Internal combustion engine
Ir	Irrididium
kg	kilogram
lph	liter per hour
lpm	liter per minute

Mb/d	Million barrel per day
min	minute
ml	milliliter
MW	molecular weight
m^3	meter cube
NaOH	Sodium hydroxide
Na_2CO_3	Sodium carbonate
Ni	Nickel
NiO	Nickel oxide
Ni_3Al	Nickel aluminide
Ni_3Sn	Nisnite mineral
Ni/Al_2O_3	Nickel support alumina oxide
Pd	Palladium
PEM	Proton exchange membrane
PFD	Process Flow Diagram
PI 101	Pressure indicator (101 = referring number of unit)
PSA	Pressure swing absorber
PtGe	Platinum Germanium
PV	Process value
Pt	Platinum
P&ID	Process & Instrumentation Diagram
RBDPO	Refined Bleach Deodorized Palm Oil
Rh	Rhodium
Ru	Ruthenium
R-101	Reformer (101 = referring number of unit)
s	seconds
SOP	Standard Operating Procedure
SMR	Steam methane reforming
S-101	Separator (101 = referring number of unit)
SSC-101	Superheated steam converter (101 = referring number of unit)
SS304	stainless steel grade of 304
SS316	stainless steel grade of 316
TI 101	Temperature indicator (101 = referring number of unit)
V-101	Ball valve (101 = referring number of unit)

W	weight % catalyst
WGS	Water gas shift
WHSV	Weight hourly space velocity
X_{CH_4}	Methane conversion
Å	Angstrom measurement
°C	degree Celsius
ΔH	Enthalpies
wt%	weight percent
2θ	Bragg reflection
µl	Micro liter
$\dot{\xi}_1$	Extent reaction for SMR equation
$\dot{\xi}_2$	Extent reaction for WGS equation
$(\dot{m})$	Steam mass flow rate
$\dot{n}_i$	Mole flow rate of species exit the reactor
$\dot{n}_{o,i}$	Mole flow rate of species into the reactor
$-r'_{CH_4}$	Rate of reaction (mol CH_4 /g catalyst.s)
$-r_{CH_4}$	Rate of reaction (mol CH_4 / dm^3.s)

LIST OF APPENDICES

CHAPTER 1

INTRODUCTION

1.1 Research Background

It is reported the distribution of proved fossil fuel reserves from 1996 to 2016 had showed that the global oil demand grew by 1.6 million barrels per day and the oil reserves also increased at 1706.7 thousand million barrels in 2016, in consequences of both demand and supply trending (British Petroleum, 2017). It is believed that possibility of demand shortage will occur since fossil fuel is non-renewable. In addition to the cost and demand of fossil fuel energy, there was a significant environmental concern regarding petroleum fuel based usage. The recent analysis estimated that pollutants may be high enough to bear on public health and the environment in areas where 50% of develop country exist. Report by Daud, (2006) and Kamarudin et al., (2009) air pollution by transportation and industrial sectors are principally due to the using of fossil oil and natural gas as their source of fuel. Figure 1.1 shows the projection of production and demand of fossil fuel generally at world level and specifically at Malaysia level. Apparently, extreme depending on the fossil fuel lead to shortage of fuel energy sources and high potential of pollutant as the emission from combustion of the fossil fuel. Thus, in order to deal with these issues, there has been an effort to diversify energy supply for better energy efficiency and cleaner fuels. The utilization of renewable energy, capable to encounter the energy demand and to reduce the growth rate of greenhouse gases (GHG), which mainly concentrate of Carbon Dioxide (CO_2) as the emission from the fossil fuel usage. In Malaysia, renewable energy development is mainly focused on biomass-based power generation (BIOGEN), solar and hydrogen energy. It's believed that, the GHG impact from industrial sector and transportation should be reduced by 3.8% within 5 years

(Daud, 2006, Holladay, et al., 2009; Kamarudin et al., 2009). The hydrogen energy at a smaller extent identified as most viable long term renewable energy as alternative fuel compared to the fossil fuel.

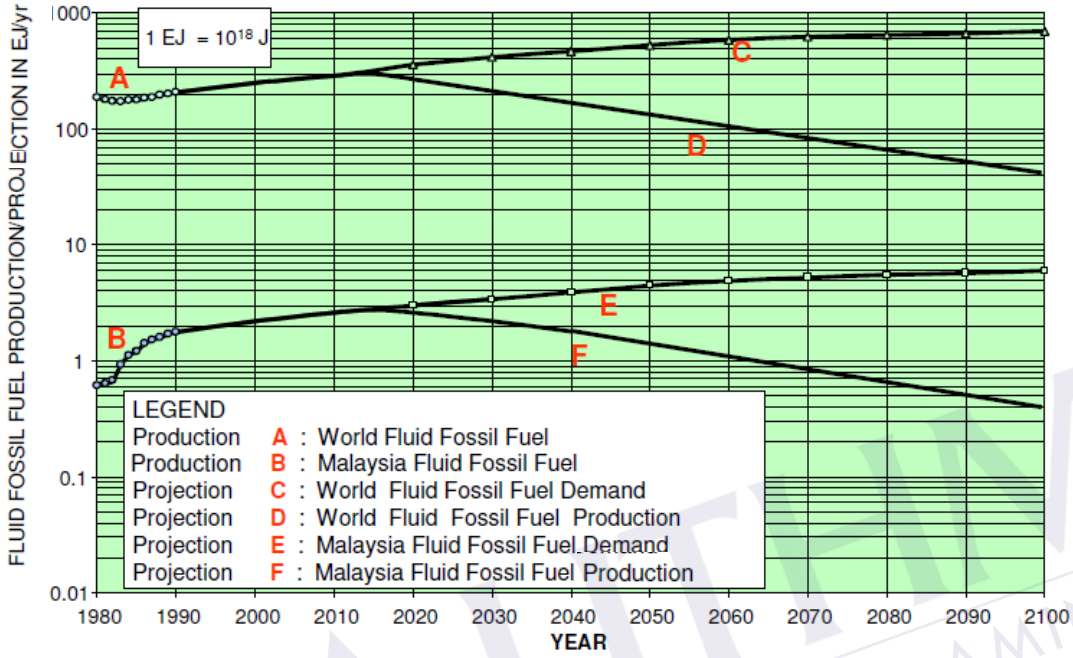

Figure 1.1 : Fossil fuel projection of production and demand (Daud, 2006).

It is widely accepted that hydrogen energy was among the clean, efficient and pollution free energy source in the future. The hydrogen energy becomes the main energy sources as fuel in fuel-cell system especially for the transportation sector. Besides that, this hydrogen is widely utilized as feedstock for food processing, chemical production and refining industries. Reported by Daud, (2006), Kamarudin et al., (2009) and Khan et al., (2010) the demand for hydrogen is expected to rapidly increase due its potential as major energy sources in the future. Figure 1.2 describes the route map of hydrogen energy, specifically in Malaysia which had been exhibited at International Seminar on The Hydrogen Economy for Sustainable Development, Reykjavik Iceland (Daud, 2006). The R&D of the hydrogen production and storage technologies has been started as early as 2002. This road map has become the baseline for hydrogen research area in Malaysia. This road map is mainly focused on transportation sector whereby the Hydrogen is used as energy sources for zero carbon emission fuel (Kamarudin et. al., 2009).

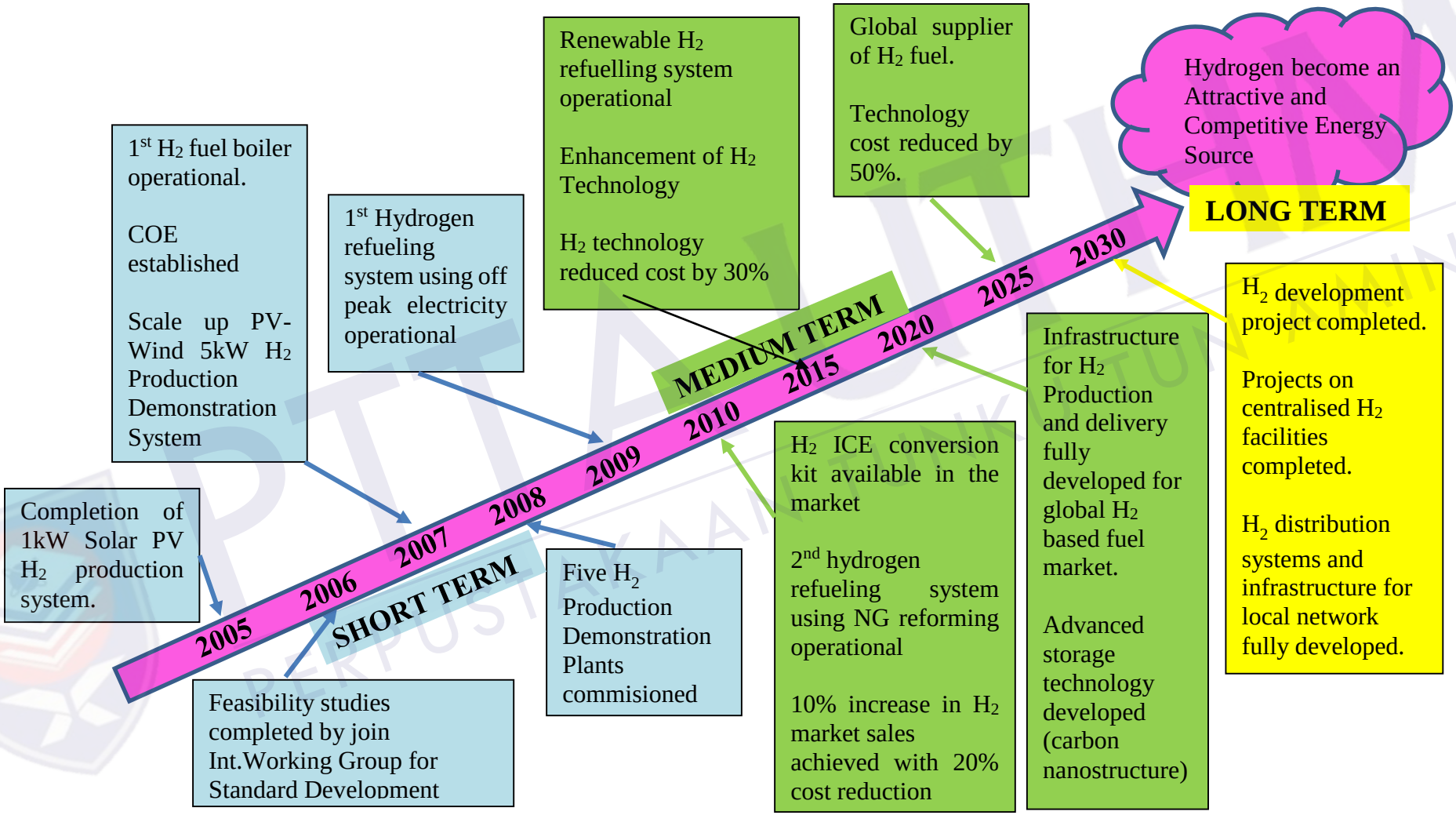

Figure 1.2: Hydrogen road map for Malaysia (Daud, 2006).

Established along the theory of stoichiometry equation for combustion reaction, Eqn. 1.1 shows any hydrocarbon produces carbon dioxide. The concentrated carbon dioxide leads to the greenhouse gas phenomenon and becomes worst polluted to the environment. Eqn 1.2 shows the combustion of hydrogen, which primarily produces water vapor. The equation demonstrate that the hydrogen is clean and zero carbon pollutant fuel (Sciazko et al., 2014; Udengaard et al., 2004; Verykios & Piga, 2000).

$$C_mH_n + \left(m + \frac{n}{4}\right)O_2 = \frac{n}{2}H_2O + mCO_2 \quad (1.1)$$

$$2H_2 + O_2 = 2H_2O \quad (1.2)$$

Reported by Holladay et. al., (2009) highlighted that the most developed and most used technology in hydrogen production was reforming of the hydrocarbon fuels, due its advantage such as highly efficient, low cost and already achieve commercial and long term stage in industry compare to non-reforming (biomass gasification, photolysis, electrolysis and etc). Furthermore, presently almost 96% of the world's hydrogen demand, including in Malaysia, is provided by traditional fossil fuels, and about half of it, comes from natural gas; which the main composition is methane (Bartels et. al., 2010; Bej et. al., 2013; Florin & Harris, 2007; Kamarudin et al., 2009; Udengaard, 2004). The production of hydrogen from various hydrocarbons, especially methane mainly comes from the chemical reaction process of catalytic reforming technologies which consist such as steam methane reforming, partial oxidation, and auto thermal reforming. Among these, catalytic steam methane reforming has the advantage of relatively low reaction temperature and high hydrogen content in the reforming products, and it is currently considered as the most cost efficient and highly evolved case of reforming for hydrogen production. Whereby, since the early 1950s, a considerable efforts have been set into the investigations of steam methane reforming (SMR) and its kinetics (Kamarudin et al., 2009; Khan et al., 2010; Wang et al., 2012; Wang et al., 2013).

The SMR is a strongly endothermic reaction inside tubular reactor with Nickel based catalyst, which requires external heating of the reactor tubes. This process is carried out by either the direct firing (as in radiant reformers) or by heat exchange with

a hot stream (as in convective reformers) which operate at pressures of 3 to 25 bars atmospheres and temperatures of 700°C to 1000°C (Graf et al., 2007; Radfarnia & Iliuta, 2014; Simsek et al., 2013). Figure 1.3 expresses the conceptual flow sheet of the fuel processing of gaseous, liquid, and solid fuels for hydrogen production.

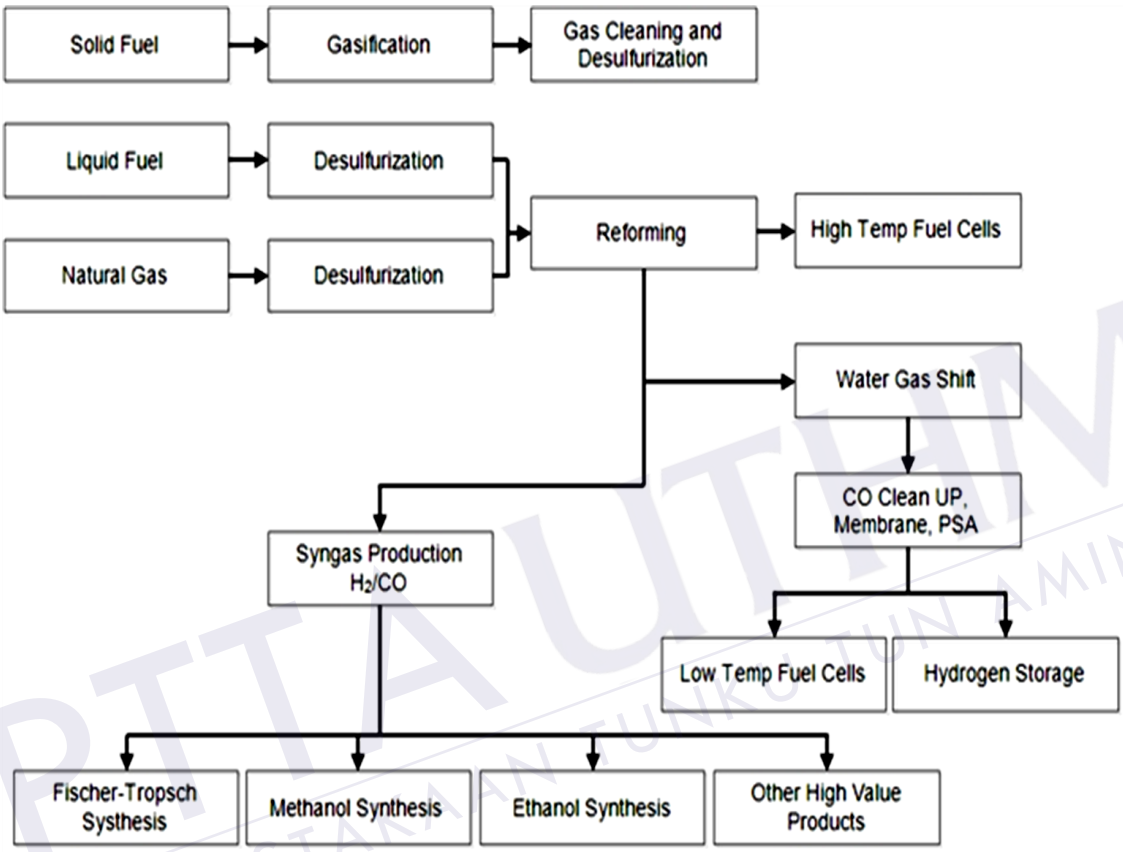

Figure 1.3 : Fuel processing of gaseous, liquid, and solid fuels for hydrogen production (Holladay et al., 2009).

1.2 Problem statement

According to Figure 1.2, current road map timeline was set on “medium term” which is an enhancement of hydrogen production technology at a reduced cost. Thus, increasing demands of running hydrogen productions, with lower capital and operating expenses, have recently built up interest in novel approaches such as process intensification. Various strategies of intensification can be realized either by integrating chemical reactions with unit operations such as the reformer, separation and heat exchange, or, more recently, by miniaturizing the characteristic flow paths

into well-defined structured geometries. The latter approach of intensification can bring added values like the possibility of operating in narrow control limits with the combination of noble catalyst, in which eliminate complexities associated with traditional scaling-up endeavors.

The catalytic steam methane reforming (SMR) is commonly supported by tubular packed bed reactor with nickel based catalysts and most widely used in the production of hydrogen. In comparison with noble metals-based catalysts, such as rhodium, palladium, platinum and ruthenium, supported nickel catalysts are less active and usually more prone to deactivation by carbon formation or oxidation. The main problem of these catalyst is the formation of coke by decomposition of methane at higher temperatures and straightly decreases the catalyst activity leading to drop in conversion of methane and hydrogen's yield. This coke is usually formed through thermal cracking of hydrocarbons or through reactions between CO molecules. Extensive coke formation will result in pore blockage in the catalyst and increased resistance to pore diffusion. In addition, coke formation will also result in an increased pressure drop. The tendencies for coke formation can be influenced by a number of catalyst and process parameters. The reformer gas will produce high concentrations of CO, and formation of metal carbonyls are possible to occur under some reaction conditions. Such reactions might result in catalyst corrosion and metal dusting (Czernik et al., 2002; Pudukudy & Yaakob, 2015; Smet et al., 2001).

Furthermore, the utilization of tubular packed bed reactor had shown a few constraints such as of heat transfer coefficient, steam to methane ratio flow and unstable kinetic rate of reaction (Bej et al., 2013; Cheng et. al., 2011; Chibane & Djellouli, 2011; Izquierdo et al., 2012; Perez-Moreno et. al., 2013; Stefanidis & Vlachos, 2010; Ye et. al., 2009; Zeppieri et. al., 2010). Several studies concentrated on the intensification of flow paths have led to the design and analysis of micro channel reactors. These miniature devices involve parallel, identical channels with characteristic dimensions and laminar flow condition, which create surface areas of 50 to 100 times higher than conventional packed bed counterparts. Presence of high surface areas, sub-millimeter dimensions, and use of metallic materials favor rapid and uniform distribution of heat to the entire catalyst. This can be either coated as a layer on the interior channel walls or packed into the channels in particulate form. The

effective heat transfer is essential for highly endothermic and exothermic catalytic processes demanding precise control of temperature and product distribution (Cheng et al., 2011; Palma et. al., 2017; Simsek et. al., 2011; Simsek et al., 2013; Zeppieri et al., 2010).

The previous work done by Stefanidis & Vlachos (2010), proved that via simulations concept, the steam methane reforming (SMR) on noble active metal such Rhodium and Ruthenium catalyst at micro scale and millisecond contact times is feasible. Thus, methane conversion can be intensified by hundred to a thousand times. But practically, SMR of Rhodium in micro reactor poses new challenges such as the catalyst deposition, methane conversion and kinetic rate of reaction. This is imputable to the SMR process that depends on micro reactor geometry configuration, thermal parameters, flow parameters, catalyst and reactant characterization (Simsek et al., 2011, 2013; Stefanidis & Vlachos, 2010; Tonkovich et al., 2004, 2005, 2007).

This technique of SMR on the noble active metal catalyst in micro reactor is still new. Relevant data in this technique are still confined in the literature. Thus, parameters such as catalyst characteristics, methane conversion rate, kinetic rate of reaction and intensification of this technique need to be measured and evaluated fundamentally, especially due to unique catalyst characteristics is being experimented (Butcher et al., 2014; Halabi et. al., 2010; Izquierdo et al., 2012; Z. Liu et. al., 2012; M. Mbodji et al., 2012; Stefanidis & Vlachos, 2010; Tonkovich et al., 2004, 2007; F. Wang et al., 2013; Zeppieri et al., 2010).

Even smaller driving forces can be achieved if the duct diameter is reduced further. Nevertheless, there is a terminal point for determining smallest passage dimensions. In universal terms, finer passages must be taken in short as possible and used in larger numbers in order to manipulate the pressure drop in a given duty. Furthermore, from the point of view of manufacturing, the attachment of flow headers and distribution arrangements with very short arrays of ducts becomes problematical, and very fine passages bring an increased risk of channel closure (Chen et. al., 2016; Haynes & Johnston, 2011; Kim et. al., 2005; Seris E.L.C, 2006; Y. Wang & Chen, 2004).

There are a lot of publications on micro reactor concepts for steam reforming have been published in the past decade. Unfortunately, within the vast majority of these publications, only a very small number of publications is focused on the overall integration of the process, from cold reactants to cooled products especially for mobile hydrogen fuel generator. This research gap has become the highest motivation for this project to be pursued. A report by Kamarudin et. al., (2009) highlighted that a major obstacle in the hydrogen fuelled transportation sector is adoption of hydrogen supply chain which is hydrogen production technology. Thus, development of a novel SMR mobile plant with noble catalyst in micro reactor is potentially suited to embrace the research gap caused by the problem statement. This project desired a fundamental based line prediction model for hydrogen intensification via SMR at micro scale reactor with noble metal catalyst. There are three main phases involved to counter the research gap loophole, which are (i) development of the mobile test rig as analysis platform, (ii) introduction of interchangeable catalyst micro reactor and (iii) SMR operating parameters.

1.3 Objectives

In order to address part of the SMR problems stated above, this research is focused on the following objectives:

i. Development of a small scale mobile steam methane reforming (SMR) test rig bench for methane conversion based platform.
ii. Design of a micro channel reactor with interchangeable catalyst modules for methane conversion process.
iii. Characterization and analysis of relationships between type of catalysts and micro reactor operational configuration as a baseline for reaction rate of Rhodium, Ruthenium and Nickel.

1.4 Scopes of study

The scopes of this research are as followed.

i. Formulation test rig development is carried out based on chemical conceptual process design system which consists of four levels, such as Level 1 (process selection), Level 2 (chemical synthesis), Level 3 (recycle stream) and Level 4 (chemical separation).

ii. Design and fabrication of main operation units such as saturated steam generator, condenser, separator, dryer and purifier.

iii. Assembly of all unit operations and validation through hot commissioning at operating temperature of 500°C to 700°C.

iv. Fabricated micro reactor should undergoes cold commissioning of a vacuum test, hydrostatic test and static pressure test.

v. Micro reactor was placed inside the box furnace at operating condition of 600°C to 800 °C and 1 bar for hot commissioning.

vi. The steam to carbon ratio test of the fabricated micro reactor vary from S:C 1 to S:C 5.

vii. Determination of methane conversion and SMR's yield for the Nickel aluminide, Rhodium aluminide and Ruthenium aluminide based catalytic steam methane reforming process.

viii. Test the methane conversion working condition at reaction temperature of 500 to 700°C and 1 bar gauge pressure for 300 minutes reaction time.

ix. The methane conversion analysis at Steam to carbon ratio of 2, 3 and 4.

x. Reformate gas from SMR conversion was analyzed by using a gas chromatography and a multi gas detector.

xi. SMR conversion and yield via mole balance for flow reactors and design of rate of reaction (methane disappearing rate) modeled by using the Langmuir isotherm principle.

1.5 Overall Project Layout

In order to simplify and determine the critical parameter approach, the interaction relation diagram for the whole process involve in steam methane reforming was defined and further analysis as in Figure 1.4. This figure shows the main parameter involve in this study, which represents of:

i. SMR reformer technologies
ii. SMR conversion platform (test rig bench)
iii. Catalyst study

The main parameter has been sorted by sub-category which represent more details of related literature activities. This defined diagram has been conducted accordingly to the input and output analysis of each sub-category. This net between input (need to form) and output (effect of form) is employed to define the factor is either causes or effects. The factors that are causes are called as Driver (lead the pathway), meanwhile the results or effects of factors are called as an Indicator (dependent). Only net value above "zero" is considered as Driver factor.

From the Table 1.1 and Figure 1.4, the driving factors are identified in order to define the correction and further review analysis. These driving factors judgment are based on the net input and output of dependent track. Thus, it turned the critical stage and interaction of each spot had become connected to be pursued in detail review. From the Table 1.1, it shows that item 1.2, 1.4, 2.3 and 3.3 are the critical main factors to be deeply considered and reviewed in order to examine and characterize novel interchangeable catalyst micro reactor of this project. Meanwhile, for the indicator factors, it can be used as support for driving factor analysis.

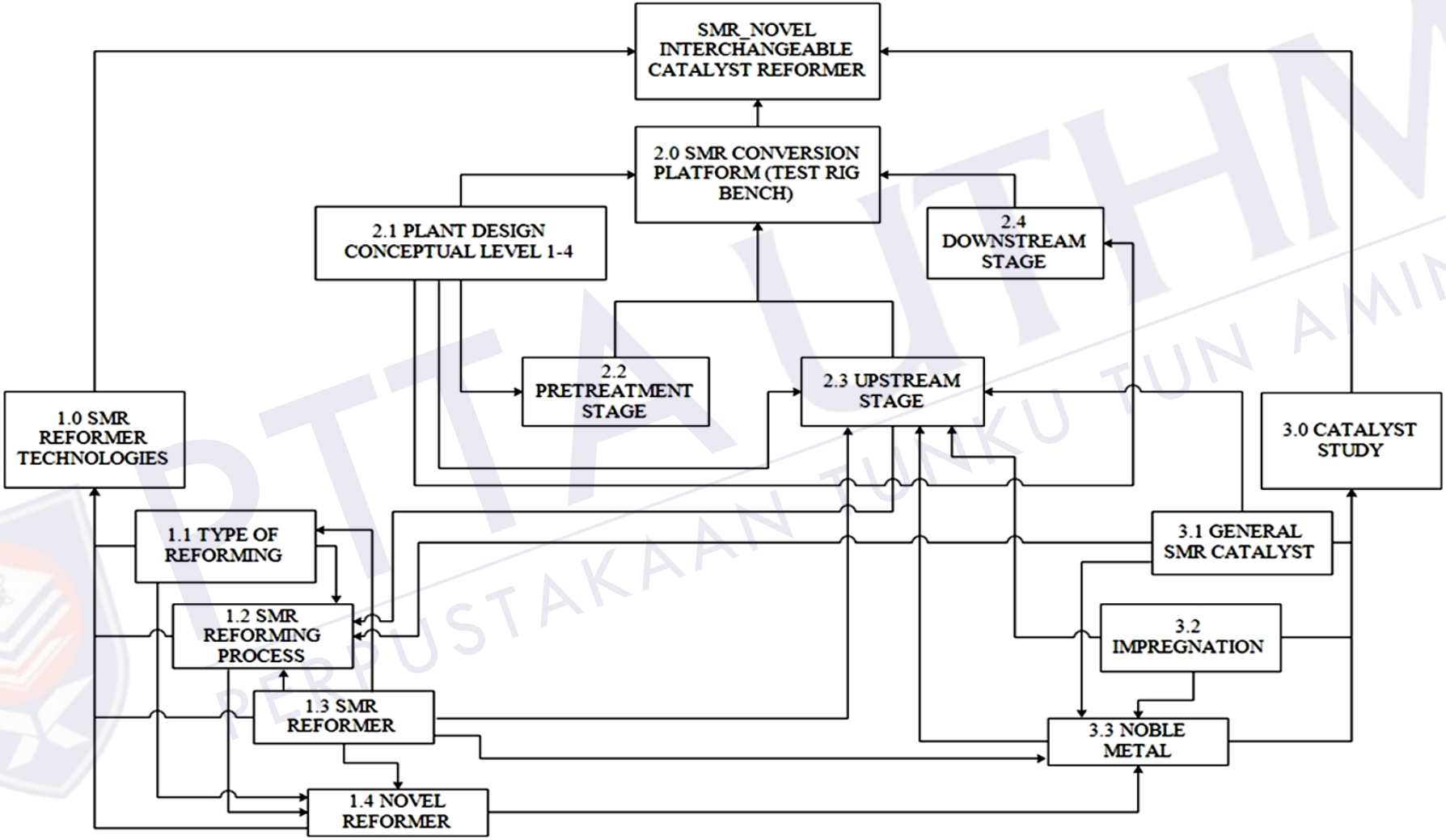

Figure 1.4 : Interaction relationship diagram of novel interchangeable catalyst reformer.

Table 1.1: Interaction relation for driving factor of novel interchangeable catalyst reformer.

No	Parameter	Input	Output	Nett	Factor
1.1	Type of reforming	1	3	-2	Indicator
1.2	**SMR reforming process**	**4**	**2**	**2**	**Driver**
1.3	SMR reformer	0	6	-6	Indicator
1.4	**Novel reformer**	**3**	**2**	**1**	**Driver**
2.1	Plant design, conceptual level 1-4	0	4	-4	Indicator
2.2	Pretreatment stage	1	1	0	Indicator
2.3	**Upstream stage**	**5**	**2**	**3**	**Driver**
2.4	Downstream stage	1	1	0	Indicator
3.1	General catalyst	0	4	-4	Indicator
3.2	Impregnation	0	3	-3	Indicator
3.3	**Noble metal**	**4**	**2**	**2**	**Driver**

The major purposes of this study were (1) design, fabricate and develop a mobile small scale SMR test bench (2) build up a micro channel reactor with substrate plate insert module (3) introduce an interchangeable catalyst of the micro channel reactor equipped with a high thermally stable catalysts that are capable of catalyzing the production of hydrogen from methane more efficiently on the coated substrate plate, (4) determination of models for reforming reaction kinetics in order to obtain a rate expression. The aim was to maximize methane conversion and hydrogen selectivity for the best performing Ni/Rh/Ru aluminide catalysts. The reasons for using this catalyst system are described in depth in chapter 2 and 3. The performance of the catalyst was tested for different process variables such as reaction temperature and

steam to carbon ratio, and the stability of the catalyst was tested by time-on-stream runs. Moreover, credit interest to study the SMR conversion at a lower reaction temperature below industrial spec which ranging from 400-700°C and operating pressure of 1 bar gauge as advantages of using a micro scale reformer

1.6 Expected outcomes

The expected outcomes of this research are outlined as follows:

i. A functioning prototype of a lab scale steam methane reforming test rig as an equipment for methane conversion for any catalyst material feasibility and performance tests.
ii. A novel multi catalyst material changeable slots in micro channel reactor for different kinetic reaction rate.
iii. Establishment of micro reactor operational configuration for intensification methane conversion rate in order to make it as a good candidate for industrial applications.
iv. Enhancement of the hydrogen yield at product stream via steam methane reforming on novel active metal catalyst in the micro channel reactor.
v. Reducing the carbon monoxide conversion at product stream via steam methane reforming on novel active metal catalyst in the micro channel reactor.
vi. A kinetic model rate of reaction (methane disappearing rate) for production's scale up through validation of relationship among catalyst, reactants characteristics and reformer geometry.

1.7 Thesis Outline

This thesis comprises of fifth chapters and listed as below:

Chapter 1 Introduction: Explains the introduction of this research, including its background, problem statement, objectives, scopes, expected outcomes, overall project layout and intention of the research.

Chapter 2 Literature Review : Background information relevant to the project's objectives and scopes, including reformer technologies, micro channel reactor, catalyst in SMR and catalyst behavior analysis.

Chapter 3 Methodology : Covering experimental apparatus, design and development process of SMR test rig bench, micro channel reactor and catalyst conversion properties.

Chapter 4 Results and Discussion : This chapter is covered the main three phases outcomes and had been briefly discussed accordingly. The first phase which covered of development of SMR test rig, focused on the design, development and commissioning of SMR test rig bench with considerations of catalyst evaluations. The second phase is covering the art of micro reactor system, design, fabrication, development and commissioning of an interchangeable micro scale reformer. The third phase is covered the reforming catalytic studies, performance of an SMR test rig bench and the micro channel reactor, an experimental work for catalytic behavior through multiple type of catalyst had been conducted and further analyze. The catalyst effect on conversion properties which covering effect of operating conditions and multiple type of catalyst.

Chapter 5 Conclusion and Recommendation: Outline the conclusion of the research output and some recommendations for future works.

CHAPTER 2

LITERATURE REVIEW

2.0 Introduction

This chapter describe a review of literature related existing research in reforming technologies, conceptual plant design (conversion platform) and catalyst profile matter. Thus, the main parameter has been sorted by sub-category which represent more details of related literature activities.

2.1 Hydrogen as a Renewable Energy

Nowadays, increasing attention is being paid to pollution related environmental and public health problems. Thus, it is essential to find an alternative way for utilizing green energy. A hydrogen economy coming from renewable energy sources would highly benefit the world. The hydrogen has been widely used in petrochemical processes such as hydro-desulfurization, hydro-cracking, and thus along. Today, hydrogen becomes more utilized as a feedstock in the synthesis of methanol/dimethyl ether (DME) and the Fischer Tropsch reactor to produce liquid fuels from natural gas. Besides that, hydrogen serves as the ideal fuel for fuel cell, such as for proton exchange membrane (PEM) which converted to electricity for vehicle or directly combusted in ICE for vehicles with special traits of zero carbon emission. Thus, demand for low-cost hydrogen production is desired either for mass production or for distributed applications (Armor, 1999; Bartels et al., 2010; Cheng et al., 2011; Langé & Pellegrini, 2013; Maluf & Assaf, 2009; Pirez et al., 2016).

Hydrogen contains the highest energy per unit weight (120.7 kJ/g) and becomes most suited potential energy carrier of the future. Advances in fuel cell technology turn out hydrogen more important as a new energy source for both stationary and mobile applications. As such, the demand for hydrogen in fuel cell application and also in the chemical industry is continually increasing (Bej et al., 2013; Beurden, 2004).

2.1.1 Optimization of Future Hydrogen Energy in Transportation Sector

The potential use of hydrogen as an energy sources in transportation sector had create brighter future to encounter the environmental pollution issue as compared to the current energy supply of petroleum based products such as gasoline and diesel. The International Energy Agencies predict the increasing of world population at 10 billion people by 2050. Thus the transportation sector is growing proportionally to the population. Thus, the need of zero carbon emission energy sources is essential to minimize the impact of transportation sector pollution especially in GHG. It is believed that hydrogen is the potential energy carrier because it can be combusted, like gasoline and natural gas without any carbon emission at the point of use. Malaysia is also targeting hydrogen as future fuel for transportation sector either based on fuel cell technology or direct combusted for ICE. (Cheng et al., 2011; Kamarudin et al., 2009; Khan et al., 2010; Maluf & Assaf, 2009).

Reported by Kamarudin et. al., (2009), the major obstacle in adoption of hydrogen fuelled vehicle is the lack of a hydrogen delivery system. A full scale hydrogen infrastructure with production lines, distribution platform and refilling stations is very expensive to be execute. The current research of hydrogen delivery system, is mainly focused on the hydrogen supply chain area which covered the technology of production, storage, distribution and refilling platform. Hereby, the hydrogen supply chain on production stage had cause a problematically loop in term of operation process, cost and feasibility performance.

The ideas of compacting and scaling down of SMR plant to a novel SMR mobile plant with noble catalyst in micro reactor for hydrogen production technology had

become the highest motivation to execute this project. This novel SMR mobile plant with noble catalyst in micro reactor's outcome should be able to run the prediction model of methane conversion, SMR's yield, rate of reaction and feasibility studies. This project should be able to improvise and covers the loop hole in hydrogen supply chain especially for production stage.

2.2 Reformer Technologies

In this context, reforming is defined as the thermochemical processing of a hydrocarbon feedstock in high temperature chemical reactors in order to produce a hydrogen-rich gas. Reforming is usually achieved by reacting a hydrocarbon (NG) with superheated steam at high temperature and pressure in the presence of a catalyst. Basically, the overall reaction is endothermic, therefore energy must be added to drive it. Unless there is an external heat source available, this requires the consumption of a fraction of the primary fuel. The hydrogen production process takes place in several steps. First, a hydrocarbon feedstock (such as natural gas) is reformed at high temperature in the presence of a catalyst. Depending on the type of reformer, the feedstock reacts with steam or oxygen at high temperature to produce a synthetic gas composed of hydrogen (H_2), carbon monoxide (CO), carbon dioxide (CO_2), unreacted methane (CH_4) and unconverted steam (H_2O). This syngas is further processed to increase the H_2 content whereby CO and H_2O in the syngas is converted to H_2 via the water gas shift reaction (WGS). Finally, hydrogen is separated out of the mixture at the desired purity, up to 99.999% for fuel cell and any other applications (Graf et al., 2007; Lutz et. al., 2004; Raju et. al., 2009; Shinagawa, Oshima, & Sekine, 2013).

The correct reforming process lead to the plant thermal efficiency, plant size and geography, capital cost, downstream gas handling equipment and syngas composition. Basically, there are six types of reforming process technology (listed below) that available for the production of syngas (mixture of H_2 and CO) and the H_2 base of natural gas as raw; which major component is methane. Further analysis of reforming technology is shown in Table 2.1. Whereby from this table, comparison among reformer technologies proves that SMR is the most suit compare to others.

i. partial oxidation
ii. steam methane reforming
iii. auto thermal reforming
iv. carbon dioxide or dry reforming of methane
v. combination of dry reforming and steam methane reforming
vi. tri reforming of methane

The steam methane reforming (SMR), has several advantages over the others, such as low reaction temperature, high hydrogen and low carbon monoxide content in the reforming products. Therefore, the SMR is currently becoming the most suitable process technology at plant scale due to its cost effectiveness and a highly developed method for production of hydrogen on a large scale. Moreover, the natural gas used in this process is abundantly available at relatively low cost and high H_2/CO ratios are desired for H_2 production (Eswaramoorthi & Dalai, 2009; Gangadharan et. al.,2012; Ghorbanzadeh et. al., 2009; Graf et al., 2007; Liu.J, 2006; Lutz et al., 2004; Mondal et. al., 2015; Pirez et al., 2016; Rafiq & Hustad, 2011; Salhi et. al., 2011; Seungwon Park et al., 2017; Udengaard, 2004; Vagia & Lemonidou, 2008; Youn et al., 2008).

Since hydrogen is attracting much attention as a clean and efficient energy source. A lot of efforts have been made to develop efficient, low-cost catalysts for hydrogen production. Nickel catalysts are typical of them and are being widely used for hydrogen production. However, these catalyst have a drawback of the methane formation (methanation) due to the chemical reaction between product gases, H_2 and CO. This reaction ends up reducing the efficiency of H_2 production. Therefore, it is necessary to develop better catalysts without causing methanation such are written in Equation 2.1 and 2.2 (Cohron et. al., 1996; Doma et. ak., 2016; Fabas et al., 2017; Haynes & Johnston, 2011; Kr et. al., 2015; Saadi et al., 2011; Sulka & Jó, 2011; Ward-Close & Minor, 1996; Y. Xu et al., 2005).

$$CO + 3H_2 \leftrightarrow CH_4 + H_2O \quad (2.1)$$

$$CO_2 + 4H_2 \leftrightarrow CH_4 + 2H_2O \quad (2.2)$$

Table 2.1 : Comparison of syngas generation technology (Gangadharan et al., 2012; Holladay et al., 2009; Samuel, 2003).

No.	Technology	Advantages	Disadvantages	Developers/Licensors
1	Partial Oxidation (POX)	Feed stock desulfurization not required	Very high process operating temperature. Usually requires oxygen plant Low H_2/CO Soot formation/handling add process complexity	Texaco Inc. and Royal Dutch/Shell
2	Steam Methane Reforming (SMR)	Most extensive industrial experience Oxygen not required, lowest process operating temperature Best H_2/CO ratio for production of liquid fuels.	Highest air emissions More costly than POX and autothermal reformers Recycling of CO and removal of the excess hydrogen by means of membranes	Haldor Topsoe AS, Foster Wheeler Corp, Lurgi AG, International BV, Kinetics Technology and Uhde GmbH
3	Auto Thermal Reforming (ATR)	Lowest process temperature requirement than POX Syngas methane content can be tailored by adjusting reformer outlet temperature.	Limited commercial experience Usually requires oxygen plant	Lurgi, Haldor Topsoe
4	Dry Reforming (DRM)	Green house gas CO_2 can be consumed instead of releasing in to atmosphere Almost 100% of CO_2 conversion	Formation of coke on catalyst Additional heat is required as the reaction takes place at 873K	Carbon Sciences

5	Dry Reforming + Steam Methane Reforming	Best H_2/CO ratio for production of liquid fuels Coke deposition drastically reduced	Separation of unreacted methane from SMR syngas Project Installation cost	Haldor Topsoe AS
6	(DRM+SMR) Tri Reforming Methane (TRM)	Directly using flue gases, rather than pre separated and purified CO_2 from flue gases Over 95% of methane and 80% CO_2 conversion can be achieved.	Usually requires oxygen plant Low H_2/CO ratio ratios limit its large-scale application for F-T & MeOH synthesis.	Haldor Topsoe AS

2.2.1 Steam Methane Reforming (SMR)

Catalytic steam reforming of methane (SMR) is a well-known, commercially available process for hydrogen production. Currently in the United States, most hydrogen today (over 90%) is manufactured via steam reforming of natural gas. As mention previously, this SMR is the conversion of hydrocarbon mainly methane with steam into a mixture of hydrogen (H_2), carbon dioxide (CO_2), carbon monoxide (CO), unreacted methane (CH_4) and unconverted steam (H_2O). Hydrogen production is accomplished in several steps: steam methane reforming (SMR), water gas shift reaction (WGS), and hydrogen purification.

$$CH_4 + H_2O \leftrightarrow CO + 3H_2 \qquad \Delta h = +206.16 \text{ kJ/mol} \tag{2.3}$$

The SMR reaction as in Equation 2.3 is an endothermic reaction and requires external heat input. Economics favor reactor operation at pressures of 3-25 atmospheres and temperatures of 700°C to 900°C. The external heat is needed to drive the reaction is often provided by the combustion of a fraction of the incoming natural gas feedstock (up to 25%) or from burning waste gases, such as purge gas from the hydrogen purification system. This heat transfer to the reactants is accomplished indirectly through a heat exchanger mechanism. The Methane (CH_4) and steam (H_2O) react in catalyst filled tubes with typical operating condition of, the steam- to-carbon ratio is about 3 or more, in order to avoid coking or carbon build-up on the catalysts. This is due to at lower steam-to-carbon ratios below 3, solid carbon is produced via side reactions (Bej et al., 2013; Beurden, 2004; Dybkjær et. al., 2011; Eduardo et. al.,, 2009; Gangadharan et al., 2012; Graf et al., 2007; Radfarnia & Iliuta, 2014; Simsek et al., 2013; F. Wang et al., 2013; H. Wang et. al., 2012). A reduction in the steam to carbon ratio in the reformer helps reduce the magnitude of the problem, but at the risk of exacerbating the propensity to form carbon in the system (Chen, Yan, Song, & Xu, 2016; Haynes & Johnston, 2011).

This SMR process is highly endothermic, therefore in order to achieve high conversion of methane and to avoid carbon deposition due to methane cracking as in Equation 2.4, steam is introduced in excess. But this will lead to high energy

consumption, especially during the mass ratio of steam- to-carbon is about 3 or more. Even though this condition capable to increase methane conversion and hydrogen production, it's still delivering a few disadvantages such as high energy expenditure and less efficiency of hydrogen recovery from a undesired product during a final product separation stage. After reforming, the resulting syngas is sent to one or more shift reactors, where the hydrogen output is increased via the water-gas shift reaction as in Equation. 2.5. This SMR has a lower operating temperature compare to Partial Oxidation (POX) and Autothermal Refroming (ATR), and also yield a high H_2/CO ratio approximately 3:1 at the output stream (Charisiou et al., 2016; Holladay et al., 2009; Maluf & Assaf, 2009; Moghtaderi, 2007; Tonkovich et al., 2004; 2007; Udengaard, 2004).

$$CH_4 \leftrightarrow C + 2H_2 \qquad \Delta h = 75 kJ/mol \qquad (2.4)$$

$$CO + H_2O \leftrightarrow CO_2 + H_2 \qquad \Delta h = -41.15 kJ/mol \qquad (2.5)$$

Equation 2.5, the conversion of CO to H_2 and CO_2 with the excess of H_2O. This reaction is favored at temperatures of less than about 600°C, and can take place as low as 200°C, with sufficient active catalysts. The gas exiting the shift reactor contains mostly H_2 (70%-80%) plus CO_2, CH_4, H_2O and small quantities of CO. For hydrogen production, the shift reaction is frequently carried out in two phases. A high temperature shift reactor operating at about 350 to 475°C accomplishes much of the conversion, followed by a lower temperature at 200 to 250°C shift reactor, which brings the CO concentration down to a few percent by volume or less. Meanwhile the Equation 2.6 is global SMR whereby submerged from Equation 2.3 and 2.5 (Salhi et. al., 2011; H. Wu et al., 2013).

$$CH_4 + 2H_2O \leftrightarrow CO_2 + 4H_2 \qquad (2.6)$$

The hydrogen is then purified, where the level of purification depends on the application. For industrial hydrogen, pressure swing absorption (PSA) systems or palladium membranes are used to produce hydrogen at up to 99.999% purity. In a preferential oxidation system, the gas is passed over a catalyst bed, with added air. At a certain temperature and stoichiometry conditions, the reaction is strongly favored over hydrogen oxidation, so that CO is removed to the level of several ppm. These

coke formation as in Equation 2.4 is normally through thermal cracking of hydrocarbons or through reactions between carbon monoxide molecules as in Equation 2.7. Extensive coke formation will result in pore blockage in the catalyst and increased resistance to pore diffusion (Beurden, 2004; Graf et al., 2007; Radfarnia & Iliuta, 2014; Simsek et al., 2013; F. Wang et al., 2013; J. Wang et al., 2012).

$$2CO \leftrightarrow C + CO_2 \qquad \Delta h = +173.3 \text{ kJ/mol} \qquad (2.7)$$

Therefore, the constant pursuit for maximum energy efficiency in modern steam reforming plants yields both economic and environmental benefits. For a steam reforming plant to operate at maximum efficiency and deliver a high throughput of desired product composition, it is essential to keep the S/C ratio low. Operation at low S/C is often accompanied by challenges in the development of materials (Saadi et al., 2011).

The current practice of SMR is generally to react natural gas with steam over a nickel catalyst in large tubular reformers operating at temperatures ranging up to excess of 800°C. Therefore, the catalyst used is extremely activated and rate of heat transfer limits the reaction intensity that can be achieved. For large scale plant, higher heat fluxes are attainable using high-temperature radiant transfer, whereby the tubes containing the catalyst are located within a furnace, equipped with flame and combustion gasses as the heat transfer through radiation. This high temperature is needed in order to obtain high radiant heat fluxes (typical design heat fluxes being of the order of $q = 100$ kW m^{-2}), mean that the combustion gases leave the furnace at around 900^{o}C (Chen et al., 2016; Haynes & Johnston, 2011; Jianguo Xu et. al., 1989).

For heat transfer from atmospheric-pressure combustion gases, the dominant resistance to heat transfer is from the combustion gases to the wall. For flow across a bundle of tubes (containing the catalyst, diameter typically of the order of 100 mm), the external heat transfer coefficient may be estimated very crudely via Colburn's correlation (Haynes & Johnston, 2011). In practice, of course, much lower temperatures and heat fluxes must be taken, despite which the convective reformer does still provide some volume reduction relative to a radiant furnace. Nevertheless,

the radiant furnace has remained the preferred plant for large-scale steam reforming (Chen et al., 2016).

Here the Reynolds number is based on the velocity occurring in the minimum open area between the tubes a typical value would be 20 ms^{-1}. Taking physical properties of combustion flue gases at 1 bar and 900°C, a heat transfer coefficient of h ~ 70 $Wm^{-2}K^{-1}$ is obtained, which in turn would require an infeasible temperature driving force ~1428.57 K in order to achieve a heat flux of q = 100 kWm^{-2}. The Equation 2.8 is showing fundamental for the desired heat flux (Chen et al., 2016; Haynes & Johnston, 2011).

$$q = h \times K \tag{2.8}$$

Where :

q : heat flux

h : heat transfer coefficient

K : temperature Kelvin

2.2.2 Novel Reformer of SMR

The large-scale packed bed reactor with Ni catalyst supported on Al_2O_3 pellets suffers from the poor heat transfer behavior. It is inevitably resulted in the large gradients in terms of temperature (and/or pressure) in axial and radial directions. External heat may not be ideally transferred to the catalyst due to the limited heat transfer characteristics of packed beds. Thus, local catalyst temperatures may be lower than the one of desired values. Distribution of external heat to the catalyst bed has a direct impact on the efficiency of the process. This phenomenon affects the SMR product spectrum in favor of H_2 rich production. The enhanced heat transfer is observed, which may be exploited for highly endothermic reactions due to the losses of the desired heat and the suppression of hot spot formation. Another considered aspect is the optimization of slow reactions getting close to the thermodynamic equilibrium. In conventional technical reactors, the conversion of reactions close to their thermodynamic equilibrium is improved by intermediate direct (cold gas/water injection) or indirect (coolers switched between several stages of the reactor) cooling. In practice, much

lower temperatures and heat fluxes must be accepted, despite which the convective reformer does still offer some volume reduction relative to a radiant furnace. Nevertheless, the radiant furnace has remained the preferred plant for large-scale steam reforming (Haynes & Johnston, 2011; Kolb & Hessel, 2004; Murphy et al., 2013; Stutz et. al., 2006; Zhai et. al., 2011).

The general reactor type, tubular reactors the temperature in static catalyst beds with high heat loads such as reformers. It is conventionally controlled by the concept of catalyst packing inside tubes; heat sources from the outside is supplied, as the heat transfer, in order to secure and maintaining the radial and axial temperature profiles inside the tubes within acceptable bounds. Even though this concept is well known, stable and becoming a very successful strategy, it still requires the striking of a delicate balance between reaction and heat transfer within the tubes, heat transfer to the outside of the tubes, and pressure drop. Therefore, the outcome of this balance is that tubular reformers are bulky, mostly, since relatively large catalyst particles with low effectiveness are employed. The active catalyst effectiveness is less than 3% of the reforming reactions, with the active catalyst is applied to only the outer 2 mm of the considered catalyst particles. The implication is that the reforming catalyst bed could be two-orders of magnitude. It is potentially can be smaller if the effectiveness is near to 1 mm by using small catalyst particles, without any improvement of intrinsic activity. Small particles are incompatible with tubular reformers since pressure drop constraints would dictate the use of many parallel or short tubes (Dupont et al., 2008; Madon et al., 2015; Marshall, 2002; Ogden, 2001; Silversand, 2003, Kuba et al., 2016; Marshall, 2002; Ogden, 2001; Seris E.L.C, 2006; Silversand, 2003; Türks et. al., 2017).

In micro-reactors, heat-exchanging channels may be introduced for temperature profiling of the reactor according to the specific requirements of the reaction. Another way of exploiting the improved heat transfer is by using the combination of exothermic and endothermic reactions in a single reactor designed like a heat exchanger. Therefore the overcome of heat and mass-transfer limitations is a crucial for applying micro-reactors instead of conventional apparatus. Suitable criteria have to be identified to allow proper judgement of such limitations, the effect of intra-particle (or intra-coating) and temperature gradients (Haynes & Johnston, 2011; Kolb

& Hessel, 2004; Murphy et al., 2013; Stutz et al., 2006; Zhai et al., 2011). Simsek et. al., (2011) reported that heat is generated locally or supplied externally can be rapidly spread over the entire catalyst volume. It can exist either as a layer coated on the interior channel walls or as particles packed into the channels. The heat can be guaranteed nearly isothermal operating conditions without the risk of hot-spot formation. Due to the negligible pressure drop benefit of the micro channel flow, operation on the micro scale also offers the possibility to reduce residence times down to millisecond levels at which undesired and slow side reactions such as carbon formation cannot take place.

Recent developments in the intensification process provide advantage of the fact that heat transfer rates are greatly enhanced in smaller-scale systems and a number of convective reformer concepts have been advanced and demonstrated. Therefore, the reactors are regarded as being micro-structured, when carrying channels or similar fluid paths with a size below 1mm. In parallel plate reformers, the combustion and reforming processes take place in adjacent channels. By creating a heat-exchanger/reactor with the channel wall, it is providing the support for both catalysts that promote the respective processes and the heat transfer dividing wall. Since the narrow channel width employed, the flows in these systems are typically laminar, for which a characteristic Nusselt number is easily obtained as a constant value under a fully developed condition with a value of Nusselt number is Nu~8. A typical plate separation of 1 mm, the corresponding heat transfer coefficient, h, for flue gas is approximately 320 W m^{-2} K^{-1}. Therefore, for a heat flux of 100 kW m^{-2}, the temperature driving force is approximately 312.5 K, and successfully reduce 78% of driving temperature compare to the one by the conventional tubular packed bed (Chen et al., 2016; Haynes & Johnston, 2011)

The shorter passages, within the thermal development length, manage to obtain the benefits of thinner boundary layers and higher heat transfer coefficients. During fluids flow pass through a curved duct, the secondary flows (Dean vortices) are developed which lead to the transverse mixing of the fluid in the duct and straightly potentially enhance the heat transfer rate. Meanwhile, at sharp bend points, the recirculation zones may be established, which also lead for mixing of the fluid at that point. Besides that, the laminar boundary layer must be reestablished beyond the bend,

especially during the process of significantly higher (developing flow) heat transfer coefficients. Significant augmentation is possible using a combination of the above techniques, meaning that the nominal reformer heat flux of 100 kW m^{-2} can be achieved with a temperature driving force <1000 K for flow in 1 mm passages compare to the conventional tubular packed bed reformer. By applying to the reforming example, this turn allows one to think in terms of processes with close temperature approaches and very high thermal efficiency (Chen et al., 2016; Haynes & Johnston, 2011).

2.3 Micro Channel Reactor in Steam Methane Reforming (SMR)

Recently, micro-channel reactors have received much attention for the unique feature of process intensification, for example, the excellent temperature control and improved mass transfer especially in the applications of highly exothermic and endothermic reactions. A metallic structured support, with its inherent high thermal conductivity, can be used as the substrate of catalysts and integrated for micro-channel reactor applications. Researchers from Velocys and Pacific Northwest National Laboratory (PNNL) reported that, the development of a millisecond micro-reactor concept for steam methane reforming (SMR) process with the highly efficient integration of an exothermic combustion channel and an endothermic reforming channel with high thermal efficiency through the channel (metal) wall. In the meantime, a potential risk is existed due to the difference of thermal expansion coefficients between the metallic substrate and the catalyst layer. The catalyst layer would fall off during the reactions operated at high temperature. This would hinder the practical applications of the micro-channel reactor, and has not been successfully solved yet (Cheng et al., 2011; Z. Liu et al., 2012; Tonkovich et al., 2004).

Down-scaling of SMR has been a pressing demand over the last two decades in view of the world's ever growing need for cleaner, safer and more economical hydrogen production processes. This micro channel reactor naturally fits these needs owing to process intensification via miniaturization, which tremendously increases transport rates and allowing for processes running at almost the intrinsic rate of chemical kinetics (Cao et. al., 2016).

The high heat and mass transfer rates is enabled by the micro channel design capability to increase the reactor efficiency, reduce size and weight, and improve conversion, yield, selectivity, and catalyst life compare to the conventional fixed- bed reactors. For all catalysts studied, at the same weight hourly space velocity (WHSV) operating condition, this micro reactors have been reached a higher hydrogen yield and methane conversion compare to the one by fixed-bed reactors (Jin et al., 2016; Murphy et al., 2013).

The micro channel reactor is a device that is used primarily to produce hydrogen. It is often made from pieces of aluminum, iron, ceramics, glass, and more. There are many types of micro reactor produced by researchers (Simsek et. al., 2011). There is a structure called as a micro channel where the flow of liquid will flow through and react with the catalyst. Figure 2.1 to 2.3 show the micro channel reactor structure, pathway of reactant flow in micro channel and the actual micro channel reactor, respectively.

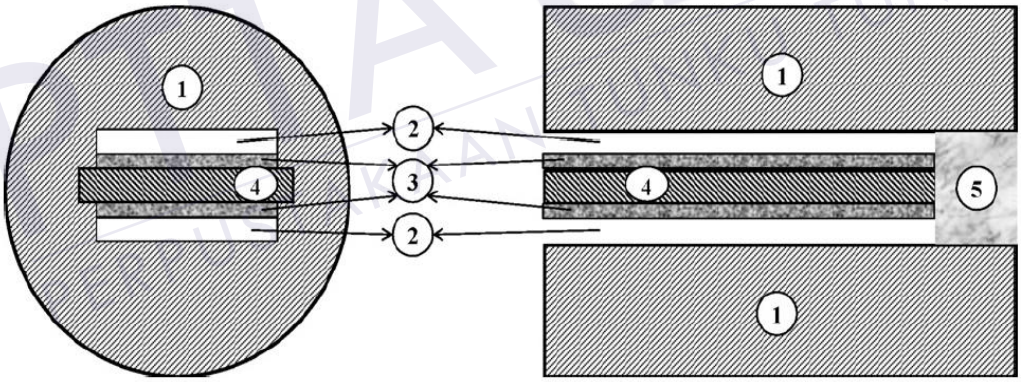

Figure 2.1 : Micro channel reactor structure:Top (at the left) and cross-sectional (at the right) views of the microchannel configuration①: engineered metal housing; ②: open microchannels;③: coated catalyst layers;④: substrate plate;⑤: ceramic wool plug (Simsek et al., 2011).

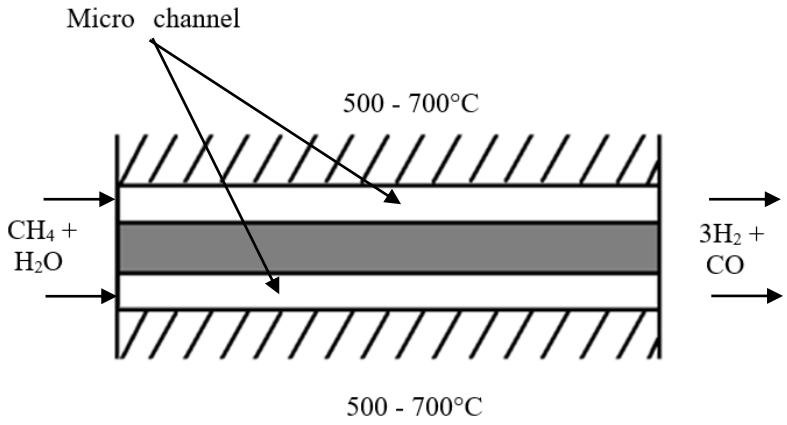

Figure 2.2 : Pathway of reactant flow inside micro channel (IP2017300009, 2017; Simsek et al., 2011).

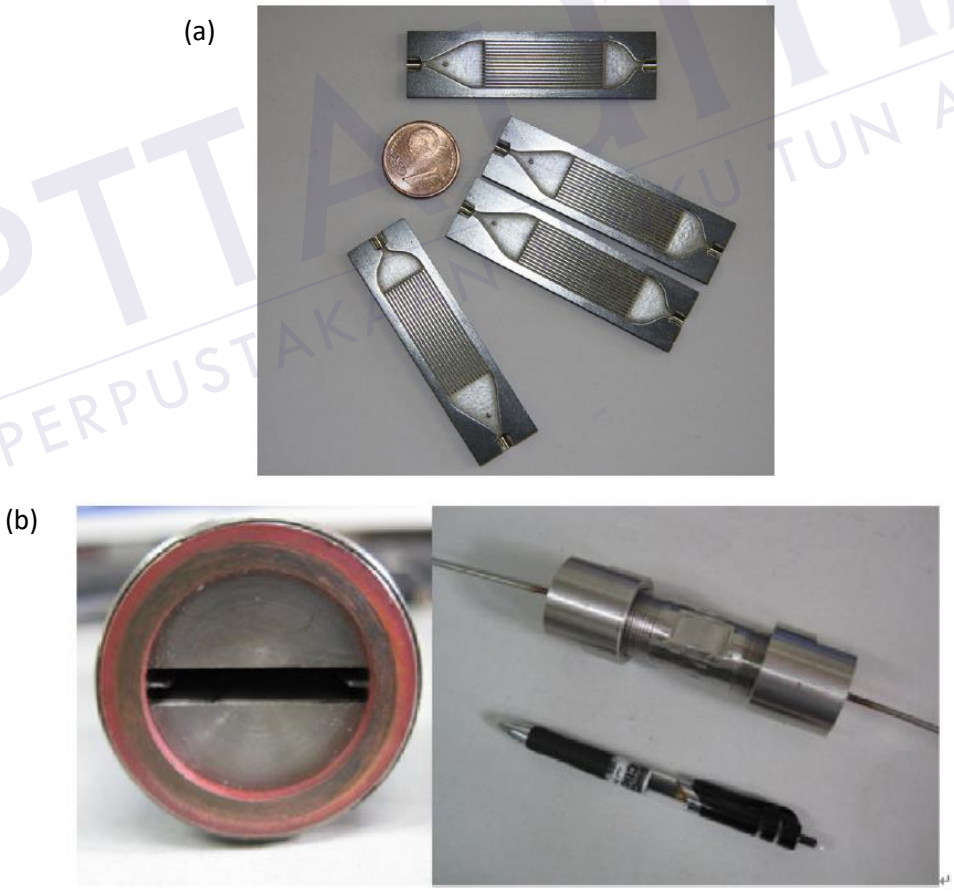

Figure 2.3 : Micro channel reactor : (a) Multi coil type (Izquierdo et al., 2012), (b) Radial pin hole type (Liu et al., 2012).

Even smaller driving forces can be achieved if the duct diameter is further reduced. However, there is a limit in determination of small passage dimensions. In general terms, fine passages should be as short as possible and can be used in larger numbers in order to control the pressure drop in a given duty. From the point view of manufacturing, the attachment of flow headers and distribution systems with very short arrays of ducts become problematical, thus, very fine passages bring an increased risk of channel blockage. There are a lot of publications have been published in the past decade about micro reactor concepts for steam reforming. Unfortunately, in the vast majority of these publications, little or no attention is paid on the overall integration of the process from cold reactants to cool products. The main focus of these previous researchers is concentrated on the reaction kinetics of novel supported catalysts and also on the configuration of the high-temperature heat supply (combustion) and heat sink (reforming) reactions (Haynes & Johnston, 2011; Kim et al., 2005; Seris E.L.C, 2006; Y. Wang & Chen, 2004).

2.3.1 Physical Properties of Micro Channel Reactor

Structural size of composite micro channel reactor system for direct transmission or restriction of gas or liquid, which has dimensions at least in one direction, is usually measured in the micro channel reactor, sometimes up to 1 mm. These structures consist of a micro-scale channels (eg, channel and slot) and pores, features a larger (e.g parallel plate) which allows fluid to flow in a thin film (Butcher et al., 2014; Morris, 2016; Tonkovich et al., 2004).

Meanwhile, the geometry is most important aspect in the micro channel reactor design. Various designs of micro channels have been highlighted by previous researchers in order to ensure that the fluids flows in the micro channel reactor actually reacts with the catalyst. The depth structure of a micro channel should be less than 1 mm to ensure full contact with the surface of the catalyst fluid flow rate. The allotted time for the fluid to react is depending on the total surface area of contact. The more surface contact between the fluid flowing to the catalyst, the faster the response time. Figure 2.4 shows the architectural structure of the micro channel (Cheng et al., 2011; Morris, 2016; Murphy et al., 2013).

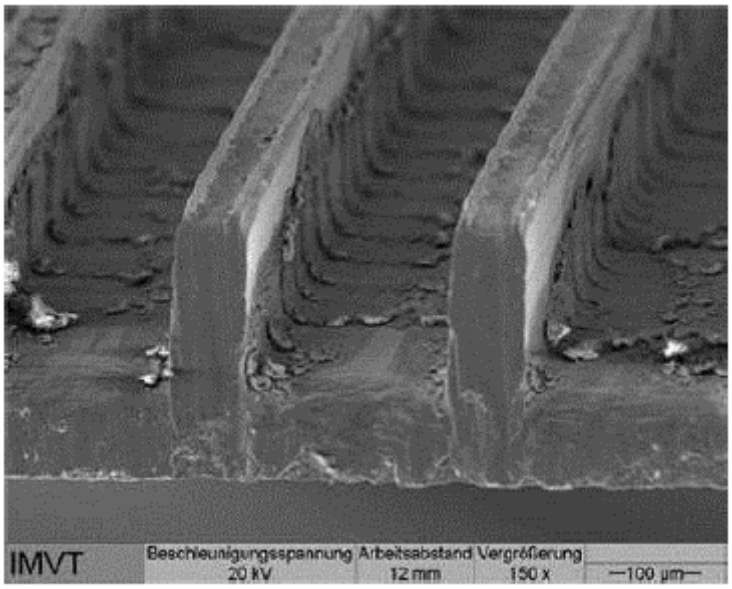

Figure 2.4 : The architectural structure of micro channel(Morris, 2016).

The reactor dimension is an important design parameter, and its effect on the performance of multifunctional micro reactors. The reactor length, the wall thickness, and the gap sizes of the two channels are three basic parameters that can be varied. Recent works on the catalytic combustion in single-channel micro reactors revealed that reactor dimensions can significantly affect the flame stability and thus reactor performance. In a single-channel micro reactors, increasing the reactor length leads to shrinking of the self-sustained combustion region, which due to the increased heat losses through the reactor solid structure. However, thermally coupled combustion-decomposition catalytic micro reactors exhibit different thermal behaviors because of the thermal coupling between endothermic and exothermic reactions (Chen et al., 2016; Deutschmann et. al., 2000; Karagiannidis et. al., 2011; Platinum & Catalytic, 2016; Reinke et. al., 2005).

Reported by Simsek et. al., (2011), studies addressing the intensification of flow paths have led to the design and analysis of microchannel reactors. These miniature devices involve parallel, identical channels with characteristic dimensions between $\sim 10^{-6}$ and 10^{-3}m and laminar flow conditions. They are constructed mostly using metallic substrates to give surface areas in the 1×10^{4} to 5×10^{4} m^2/m^3 range, which are 50–100 times higher than those of conventional packed bed counterparts.

Presence of high surface areas, sub-millimeter dimensions and use of metallic materials favor rapid and uniform distribution of heat to the entire catalyst.

2.3.2 Type of Micro Channel

The micro channel reactor is a device that has a microstructure, with dimensions at μm and domain reaction occurs continuously. Packed bed micro reactor catalyst particles requires very smaller form factor than the size of the internal micro channel. A problem often encountered by the commercial catalyst and most of the micro channel reactor is using a coated catalyst as a coating. Many studies have been done to explore the advantages of the micro channel reactor to produce hydrogen through steam reforming of methane. A micro channel reactor, which is targeting an optimum conversion and selectivity at low cost and its affected by the flow, velocity profiles, pressure drop and temperature transfer. The design, coil based micro channel reactor, as in Figure 2.5 allows high conversion, but very limited for complex solid applications. In other words, the design rectilinear channel displays a small pressure drop, but conversion is low due to the uneven distribution of mass and influenced by the Reynolds number (Hwang et. al., 2007; Karim et. al., 2005; Morris, 2016).

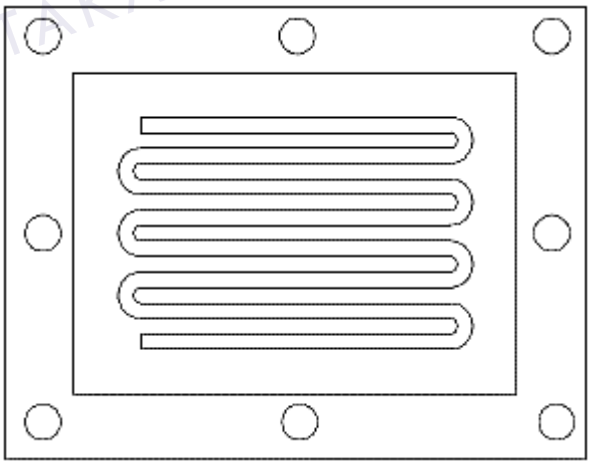

Figure 2.5 : Coil based (Morris, 2016).

Design pinhole as in Figure 2.6, has great potential for innovative applications. It shows the conversion of methane comparable to coil based micro reactor with a lower pressure drop. This design, however, shows the distribution of mass depends on the Reynolds number (Morris, 2016).

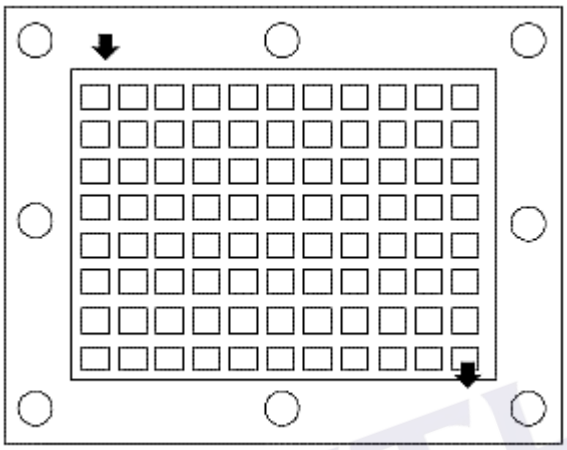

Figure 2.6 : Pinhole based (Morris, 2016).

Design radial as in Figure 2.7, has a unique design for the steam reforming of methane due to increased area for gas moving to the outlet, which leads to a lower pressure drop compared with a tubular reactor and nearly constant velocity profile (Morris, 2016).

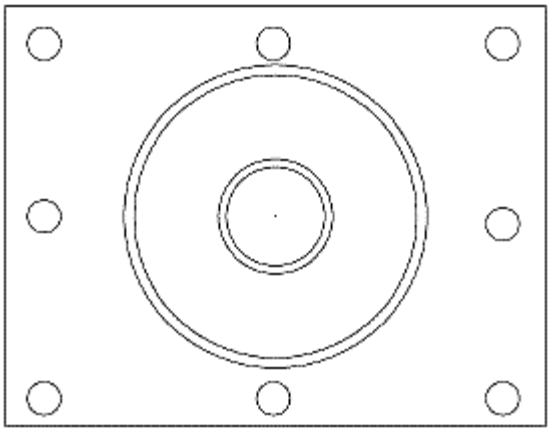

Figure 2.7 : Radial based (Morris, 2016).

2.3.3 Microstructure: Scale Up to Commercial Capacity

The micro channel reactor technology offers the promise of practical process intensification technology for the chemical industry. Capitalizing on the micro channel technology gives a few advantages such as demonstrating a scalable technology, that produces tens to hundreds of tons of product per annum. The transition from lab-scale to industrial-scale chemical processing is demonstrated. Scale-up issues, such as quantifying flow distribution and options to reduce non-uniformity are further discussed and explore. The approaches described in these excellent references however are challenging to mass manufacture as required for cost-effective commercial application (Tonkovich et al., 2005, 2007). Unfortunately, this scale up profile matter is lacked of literature. Therefore, a preliminary study at lab scale need to be done and conducted in order to accumulate related information. With the traits of changeable catalyst for the micro channel reactor lead to the at most bonuses to collect a lot of information, especially the critical parameter such reaction temperature and steam to carbon ratio. For multifunctional micro reactors, important operating principles are listed as below (Chen et al., 2016; Deutschmann et al., 2000; Haynes & Johnston, 2011; Karagiannidis et al., 2011; Platinum & Catalytic, 2016; Reinke et al., 2005) :

i. Reactant methane breakthrough: The breakthrough limit is defined herein as the flow velocity at which 99% methane conversion is achieved for complete fuel conversion in the combustion channel. For reactant flow velocities higher than the breakthrough limit, it requires more energy flux than available from the combustible stream, resulting in the incomplete methane conversion. Conversely, for reactant flow velocities lower than the breakthrough limit, the amount of combustible mixture always suffices for the complete methane conversion, but the reactor temperature becomes high and some of the combustible mixture is wasted. It is noted that this operating line is an excellent design target.

ii. Material stability: A maximum wall temperature of 1500 K is selected as a reasonable limit for stability of the reactor structural material and catalyst. That is, catalyst and wall temperatures in excess of this limit value are deemed detrimental to the reactor, although this value is chosen rather

arbitrarily. This temperature threshold is typically employed in short contact time high-temperature reactors, and it is normally termed as material stability limit. It is noted that the melting point of catalyst used should be higher respectively. The material stability determines the lower power limit for a given combustible mixture flow velocity, resulting from the high temperatures generated at low reactants flow velocities.

iii. Self-sustained operation: The self-sustained operation is determined by the extinction (i.e., the loss of reactor stability) in the combustion channel at high methane flow velocities.

iv. Maximum power output: The maximum power output corresponds to the maximum hydrogen yield, which is in the incomplete methane conversion region. This operating line is determined from the methane conversion and the combustible mixture flow velocity, caused by the trade-off between higher flow velocity and lower methane conversion.

The gap size can significantly affect transverse transport rates, pressure drop, and temperatures, along with all its effects on hot spots, reaction rates, and catalyst life time. The wall plays two roles in the thermal management of the thermally coupled combustion decomposition catalytic micro reactors, the axial heat recirculation and the heat transfer between the two channels (Chen et al., 2016; Deutschmann et al., 2000; Karagiannidis et al., 2011; Platinum & Catalytic, 2016; Reinke et al., 2005).

2.4 Catalyst in Steam Methane Reforming

Catalytic steam reforming of methane involves the reaction of methane with steam over a catalyst at elevated temperatures (400°C to 900°C) and pressures (1 to 30 bars). This catalyst functionally acts as the active site for reactant conversion. The parameter of conversion is proportional to the type and kinetic reaction of certain catalyst. In order to obtain acceptable reaction rates, a catalyst is required to accelerate the process through reducing of activation energy. Furthermore, the catalyst should be stable under extreme conditions especially during high CH_4 conversions (i.e., high temperatures and high probabilities of unwanted side reactions involving carbon deposition) (Bej et al., 2013; Roh et. al., 2012; J. Xu et al., 2008; Zhai et al., 2011).

The higher catalyst surface active area, lead to the greatest number of product molecules produced per unit time. It is reported that, dominantly the art and science of catalyst preparation deals with high surface area materials (typically 100 to 400 m^2/g). These are prepared in such a way of crystalline with well-defined microstructures and behave as an active component of the catalyst system in spite of accepted name supports. The (transition) metal atoms are then deposited in the micro pores, the sample is subsequently heated and reduced to produce small metal particles; ideally 10 to 102 Å in size with virtually all the atoms located on the surface (i.e., unit dispersion[2]) (Hou & Hughes, 2001; Rajagopal, 2007; Sciazko et al., 2014; Yang et. al., 2014).

In non-catalytic reforming, the production of syngas is dependent on the steam to carbon ratios at operating temperature of 1200°C to 1500°C without a catalyst. Therefore, in order to counter this drawback, a catalytic reforming approach had been rapidly growing among researcher and chemical plant provider. It's proven that, the catalyst approach in the production of syngas and hydrogen successfully manages to reduce the desires reaction temperature as lower from 600°C till 900°C (Gangadharan et al., 2012; J. a Liu, 2006; Rajagopal, 2007).

2.4.1 Nickel Catalyst

Nickel (Ni) catalysts have been widely used for hydrogen production. However, a disadvantage of these catalyst is the formation of methane due to the chemical reaction between product gases, hydrogen and carbon monoxide. This will reduce the efficiency of hydrogen production. Therefore, it is essential to develop better catalysts without causing methanation (Doma et al., 2016; Kim et al., 2005; Sulka & Jó, 2011; Y. Xu et al., 2005; Yamada, 2006).

A major challenge is that Ni catalysts have a high thermodynamic potential for coke formation during reforming reactions. Several methods have been discussed to synthesize coke resistant Ni catalysts. An alternative method is proposed by using structured catalyst supports such as foams and monoliths, generally ceramic-based, for the beneficial effects of low-pressure drop and high catalyst utilization efficiency in

SMR reaction. Whereas, the low thermal conductivity still limits the overall performance of the reactor (Cheng et al., 2011).

Nickel-based catalysts are widely studied for steam methane reforming (SMR). In particular, Nickle support alumina oxide (Ni/Al_2O_3) is considered as a promising catalyst for SMR due to its low cost and high catalytic activity. The present work is concerned about the steam reforming of methane over a nickel based catalyst. The catalytic activity of Ni/Al_2O_3 is closely related to both nickel content and nickel dispersion, but the effects of these two factors on the catalytic activity are contradictory. While the catalytic activity of Ni/Al_2O_3 increases with nickel content due to increased number of active nickel sites, the nickel dispersion decreases as nickel content increase due to the aggregation of nickel, thereby decreasing the catalytic activity. In general, nickel content of conventional Ni/Al_2O_3 catalysts used in steam reforming does not exceed 12 wt% to avoid severe aggregation or sintering of nickel particles during the reaction. The catalyst loading 10wt% of Nickel, has been proven as the most optimum catalyst impregnation on substrate plat via dip coating method (Bej et al., 2013; Madon et. al., 2016; K. I. Sarwani et al., 2016; M. K. I. Sarwani, 2017). However, this Ni/Al_2O_3 catalyst stability is declining with the increasing of reaction temperature, which lead to carbon formation and active area coking (Bej et al., 2013; Maluf & Assaf, 2009; Monzon et al., 2006; Radfarnia & Iliuta, 2014; Salhi et al., 2011; Zhang et. al., 2017).

Beside the utilization of Ni/Al_2O_3, some intermetallic compounds are known to have good catalytic selectivity and activity. For example, Ni_3Sn increases the selectivity for hydrogen production, and PtGe and CoGe do for hydrogenation and dehydrogenation. In Ni–Al system, intermetallic compounds of Nickel aluminide (Ni_3Al : Ni–50 wt% Al) is used as a precursor alloy for Raney nickel catalysts. This Raney nickel catalysts are produced from the precursor alloy by leaching aluminum in a concentrated NaOH solution. For this Ni_3Al, very limited studies have been carried out on the catalytic properties. Probably, it has been thought difficult to effectively leach aluminum from them because of their low aluminum concentration, and thus high catalytic activity has not been expected, particularly for Ni_3Al. Until now, Ni_3Al has been known as promising high- temperature structural materials because of its excellent high temperature strength and corrosion/oxidation resistance, thus, many

studies have been focused on the mechanical properties and the microstructures (Fabas et al., 2017; Kim et al., 2005; Saadi et al., 2011; M. K. I. Sarwani, 2017; Sulka & Jó, 2011; Y. Xu et al., 2005).

Utilization of carbon dioxide into methane reforming can lead to carbon deposition and subsequently to catalyst deactivation. However, catalyst stability test performed in the present study revealed that stable activity of the catalysts could be maintained for over 20 hours for the Ni–Al system catalysts, under appropriate experimental conditions. But this Ni–Al system catalysts, capable to become stable in a shorter reaction time, therefore, stable time operation is suited to be controlled at first 5 hours. The assumption of carbon deposition is negligible, to be adopted here, in order to develop a theoretical model for describing a steady-state operation of the experimental reactor, at least during the initial stages of methane reforming (Charisiou et al., 2016; Pudukudy & Yaakob, 2015; Pudukudy, Yaakob, & Akmal, 2015).

2.4.2 Noble Metal Catalyst

The activity of a catalyst is related to the metal surface area (i.e., the number of active sites). This implies that, generally, the catalytic activity benefits from a high dispersion of the metal particles. Common dispersions for Ni catalysts is variable from 2 to 15%, with metal particles of 20–50 nm. There is an optimum beyond which an increase in Ni-content does not produce any increase in activity, usually around 15–20 wt% (depending on support structure and surface). Although the nickel surface area is generally increased with higher loadings, the dispersion or utilization of the nickel tends to decrease with increasing nickel content. Hence, the activity will not increase any further (Bej et al., 2013).

Apart from the amount of available metal surface area, also the structure of the available surface area also has a significant influences on the catalyst activity. For instance, the close-packed surface of nickel is less active than the more open surface. For instance, it is known that Ni particles are composed of a number of single crystals (i.e., the metal particles are polycrystalline), which are not completely 'space filling'.

Therefore, some lattice distortion is required and these dislocations are expected to play a role in the catalytic reaction (Bej et al., 2013).

The activity per unit metal surface area (the specific activity) decreases with increasing dispersion (i.e., with smaller metal crystal size). This effect may be explained by a decrease of large ensemble landing sites on the smaller particles (i.e., an entropy-effect). Alternatively, it may be explained in terms of a change in electronic state of the metal particles showed for Rh-based catalysts, that a higher dispersion may result in a less metallic and hence less reactive character of the Rh particles. However, the causes of these discrepancies remain unclear. The synergism between different metals has also been investigated. For instance, Rh promoted $NiAl_2O_3$ is found to possess higher activity than either $NiAl_2O_3$ catalysts in the methane reforming with CO_2. In this case, Rh improved the dispersion of Ni, retarded the sintering of Ni, and increased the activation of CO_2 and CH_4 (Bej et al., 2013; Schädel et. al., 2009; Zeppieri et al., 2010).

The precious noble metals such as rhodium Rh, ruthenium Ru based catalysts have been reported to be more effective catalysts for steam reforming by preventing the carbon deposition. Its have been proposed to replace conventional base metal for steam reforming in fuel cell applications. This Ruthenium and Rhodium supported by aluminide is a noble metal catalyst, which capable to enhance the SMR yield at multiple time greater than the conventional catalyst event at a small amount of loading (Beurden, 2004; Rajagopal, 2007; Stefanidis & Vlachos, 2010; Yang et al., 2014). The catalytic activity of catalysts with different loadings of Ru or Rh on alumina or aluminide supports specifically, found that CH_4 reforming turnover rates increases as the size of Rh and Ru clusters decreases, suggesting that coordinative unsaturated of Ru and Rh surface atoms prevalent in smaller clusters activate C–H bonds more effectively than atoms on lower-index surfaces (Bej et al., 2014; Schädel et al., 2009).

However, the fact that these noble metals are expensive and of limited availability makes the development of new supports and/or the addition of promoters or additives to improve the performance of catalysts based on nickel, which produces a challenge to the catalytic scientific community. The addition of metal additives into nickel-based catalysts could be relatively simple. Effective method to increase its

resistance of coking have proposed that the addition of molybdenum and tungsten into the nickel based catalyst will decrease carbon deposition, while entailing no change in catalyst activity. If these expensive materials have to be used often, the catalysts can be prepared in nanometer sized particles, supported on an inert, porous structure (Rajagopal, 2007; Yang et al., 2014). From Table 2.2 is showing the relative rate of catalyst conversion ability with correlative to the mass %. It is highlighted that Rh managed to achieve 27 times greater rate compares to Ni, follows by Ru at 24 times greater. Hence, in this research, Ru and Rh are chosen as the best active metal catalyst. The validation will be done by using the fabricated test rig and micro channel reactor.

Table 2.2 : Relative activities for SMR at operating condition of 550°C, S/C: 4, and 1 bar (Beurden, 2004).

Catalyst metal content (wt%)	Relative rate
Ni (16)	1.0
Ru (1.4)	2.1
Rh (1.2)	1.9
Pd (1.2)	0.4
Ir (0.9)	1.1
Pt (0.9)	0.5

2.4.3 Catalyst Deposition

In practice, different catalyst preparation methods have been used to adjust the structure of supports. Consequently, physical and chemical properties of the catalysts are modified. The co-precipitation and impregnation methods are described in detail below since these two methods are used to prepare the catalysts for this work (Yang et al., 2014).

i. Co-precipitation:- In this method of preparation, the catalytically active component and the support give a mixture that is subsequently dried and calcined, thus, reduced to yield porous materials with high surface area. Solutions of salts of these two components are prepared and a precipitating

agent such as Na_2CO_3 and/or NaOH is added to the solutions. This gives carbonates and/or hydroxide precipitate and form a homogeneous mixture, that is filtered off. A porous catalyst could be obtained by removing CO_2 and water during drying and calcination, by removing oxygen during reduction. The process is difficult to control since the solution should be kept homogeneous to allow the two components to precipitate simultaneously, thus variation of pH throughout the solution should be avoided.

ii. Impregnation: - Involves filling the pores of the support with the solution of the catalytically active element, then drying it and converting it into an active form. On the other hand, various interactions are possible between the dissolved catalyst precursor and the surface of the support in this process; which can be used to obtain a good dispersion of the active component over the support. Silica and alumina supports contain several types of hydroxyl groups, which play a very important role in catalyst preparation. Its represent anchoring sites where catalysts precursors can be attached to the support. This simple method has one disadvantage in that migration of the solution to the external surface takes place during the drying. Thus leaving some of the internal surface uncovered.

2.4.4 Rate of Reaction

There are various forms of kinetic rate expressions for a chemical reaction. In the current study, the Langmuir–Hinshelwood model is chosen for the reaction of the complete oxidation of methane. The rate expressions for steam reforming and water gas shift reactions) are based on the analysis (Hoang et al., 2005; Hou & Hughes, 2001).

The physical interpretation, Langmuir's model is employed for the adsorption of a gas on a solid catalyst. From Figure 2.8 had shown that the light gray area is representing the surface of the catalyst. Meanwhile the black dots on the site are the catalyst which available to adsorb gas. Next to the white ovals are the adsorbed of

steam molecule and lastly for the pink ovals are the adsorbed methane molecule. The adsorbed molecule is undergoing reaction of steam and methane cracking to produce hydrogen (H^+) atom. This hydrogen atom (H^+) desorbed from the catalyst active site and merge among the other atom to form hydrogen (H_2) gas molecule. The equation involve for determination of methane conversion, SMR's yield and rate of reaction (methane disappearing rate) will be further explained in subchapter 3.7.3 in Chapter 3. Reported by Charisiou et al., (2016), in order to examine the reproducibility of all experimental results, a 95% confidence interval of the mean value is analyzed for at least three time repetition works.

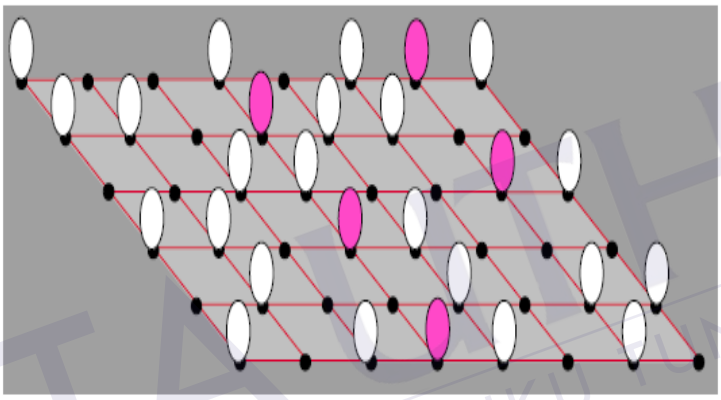

Figure 2.8 : Physical interpretation of Langmuir-Hinshelwood model (Hou & Hughes, 2001).

2.4.5 Catalyst in Micro Channel Reactor

Syngas production from methane in micro channel or structured reactor geometries has been rapidly investigated. Studies that exploit the differences of micro channel reactors with conventional packed counterparts are scarce. The comparison of steam methane reforming in a packed bed reactor and an engineered micro channel reactor made by metal based felt inserts of specific dimensions using the same catalyst and it is reported that the latter led to higher methane conversions and CO selectivity's (Simsek et al., 2011, 2013).

Reported by Simsek et. al., (2011), SMR studied in micro channel is mainly composed of wall-coated and packed bed reactor for catalyst deposition. The wall-

coated configuration is free from any transport limitation, meanwhile the packed bed reactor operation is limited by heat transfer, thus influence the methane conversion and SMR's yield properties. It is proved that, the wall-coated reactor configurations minimize transport resistances, thus, provide uniform temperature distribution in the catalyst layer. Therefore, methane conversion rates, H_2 and CO production rates, reached in coated micro channels are much higher than those in packed micro channels under the reaction conditions covered for all catalysts.

2.5 Conversion Platform

A feasibility study regarding general unit operation involves inside steam methane reforming is shown as in Figure 2.9. This process flow diagram (PFD) is at most been used and accepted technologies for SMR. Hence this PFD will become the trademark as a basis SMR conversion platform (Holladay et al., 2009; Madon et al., 2015; Mbodji et. al., 2014; Seris E.L.C, 2006). The feed reactant is flowing into mixer to produce homogenous reactant as pretreatment stage. Then it flows into reformer, high and low temperature shift for reactant conversion as upstream stage. The process then follows by a condenser and pressure swing absorber as downstream stage.

Steam to carbon ratio (S:C) is defined as the ratio of the number of moles of steam to that of methane at the inlet. As it works as a catalyst, the steam to carbon ratio is affecting the SMR yield either highly product conversion or lowest carbon formation. Accordingly, to the review, the methane conversion is proportional to the ratio, and the optimum condition laid on steam to carbon ratio of 3. Typically, the mass ratio of steam- to-carbon is about 3 or more to avoid "coking" or carbon build-up on the catalysts. At lower steam-to-carbon ratios, solid carbon can be produced via side reactions (Bej et al., 2013; Beurden, 2004; Graf et al., 2007; Radfarnia & Iliuta, 2014; Simsek et al., 2011; F. Wang et al., 2013; H. Wang et al., 2012). Therefore, in order to eliminate the coke formation, the steam to carbon ratio is kept above stoichiometry for SMR over Ni at a range between 2.5 and 3.5. For this study, the steam to carbon ratio initially is fixed at 3 because it is already reported that proven to yield optimum condition (Eduardo et al., 2009; Gangadharan et al., 2012; Graf et al., 2007; Holladay et al., 2009; Maluf & Assaf, 2009; Moghtaderi, 2007; Radfarnia & Iliuta, 2014; Simsek

et.al.,, 2011; Simsek et al., 2013; A. L. Y. Tonkovich et al., 2007; a. Y. Tonkovich et al., 2004; Udengaard, 2004; F. Wang et al., 2013).

Meanwhile for the catalyst loading 10wt% of Nickel aluminide, it has been proven as the most optimum catalyst impregnation on substrate plat via at most method of dip coating method (Bej et al., 2013; Madon et. al., 2016; K. I. Sarwani et al., 2016; Sarwani, 2017). According to the previous researcher works, the working catalyst will show stability less than 500 minutes. (Bej et al., 2013; Maluf & Assaf, 2009; Pudukudy & Yaakob, 2015; Pudukudy et al., 2015).

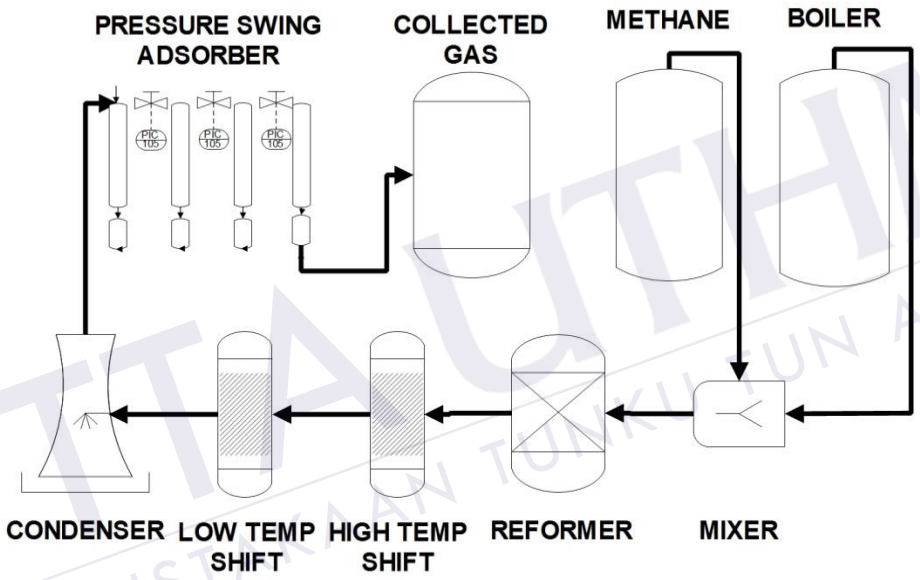

Figure 2.9 : General steam methane reforming (SMR) process flow diagram (PFD) (Madon et al., 2015).

Currently, the chemical plant growth rapidly becomes larger. However, due to the reduction of economies of scale, the capital component, especially of the unit costs within production, indutries switch to centralize it to share a site zoning and utilities such as power, steam, and cooling water. These factors have led to an inexorable growth in the size and concentration of chemical plant, with globalization and international trade working to penalize sub-‘world scale’ production (Aloisi et al., 2017; Dupont et. al., 2008; Kuba et. al., 2016; Madon et al., 2015; Marshall, 2002; Martin et. al., 2015; Mamadou Mbodji et al., 2014; Molburg & Doctor, 2003; Nexant Inc., 2006; Ogden, 2001; Seris E.L.C, 2006; Y. Wang, 2005).

The potential advantages of distributed chemicals manufacture in smaller on-site, or regional facilities have long been recognized. It is not only could such a plant be cheaper to build (as the economy of scale is shifted from the chemical product in the production of the plants themselves), it would also offer the improvement in safety (both in the process and in the bulk storage and trans- port of chemical products), and better reliability and continuity of supply. At the moment, risk of terrorist assaults can be reduced on major hazardous facilities as a further driver for distributed manufacture. Hence this motivation had lead to the successfulness of this project (Barelli et. al., 2008; Seris E.L.C, 2006; Smith, 2005).

Currently, advanced manufacturing techniques are needed in order to produce the basic plant modules in large numbers. Such a different scale of operation can be achieved by simply increasing the number of systems rather than through custom designs for each application in the limit, one could go from bench-scale to industrial scale in a single step. This scaling by 'numbering up' the systems further allows capital investment and market growth to be coupled, thus further reducing the financial risk of building large new facilities. Furthermore, mini plants cannot be developed simply by implementing existing processes on a minute scale: The new process designs are needed in order to ensure it complies to the increasing demands for energy efficiency and environmental performance, thus, these new designs must especially show significant improvements in these areas, relative to existing practice (Kook et. al., 2013; Seris E.L.C, 2006; Vidal Vázquez et. al., 2016).

2.5.1 Route of Process System

Advanced manufacturing techniques are needed to produce the basic plant modules in large numbers. Different scales of operation can then be achieved by simply increasing the number of systems rather than through custom designs for each application in the limit, one could go from bench-scale to industrial scale in a single step. Scaling by 'numbering up' the systems further allows capital investment and market growth to be coupled, thus further reducing the financial risk of building large new facilities. Mini

plants cannot be developed simply by implementing existing processes on a minute scale; new process designs are needed. In keeping with increasing demands for energy efficiency and environmental performance, these new designs must especially show significant improvements in these areas, relative to existing practice (Marshall, 2002; Mamadou Mbodji et al., 2014; Nexant Inc., 2006; Ogden, 2001; Seongho Park et al., 2016; Seris E.L.C, 2006; Silversand, 2003; Y. Wang, 2005).

In recent years there has been a growing interest in developing microsytem technology by employing characteristic length scales in the range $10 to $1000 per mm for chemical processing. The main focus has been concentrate on repetitive synthetic and analytical chemistry, but the development of micro reactors for bulk chemical manufacturing systems is also attracting interest. While many examples of highly miniaturized components have been described in previous work, but there are very few demonstrations of integrated micro-process plants of practical significance (Butcher et al., 2014; Cheng et al., 2011; Ogden, 2001; Silversand, 2003; a. Tonkovich et al., 2005)

2.5.2 Process Overview

For the present application of SMR plant, it is scaled to produce hydrogen to fuel a notional around 15 kWe PEM fuel cell. This syngas sequent is used for further processing, in example, to produce methanol, ammonia, or Fisher- Tropsch liquids. Indeed, currently development of such processes is integrated with the syngas production. From Figure 2.10, shown that, the plant is composed of four major modules:

i. pre-reforming module including the high temperature shift reactor
ii. reforming and combustion module
iii. low temperature shift reactor
iv. steam drum

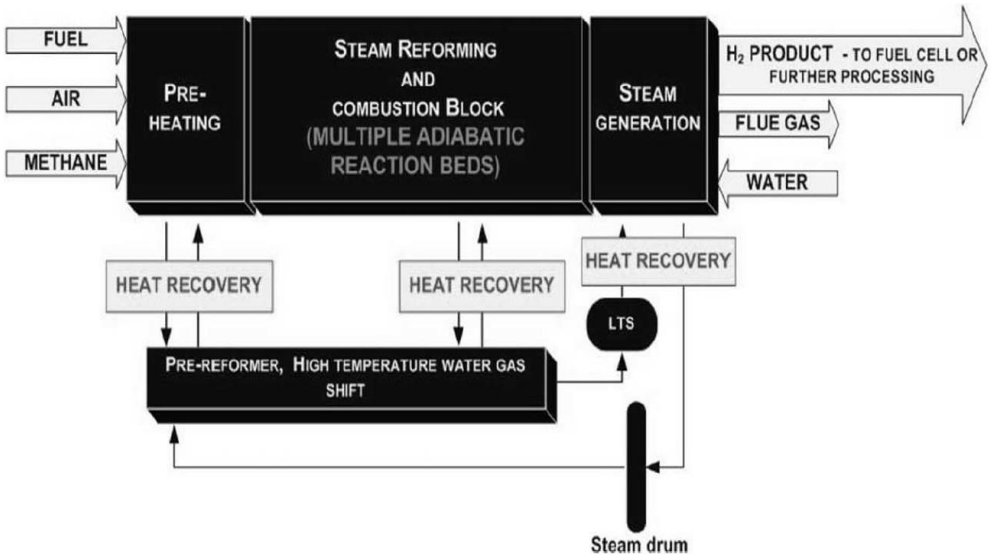

Figure 2.10 : SMR Process overview (Seris E.L.C, 2006).

The only heat input to the process is provided by the catalytic combustion reactions in the reforming and combustion module. A highly complex network distributes the heat to the other parts of the process (pre-reformer module, steam generation, pre-heat of the reactants). The CO is oxidized to become CO_2 in the high and low temperature water gas shift reactors. The selective oxidation is not considered because of its low impact on the heat integration. However, this would be needed for implementation as a fuel processor for a PEM cell (Kuba et al., 2016; Marshall, 2002; Ogden, 2001; Seris E.L.C, 2006; Silversand, 2003; Türks et. al., 2017).

2.5.3 Micro Plant Design Basis

The basic design of steam methane reforming pilot plant, especially at the micro scale, is taken to fulfill certain conditions in order to yield optimum production. Previous work has been highlighted that, there is a demanding of combination between oxidizing, carburizing and dusting conditions in the reformer and heat recovery system. Basically, the pilot plant is conceived as a short-term process testing facility by using relatively low temperatures (<815^{o}C) and low pressures (about 2 bars), for which austenitic stainless steel provides an acceptable of construction. At the beginning, most of the earlier prototype has shown corrosion after running a few hours of operation. Therefore, a lot of various approaches for extending component lives

spent had been investigated. It is very important for relative cost effectiveness, including the use of high nickel alloys, aluminide coatings and process re-design to eliminate the most aggressive dusting conditions (Dupont et al., 2008; Madon et al., 2015; Marshall, 2002; Ogden, 2001; Silversand, 2003, Kuba et al., 2016; Marshall, 2002; Ogden, 2001; Seris E.L.C, 2006; Silversand, 2003; Türks et. al., 2017). A few assumptions are revealed for basic design of small scale micro reactor plant, such as:

i. Stand-alone system which manage to reduce the scope of export-import steam (heat rejection or sink out).
ii. Simple, robust control required no more complex than for industrial.
iii. High efficiency, compact and robust, for ease of transport and installation.
iv. Suited for low-cost manufacture.
v. Sulphur-free methane feed.
vi. Ease of catalyst deployment in the reactors (crushed catalyst pellets or monolith and coating impregnation).
vii. Conservative design with respect to carbon formation. The temperature of the reforming stages is gradually increased throughout the process to avoid coking.
viii. Material of construction: austenitic stainless steel for testing purposes.
ix. Easy scale up by multiplication. The size of the local plant can be matched to the local demand in a single step.
x. For micro reactor basis design should consists a few basic principles such below:

    a) The width of the reaction channel is significantly larger than the height

    b) The flow in the reaction channel is laminar

    c) Steady-state operation of the reactor has been reached

    d) Gas-mixture can be treated as incompressible ideal gas (the density of the mixture can be calculated from ideal gas law)

    e) Gas phase non-catalytic reaction can be neglected

    f) The porous catalytic wash coat is isotropic and in local thermal equilibrium with the gas mixture.

2.5.4 Development of Conceptual Design

Basically, this project has been divided into three major phases. The first phase covers the design, fabrication, development and commissioning of steam methane reforming test rig bench system. Phase 1 was focused on the design, development and commissioning of SMR test rig bench with considerations of catalyst evaluations. This covers several unit steps of the process such as below:

i. Development of Process Flow Diagram (PFD) and Process & Instrumentation Diagram (P&ID).
ii. Fabrication of major unit operation such as saturated steam generator, reformer, condenser, liquid/gas separator, dryer and a purifier.
iii. Assembly of all units in item (ii) and trial run for cold and hot commissioning.
iv. Safety precaution, reliable and repeatable of SMR's test rig operation method via Standard Operating Procedure.

Thus, in parliamentary procedure to execute this phase, a control strategy was developed and discussed. This phase covers basic builds up test rig from level 1 until 4 of chemical conceptual process design systems as reported by Douglas, (1988) and Seider et al., (2003), as listed below:

i. Level 1 (process selection)
ii. Level 2 (chemical synthesis)
iii. Level 3 (recycle stream)
iv. Level 4 (chemical separation).

The Figure 2.11 shows a conceptual design of flow analysis for the SMR route process. Each level has output goal to be achieved. Thus, the main outcome of the analysis is development of PFD and P&ID as the core blue print in SMR test rig bench workout and project phase.

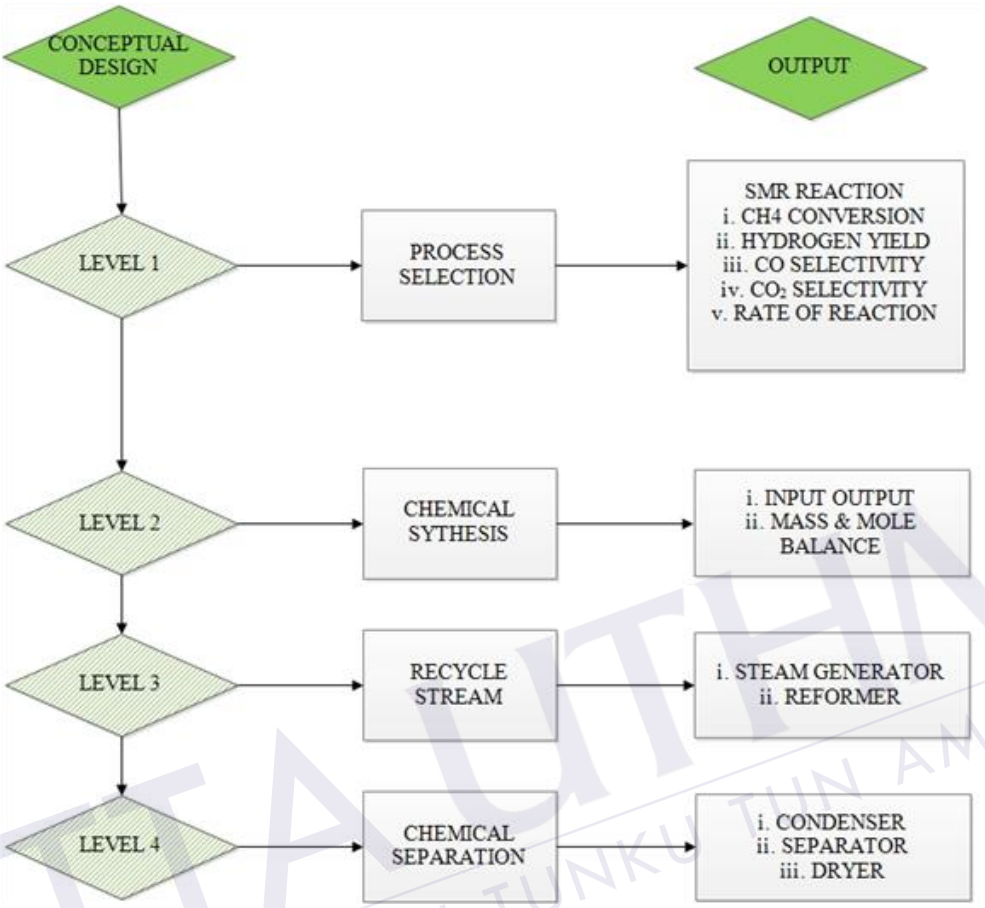

Figure 2.11 : Conceptual design flow analysis of a chemical process.

2.5.4.1 Conceptual Design Level 1 – Process Selection Overview

The catalytic steam reforming of methane involves the reaction of methane with steam over a catalyst at elevated temperatures of 400 to 900°C and operating pressures of 1 to 30 atm (Bej et al., 2013). Generally, the steam methane reforming is endothermic and required external heat input. The reactant feed of steam and methane has been run through a catalyst for conversion syngas purposed as in Equation 2.9. After the complete reforming stage, the resulting syngas has been sent to one shifter reactor, where the hydrogen output is increased via water gas shift reaction as in Equation 2.10 which converts the CO to H_2. The resulting of this two-main equation is H_2, CO, CO_2 and unreacted of CH_4 and Steam. Further details about the process of methane cracking to produce hydrogen and carbon is shown as in Equation 2.11. Beside those main

equations, there is also another consequence potential reaction which is carbon formation as in Equation 2.12. It is noted that the carbon formation had decreased catalyst activities.

Steam methane reforming: $CH_4 + H_2O \leftrightarrow CO + 3H_2$ (2.9)

Water gas shift: $CO + H_2O \leftrightarrow CO_2 + H_2$ (2.10)

Methane cracking: $CH_4 \leftrightarrow C + 2H_2$ (2.11)

Soot formation: $2CO \leftrightarrow C + CO_2$ (2.12)

2.5.4.2 Conceptual Design Level 2 –Chemical Synthesis

The second level of the process design involves defining the input and output structure of the process and deciding if the process requires recycle of the gaseous reactant. Once the input-output structure has been determined, the material balance of each component is being developed for mole balance of flow reactors. The Figure 2.12 shows the input-output schematic diagram. The process and instrumentation diagram has been setup according to the three main stage. The first phase is pretreatment stage, follow by the second stage of upstream stage and lastly downstream stage as the phase three.

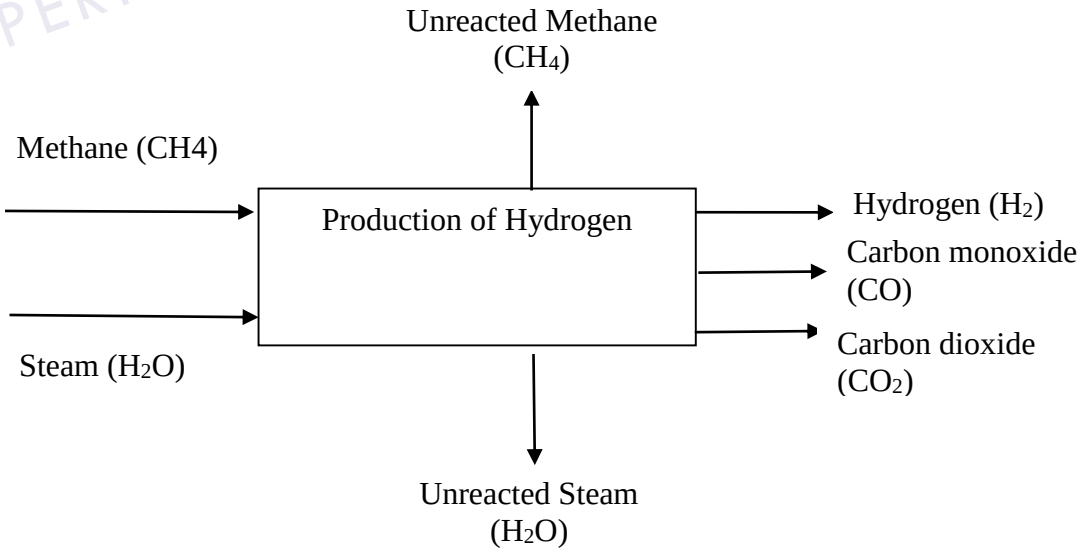

Figure 2.12 : Input-output of Steam Methane Reforming process.

2.5.4.3 Conceptual Design Level 3- Recycle Stream

In this stage, the components which involved phase or reactant changes have been defined and analyzed, such as steam generator, superheated steam converter and reformer properties.

i. For the steam generator system, fresh distilled water has been pumped into stainless steel coil inside hot oil bath tank. Here, the distilled water was converted to saturated steam. Hence, the steam generator systems have been designed, fabricated and develop according to the desired steam mass flow rate (gram/seconds).
ii. For the superheated steam converter, it is a system where mixture of steam and methane passed before entering micro reactor. The saturated steam is converted to superheated phase by supplying high energy transfer.
iii. For the reformed system, an assortment of steam and methane is flew into stainless steel tubing through a micro scale reformer, which is known as micro reactor. This micro reactor has been designed, fabricated and developed based on the catalyst plat type, which consists of an insert module slot.

2.5.4.4 Conceptual Design Level 4 – Chemical Separation

The next level of the conceptual design involves defining the chemical separation system. This system is required to perform the separation of the materials produced from the reactor i.e. product, by-product, waste. The typical separation process considers either liquid, two phase mixtures or all vapor separations by using a distinctive technique or method. This method specifically applies after all the reactant pass through micro channel reactor for conversion process. The output of steam methane reforming and water gas shift reaction, the reactant is converted to two main components including liquid (water) and gasses (hydrogen, carbon dioxide, carbon monoxide and unreacted methane). Water is removed through the use of a Separator vessel unit. As additional, the moisture is fully removed by using Dryer unit at

reformate gas stream. In general, the process of producing hydrogen from SMR involves the below separation system:

i. Condenser –to cool down the reformate gas stream after micro channel reactor in order to ensure unreacted steam is condensed to liquid phase.
ii. Separator – to remove soot and water from a reformate gas stream
iii. Dryer – to eliminate all moisture content inside the reformate gas stream

Meanwhile, the micro channel reactor has been built and evaluated during Phase 2 of the project. Some changes are carried out into the P&ID-schematic diagram and the complete system were assembled, commissioned and evaluated through an experiment. The objective of Phase 1 and 2 is to verify the design work performed according to the SMR theoretical and to suggest improvements concerning the catalysts, the reactors and system including the control strategy.

2.6 Gap Analysis Work Studies

From the Table 2.3, show that comparison of related works done by previous researchers. This comparison helps to define potential loop, especially in SMR through micro reactor at noble catalyst based. The results of simulation and experimental from works of previous researcher, highlighted that micro reactor geometry (width), noble catalyst deposition and reaction condition (operating temperature) are the most potential loop to be explored and depth review.

Meanwhile, from Figure 2.13, clearly shown the flow chart of gap analysis work for this project, whereby the novelty of the interchangeable catalyst reformer is further reviewed and discussed. In order to create a potential system for the production of rich hydrogen gas, there are three main literatures have been considered which are reforming technologies, conceptual plant design and lastly catalyst profile matter. From all literature, the gap has been defined accordingly to the project done from previous.

As the point of view from reforming technologies, literature has been considered once for each parameter, so that a micro scale reformer has been obtained a lot of opportunity to be explored due to limited access info. Almost all micro scale reformer done in literature is a one off used for each catalyst test. It is quite a lot of reformer are needed for SMR analysis. Therefore, an idea of interchangeable catalyst platform for a conversion test has led to a great novelty. Through this project, main outcomes are design, fabricate and develop a fix rigid micro scale reformer with an insert slot module for any catalyst test. Meanwhile, for the conceptual plant design, formulation, a gas conversion test rig which complies for any feed and reactor used, is managing to be defined according to the basic chemical process flow. Whereby, upstream stage is sequent to the micro scale reformer operating condition including catalyst impregnation method. According to the Table 2.3, the most suit novel deposition techniques is a substrate plate coating which is easily installed (slot-in) inside the interchangeable platform of micro reactor. This special concept of interchangeable micro scale reformer has not been deeply studied by any researcher, therefore, its lead to a bright future of novelties in contribution to knowledge due to it has a lot point of view to be explored and studied.

Table 2.3 : Comparison of related work done by previous researcher.

No.	Parameters	(Stefanidis & Vlachos, 2010)	Simsek et. al., (2011)	Simsek et. al., (2011)	(Cao et al., 2016)
1	Validation works	Simulation	Experimental	Experimental	Simulation
2	Catalyst deposition	Plate coating	Packed	Plate coating	Plate coating
3	Reaction temp	927°C	750°C	750°C	900°C
4	Steam to carbon	2	3	3	3
5	Catalyst (weight) (CH_4 conversion)	Rhodium (reaction kinetic time scale 1 seconds to 200µseconds) (97%) Nickel (reaction kinetic time scale 1 seconds to 1mseconds) (85%)	Nickel (10%) (23.9%) Ruthenium (2%) (18.2%) Rhodium (2%) (33.5%)	Nickel (10%) (53.9%) Ruthenium (2%) (37.6%) Rhodium (2%) (71.6%)	Nickel (15.2%) (88.5%)
6	Micro channel depth	200 µm	N.A	500 µm	800 µm

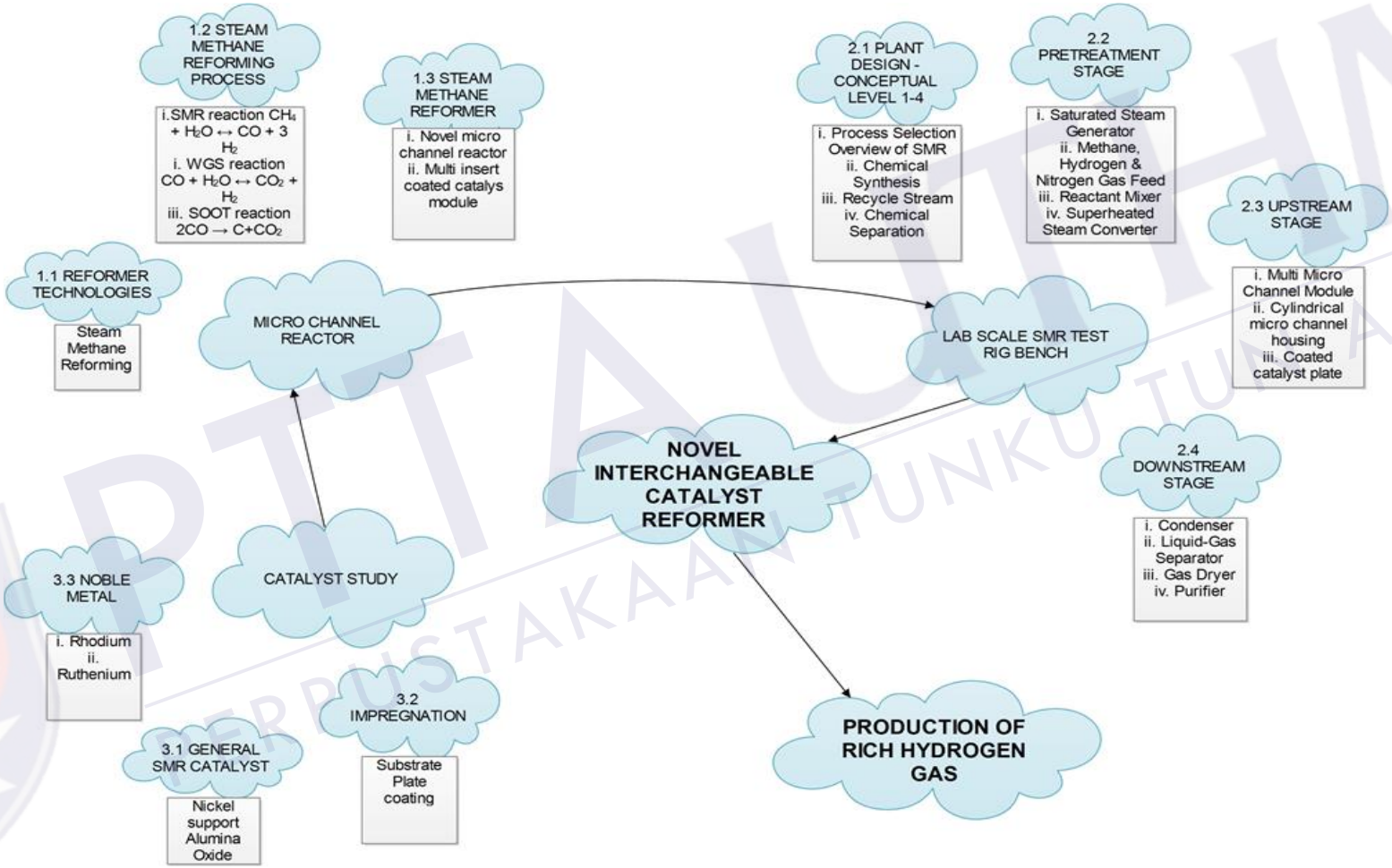

Figure 2.13 : Gap analysis works.

CHAPTER 3

METHODOLOGY

3.1 Introduction

The methodology generally is determined as a pathway process flow in order to identify process of a research project and implemented starting from the commencement of early stage until the last phase. It is ascertained that such project can be carried out smoothly, systematically and function properly according to design. This chapter identifies the method for conducting the whole experiment, which included material used and the design of experiments (DOE) set up. Figure 3.1 shows the whole procedure called for this entire experiment.

Basically, this project has been divided into three major phases. The first phase covers the design, fabrication, development and commissioning of steam methane reforming test rig bench system. For this study, further details of upstream or downstream operations such as gas compression, or syngas conversion to other products is less concern due to basic principle of plant design is highlighted that chemical synthesis must began from the main equation involve leads to the cogent evidence of a conceptual route (Douglas, 1988). The second phase is the stage to build up an interchangeable micro scale reformer. Lastly, for the third phase is the process to affirm and prove that correlation of first and second phase manages to generate the methane conversion accordingly to the theory based on material catalyst used. This new process design is needed in order to ensure it complies with the increasing demands for energy efficiency and environmental performance. Therefore, these new designs must show significant improvements in these areas, relative to existing practice.

3.2 Methodology Chart

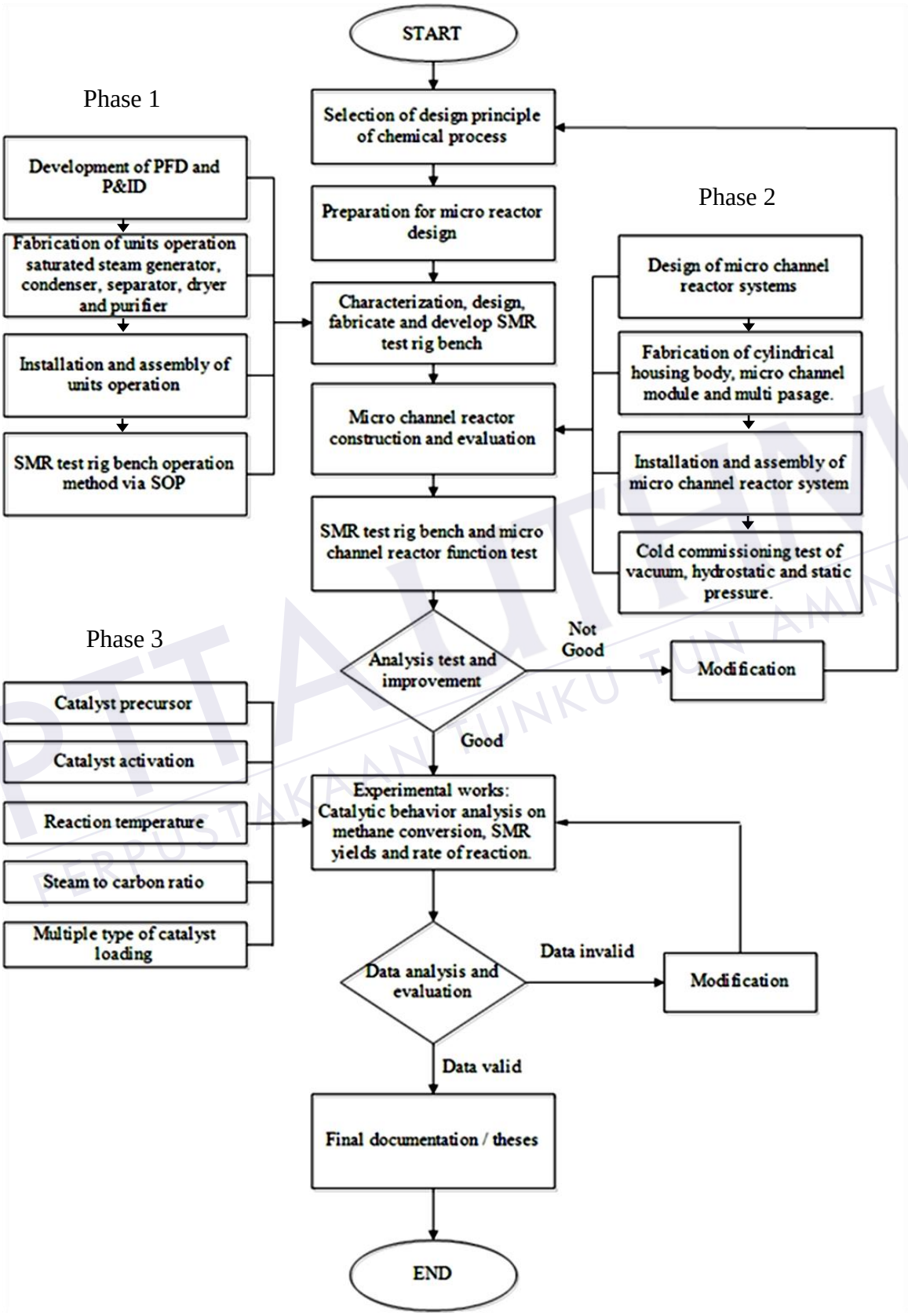

Figure 3.1: Methodology Flow Chart.

3.3 Conceptual Design of Mobile Steam Methane Reforming's Test Rig

Phase 1 of this project is the development of SMR test rig bench. This phase is focused on the design, development and commissioning of SMR test rig bench with considerations of catalyst evaluations. It included conceptual design stage, which the main target is to design, fabricate, build and evaluate a platform system for the novel micro reactor operation. This covers several unit steps of the process as below:

i. Development of Process Flow Diagram (PFD) and Process & Instrumentation Diagram (P&ID).
ii. Fabrication of major unit operation such as saturated steam generator, reformer, condenser, liquid/gas separator, dryer and a purifier.
iii. Assembly of all units in item (ii) and trial run for cold and hot commissioning.
iv. Safety precaution, reliable and repeatable of SMR's test rig operation method via Standard Operating Procedure.

3.3.1 Development of Process Flow Diagram (PFD) and Process & Instrumentation Diagram (P&ID)

Douglas (1988) highlighted that a chemical synthesis should begin from the main equation leads to the synthesis route. Thus, Equation 3.1 and 3.2, a basic process flow diagram (PFD) has been designed as in Figure 3.2. From Figure 3.2, the PFD is divided into three main sections which are pretreatment, upstream and downstream stage.

Steam methane reforming: $CH_4+H_2O\leftrightarrow CO+3H_2$ (3.1)

Water gas shift: $CH_4+H_2O\leftrightarrow CO+3H_2$ (3.2)

The pretreatment stage is covered reactant feed supply of steam and methane, reactant mixture point and preheating. This point is important since reactant is needed to prepare in order to fulfill the vital requirement before entering the upstream stage. In order to obtain superheated steam, the steam supply unit is developed to produce saturated steam as preparation inside superheated steam converter coils. This is also important to ascertain at the mixing point, as the saturated vapor mixture is ready.

Meanwhile, for the methane feed supply, it is already in the gas phase. Thus, at mixing point both feed reactants should already achieve gas phase and straightly lead to a well-mixed phase. Next, the mixed reactant undergoes superheated steam converter before entering the reformer.

The upstream stage consists of a reformer as the module to install catalyst for conversion process. Hereby, the reaction as in equation 3.1 and 3.2 took place. At this stage, the reformer was operated according to the reaction operating condition of reaction temperature at ranges from 500°C to 700°C, steam to carbon ratio of 2, 3 and 4, and multiple type of catalyst.

Side by side, the converted reactant, is pursued into the downstream stage. At this stage, the reaction yields are screened to ensure undesired products substance has been eliminated from the main products. The conversion of methane, product yield and undesired product selectivity is determined through a gas chromatography (GC) analysis, meanwhile a multi gas detector is used to specify the carbon monoxide conversion content in the undiluted outlet stream.

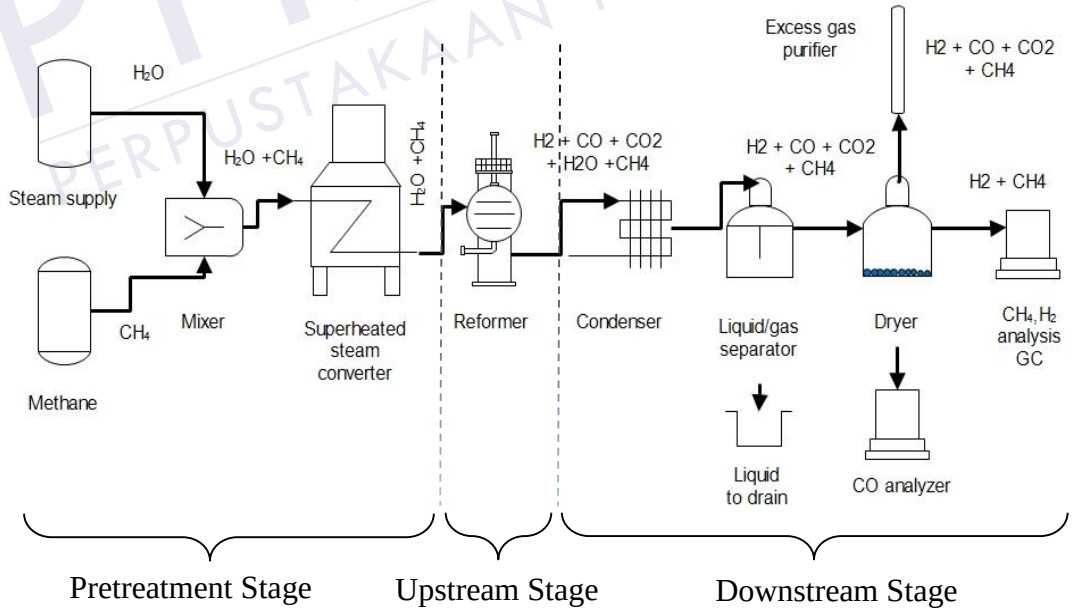

Figure 3.2 : Process flow diagram of steam methane reforming test bench.

The Process and Instrumentation Diagram (P&ID) contains more details and specific compare to the PFD. This P&ID is discussed more details for each stream and unit operation properties. Based in Figure 3.3, the P&ID of version 9 is classified more depth into three main stages, which developed with it own unit operation such as:

i. Pretreatment stage
    a. Saturated steam generator
    b. Reactants mixer
    c. Superheated steam converter

i. Upstream stage
    a. Micro reactor system

ii. Downstream stage
    a. Condenser
    b. Liquid/gas separator
    c. Dryer
    d. Purifier

3.3.2 P&ID Pretreatment Stage

The pretreatment stage consists reactant feed supply of steam and methane, reactant mixture point and superheated steam converter. Established in the Figure 3.4, the details process flow for this level as below:

i. The steam supply is created by the steam generator unit H-101. The distilled water is pumped by using a high pressure pump at working pressure 5.5 bar gauge into the heating coil inside the unit H-101. Essentially, there are two valves, called as V-101 and V-102 at the outlet pump P-101. The V-101 is functionally acted as return valve line and V-102 is for delivery valve. Both valve working principles are dependent on each other; it is implementing ‘open to closed’ and ‘closed to open’ simultaneously. It is essential to define the optimum opening degree for both valve, in parliamentary procedure to assure that the distilled water is totally changed to become saturated steam. The pressure inside heating coil H-101 was increases rapidly up to 2 bar gauge. It is important to have both valves, in order to ensure that zero back pressure during the transfer of the

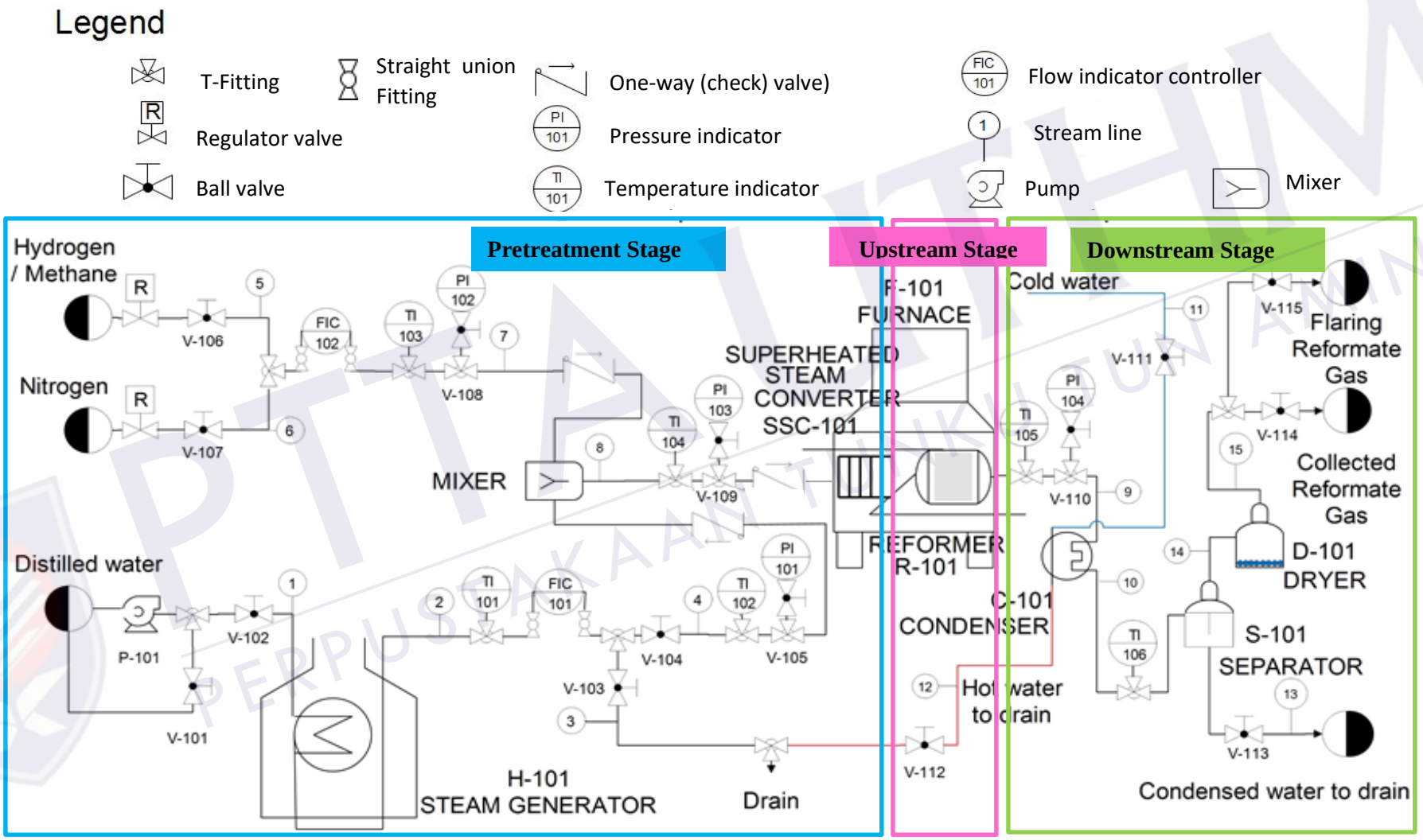

Figure 3.3 : Overall view of process and instrumentation diagram of SMR test rig bench.

distilled water into the coil. Furthermore, the P-101 is a direct diaphragm pump which works at 5.5 bar liquid delivery.

ii. The produced saturated steam is monitored by temperature indicator TI-101 (°C unit). It is unnecessary to have a pressure gauge on this streamline since the pressure value can be defined according to TI-101 and the steam at this point is not critical for evaluation. The flow indicator controller FIC-101, controls the volumetric flow rate of the saturated steam. In order to determine the mass flow rate, relationship of density and volumetric flow rate is used. Based on steam properties table, the density is obtained from the consequence reading of TI-102 (°C unit) and PI-101 (bar gauge unit) by taking up that mass in streamline 4 which is equivalent to the FIC-101 (liter per hour unit) output. Meanwhile, the V-103 and V-104 are purposely installed as safety pressure relief valves and steam preparation before entering the upstream stage. In order to secure and keep off the saturated steam back flow, a one-way valve is installed in streamline no 4.

iii. For the methane gas feed, this gas streamline is shared with nitrogen and hydrogen gas feed. The hydrogen gas is used for catalyst activation stage. Meanwhile the nitrogen gas acts as pre-heating substance before SMR operation at desired condition. It is a flushing agent to avoid from contamination inside streamline. It is also applied to create pressurized condition inside the streamline and most specifically inside the micro channel reformer. The pressure regulator for each gaseous is controlled at 4 bar gauge. The V-106 and V-107 act as a safety and switching line valve. The desired gas volumetric flow rate is regularly checked and placed based on correlation of FIC-102 (ml per minute unit), TI-103 (°C unit) and PI-102 (bar gauge unit). In order to define the mass flow rate, relationship of density and volumetric flow rate were used. From methane properties table, the density can be obtained from the consequence reading of FIC-102, TI-103 and PI-102. In order to secure and keep off the gaseous back flow, a one-way valve is installed in streamline no 7.

iv. The most critical path is laid on a mixing point which merging streamlines 4 and 7 to get streamline 8. In order to ensure homogenous mixing, the streamline 4 is carried only saturated steam, and reactant pressure range 0.2 – 1 bar gauge for both streamline 4 & 7. Last but not least, the installation of one way valve is done for each streamline.

v. The output from mixing point which is streamline 8, flows directly into the upstream of the reformer. On this streamline, TI-104 (°C unit) and PI-103 (bar gauge unit) are established to monitor temperature and pressure changes after mixing. Theoretically, the pressure changes as temperature changes inside reformer, therefore, a one way valve at streamline 8 is installed to ward off any pressure transition.

vi. Lastly, the superheated steam converter coils unit SSC-101 is installed. This unit is built from SS316 1/4 inch tubing inform of coil shape. This SSC-101 unit is attached together with the micro reactor system inside the box furnace. This SSC-101 is the most critical process, in order to convert the saturated to become superheated steam, where a large amount of heat is needed. Furthermore, once the SSC-101 is attached to the micro reactor system, it manages to extinguish any potential of pressure drop and heat loss since the superheated reactants are directly fed into the micro reactor system.

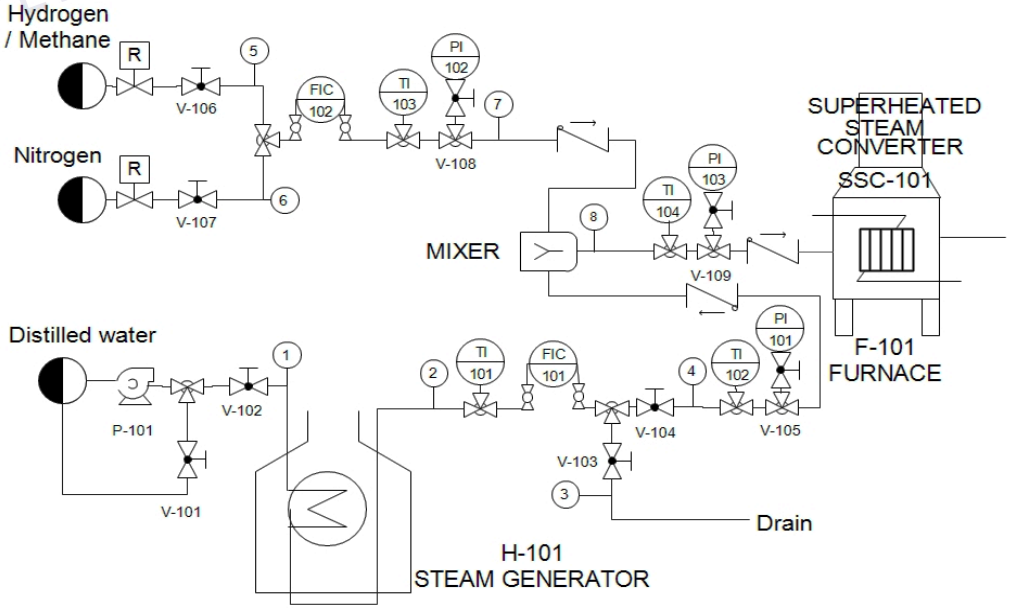

Figure 3.4 : Process and instrumentation diagram of pretreatment stage.

3.3.3 P&ID Upstream Stage

The upstream stage, which was covers reformer unit R-101, has been installed inside box furnace F-101 as shown in Figure 3.5. The details of process flow at this stage as below:

i. The output of preheat is directly fed into R-101. Hereby, the coated plat catalyst is installed inside multi micro channel passage. The active area of catalyst acts as the conversion site for the reaction as in equation 3.1 and 3.2.

ii. All reformate gases flow inside streamline 9. The TI-105 (°C unit) and PI-104 (bar gauge unit) is utilized to monitor the reaction operating condition. This is important in order to regulate the box furnace temperature.

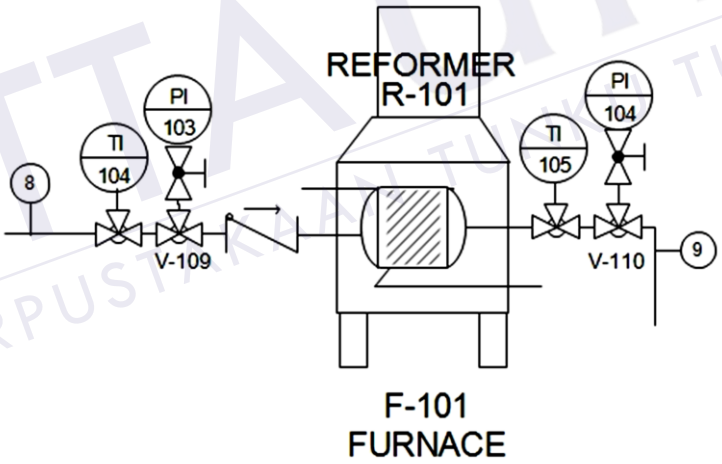

Figure 3.5 : Process and instrumentation diagram of upstream stage.

3.3.4 P&ID Downstream Stage

The downstream stage consists of unit operation such as condenser C-101, liquid and gas separator S-101, dryer D-101 and flaring unit as indicated in Figure 3.6. The details of process flow at this stage as below:

i. The condenser unit C-101, functions to cool down the reformate gas from the micro reactor systems in order to condense the excess water content after reaction as in Equation 3.1 and 3.2. The cooling medium of 27°C at streamline 11 flows into C-101 and goes out as hot medium in streamline 12 at an average of 75°C. The hot reformate gases directly flown into C-101 via SS316 1/4 inch cooling tubing coil. The cooling medium flow is controlled via V-111 and V-112 that act as a safety and drain valve. The streamline 10 is cooled down till below 40°C and flown out to the next stage, which is liquid /gas separator S-101. The TI-106 (°C unit) is used to monitor C-101 output in order to regulate V-111.

ii. Continues from C-101, the condensed water is separated inside S-101. The basic separation of liquid/gas is laid on the mechanism of the inlet stream dipping in raw water, meanwhile the outlet is floated above raw water. The separated reformate gases are continuously flow into the next stage which is dryer D-101. At this point, the V-113 act as a drainage valve.

iii. Even though the reformate gases already been separated from the condensed water, it still needs to be dried for gas chromatography analysis. The basic dryer D-101 mechanism is laid on the principal of the inlet stream located inside silica gel (500 gram load), meanwhile the outlet is floating above the silica gel.

iv. The dry reformate gases are flared at V-115. The flare unit functionally acts as a combustor of the reformate gases to comply with the purifier concept of converting a toxic compound to an environmentally friendly gas. For the GC analysis and Dräger MSI EM200, the sample is collected at V-114.

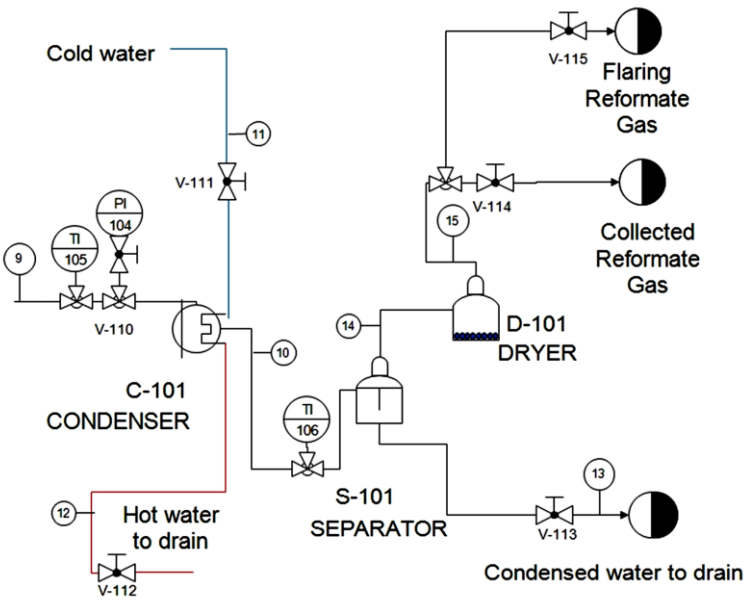

Figure 3.6 : Process and instrumentation diagram of downstream stage.

3.4 Design and Fabrication of Unit Operation

The main layout of the first phase execution began as in Figure 3.7, which shows basic flow diagram of hydrogen production. This figure was showing the flow of production hydrogen from steam and methane as a reactant, through the conversion process of steam methane reforming. Beside hydrogen as products, there are a few other yields, such as carbon monoxide and carbon dioxide.

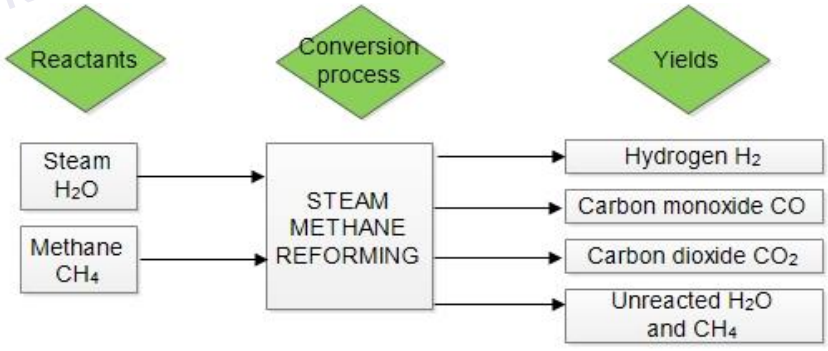

Figure 3.7 : Basic flow diagram of hydrogen production.

Once the development of PFD and P&ID was established, the next step is designing and fabrication of major unit operation such as a saturated steam generator, condenser, liquid/gas separator, dryer and a purifier. This unit operation has been

constructed accordingly to the basic theory as reported by Douglas (1988) and Marshall (2002). Figure 3.8 shows the flow analysis of unit operations, which is involves in steam methane reforming process. The unit operation had been sorted out accordingly to the conversion process stage and is further discussed briefly.

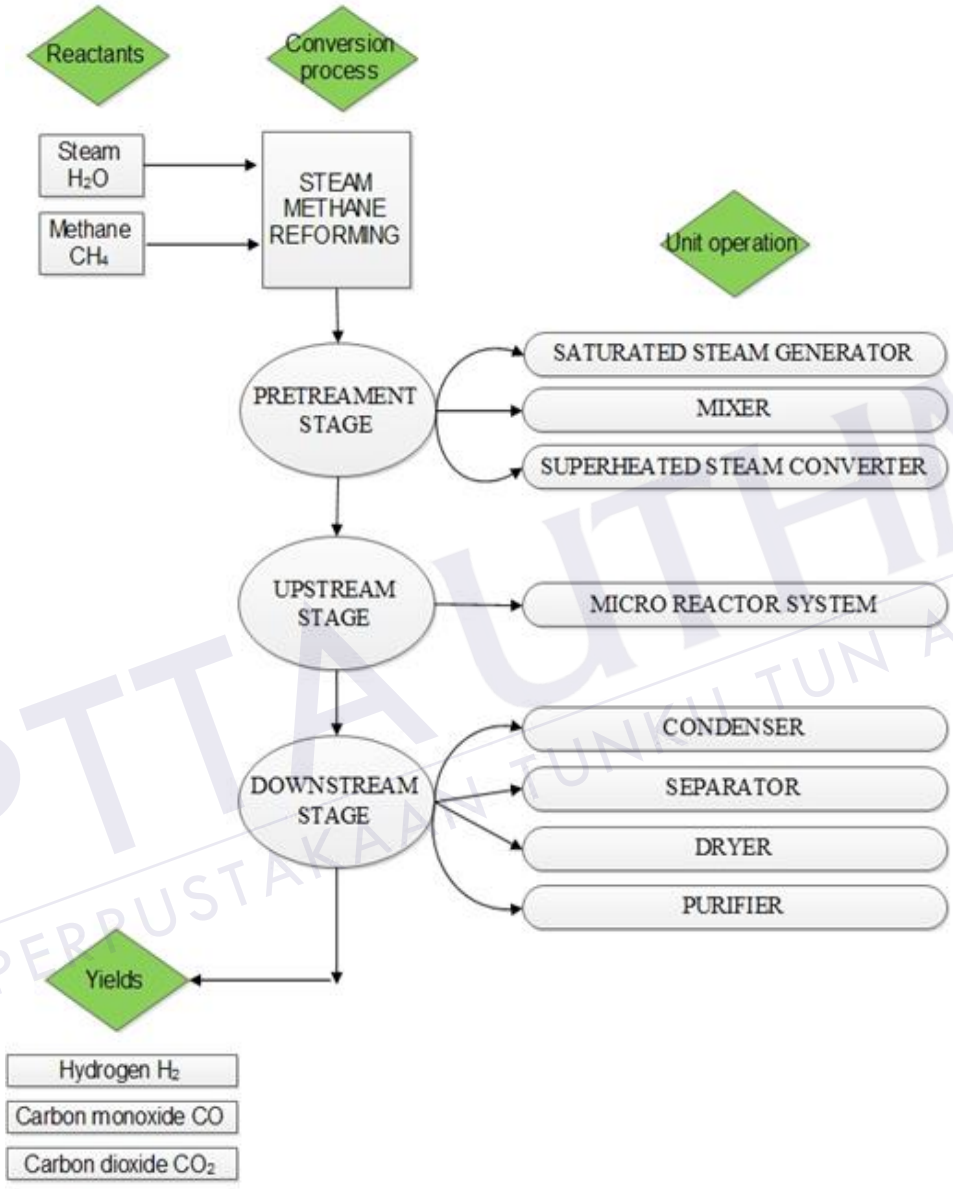

Figure 3.8 : Flow analysis of unit operation involves in steam methane reforming process.

3.4.1 Steam Generator

The steam generator functionally acts as a saturated steam converter. At this stage, the lab scale steam generator has been designed, fabricated and tested. All items needed such as tank, heater, oil and preheating coil have been determined based on the heat transfer rate. The related energy analysis of steady flow has been applied in this process.

i. Energy analysis from the dip heater into the oil bath as shown as in Equation 3.3, by assuming that insulated tank has been applied and further. So the power of dip heater is a 100 % transfer to oil bath.

ii. Energy analysis from oil bath into a water coil as in Equation 3.4 is assumed by the water mass flow rate at enthalpy changes inside the coil was a steady flow during entering the steam generator tank.

iii. This lab scale steam generator has been fabricated by using stainless-steel tubing (SS316) of 1/4 inch outer diameter size. For the oil bath medium, refined bleach deodorized palm oil (RBDPO) had been chosen for its good thermal transfer properties and edible character. For the heating element, dip heater of 1500W has been used. Lastly the vessel has been made of insulated mild steel tank with single inlet and outlet of preheating coil. The saturated steam volume flow rate inside coil has been set at 40 liter per hour, which equivalent to the steam to carbon ratio of 3. Therefore steam absorb can be used as in Equation 3.4, thus the system thermal efficiency as in Equation 3.5.

$$\dot{Q}_{\text{in oil bath}} = \dot{Q}_{\text{out dip heater}} \tag{3.3}$$

$$\dot{Q}_{\text{in oil bath}} = \Sigma_{\text{steam}}\, \dot{m}(\Delta h) \tag{3.4}$$

$$\eta_{\text{th}} = \frac{\Sigma_{\text{steam}}\, \dot{m}(\Delta h)}{\dot{Q}_{\text{oil bath}}} \tag{3.5}$$

Where :

$\dot{Q}$: power

$\dot{m}$: water mass flow rate

Δh : enthalpy change

η_{th} : thermal efficiency

The design, fabrication and development of saturated steam generator are done according to the desired net heat transfer as illustrated in Figure 3.9. Meanwhile, the thermal efficiency is defined based on type of tubing and dip heater power supply. The system physical properties are shown in Table 3.1 and technical drawing as in Appendix D.5, D.6 and D.7.

Table 3.1 : The saturated steam generator physical properties

No.	Part	Dimension	Material
1.	Tank	235 mm OD x 350 mm H	Mild steel
2.	Heating coil	90 mm OD x 14 coils	Stainless steel
3.	Oil bath	8.5 liter	RBD palm oil
4.	Dip heater	1500 watt	Steel

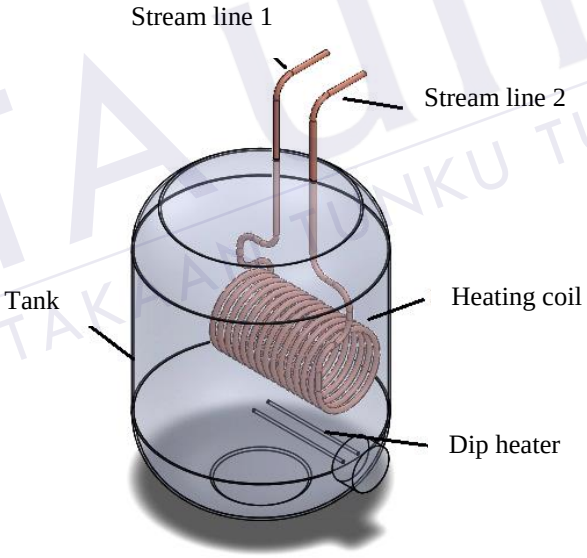

Figure 3.9 : Saturated steam generator unit

The heating coil design has been selected due to its good thermal conductivity design, easy to construct and easy induction. Moreover, the number of 14 coils is chosen as the optimum in order to give enough space and time for the distilled water to convert into saturated steam. This is also due to consideration of limited compartment space as a sequel to the used tank. The single input and output flow direction as refer to the fundamental net heat transfer control strategy. In order to

ensure the heating coil getting an optimum heat transfer from the 1500-watt dip heater, it was placed 10 cm above tank bottom surface. It is because, the heat convection direction from the dip heater and oil are moving cylindrically upwards. As for the oil bath, it is important to ensure that heating coil is fully dipped. The oil bath material is needed to be heated up to 250^{o}C as a safety precaution. The usage of 1/4 inch tubing is the most optimal for this lab scale connectivity streamline, since 1/8 inch tubing has created problem such as difficulties for instrumentation (pressure gauge, thermocouple) installation and steam flow clogged. Meanwhile, the 3/8 inch has lead to the condensed steam line problem.

3.4.2 Condenser

The condenser functionally acts to cool down the reformate gas from microreactor systems. This was very important in order to condense the excess water content after SMR and WGS reaction. The condensed water has been cooled down till 40°C and flown out to the next stage which was a separator.

By using the heat exchange mechanism, the cooling medium used a fresh tap water at inlet of 30°C and stored as water bath, whereby the hot medium is flown inside stainless-steel tubing (SS316) of 1/4 inch outer diameter size. At this stage, the lab scale condenser has been designed, fabricated and develop accordingly to the reformed gas mass flow rate based on steam to carbon ratio of 3. All items needed such as tank, condenser coil, cold and hot medium management are defined based on the heat transfer rate. Moreover, the condenser only applies to use stainless steel SS316 tubing instead of copper tubing. This is due to copper tubing chemical properties, which is oxidized if react to high temperature (>350°C) substrate especially reformate gaseous.

At the initial stage of design, it is assumed zero conversion of steam and methane. This is very important in order to prepare the basis of net heat transfer. Thus, the energy analysis of hot medium steady flow is used as in Equation 3.6.

$$\dot{m}_{water}\left(h_{water,in} - h_{water,out}\right) = \left[\dot{m}_{CH_4}\left(h_{CH_4,out}\right) + \dot{m}_{steam}\left(h_{steam,out}\right)\right] - \left[\dot{m}_{CH_4}\left(h_{CH_4,in}\right) + \dot{m}_{steam}\left(h_{steam,in}\right)\right] \quad (3.6)$$

Where :

$\dot{m}_{steam}$: steam mass flow rate

$\dot{m}_{CH4}$: methane mass flow rate

h_{steam} : steam enthalpy

h_{CH4} : methane enthalpy

The design, fabrication and development of the condenser are done according to the net heat transfer desired as shown in Figure 3.10. The thermal efficiency is defined based on the mass flow rate of the cooling medium. The basic concept of condenser flow is counter current among hot and cold medium direction. Table 3.2 shows the physical properties of condenser system and technical drawing as in Appendix D.8 and D.9.

Table 3.2 : Physical properties of condenser system

No.	Part	Dimension	Material
1	Tank	120 mm OD x 300 mm H	Stainless steel
2	Condenser coil	90 mm OD x 10 coils x ¼" tubing	Stainless steel
3	Cooling medium	Mass flow rate (g/s)	Tap water

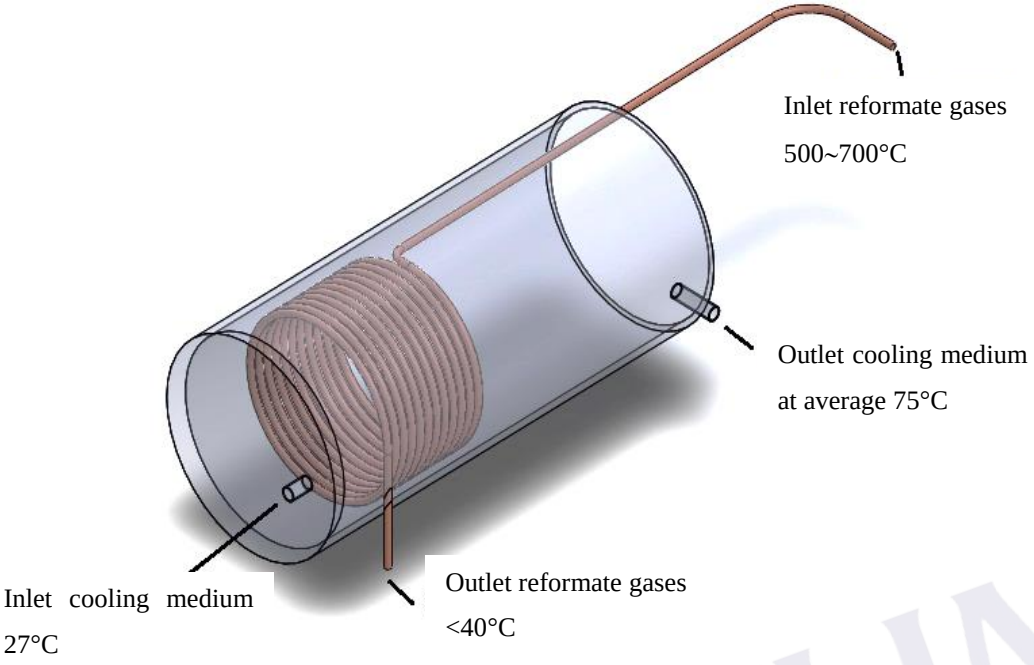

Figure 3.10 : Illustration of condenser

The condenser unit functionally acts to cool down the reformate gases from the micro reactor systems in order to condense the excess water content after SMR and WGS reaction. Figure 3.10 shows that the cooling medium of 27°C at streamline is flowing directly into the condenser and went out as a hot medium in streamline. Meanwhile that, the hot reformate gaseous directly flow into the condenser as counter flow to the cooler medium direction. The reformate gaseous inlet temperature varies from 500 to 700°C and outlet temperature is controlled approximately below 40°C. Therefore the mass flow rate of cooling medium is regulated to secure the output stream. The stainless steel tubing is used to secure the reformate gaseous from being oxidized unlike copper tubing.

3.4.3 Separator – Liquid & Gas Recovery

Pursued from condenser stage, the condensed water is distinguished at this point. The basic separation is laid on the mechanism of the inlet stream dipping in raw water, meanwhile the outlet is floating above raw water. The separated reformat gaseous is continuously flowing into the next stage, which is a dryer.

The basic separator as shown in Figure 3.11 is placed on the mechanism of the inlet stream dipping in raw water, meanwhile the outlet is floating above raw water. The separated reformate gases continuously flow into the next stage, which is a dryer. Table 3.3 shows the physical properties of liquid gaseous separator and technical drawing as in Appendix D.10. The volume of condensed water is collected at an intervals of 30 minutes up to 60 minutes.

Table 3.3 : Liquid-gas separating system

No.	Part	Dimension	Material
1	Tank	88 mm OD x 220 mm H	Pyrex glass
2	Tubing inlet	L shape ¼" 250mm	Glass
3	Tubing outlet	L shape ¼" 50 mm	Glass

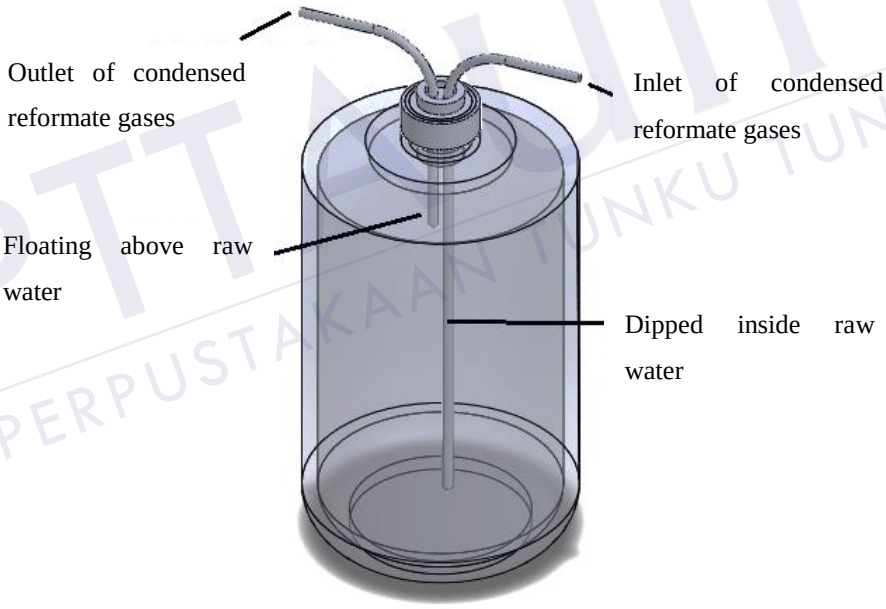

Figure 3.11: Illustration of separator

3.4.4 Dryer – Vapor Recovery

Even though the reformat gaseous already been separated from the condensed water, it still needs to be dried for gas chromatography analysis. The basic dryer mechanism is laid on the principal of the inlet stream located inside silica gel, meanwhile the outlet is floating above silica gel.

The basic dryer mechanism, as in Figure 3.12, is laid on the inlet stream located inside silica gel, meanwhile the outlet is floating above silica gel. The pattern and fabricated dryer are shown as below. Figure 3.12 shows, the dehydrolysis reformat gases are directly flowing inside the silica gel. It is determined that 500g silica gel is already more than enough to absorb all remaining moisture content. Table 3.4 shows the physical attributes of the vapor dryer system and technical drawing as in Appendix D.11.

Table 3.4 : Dryer system physical properties

No.	Part	Dimension	Material
1	Tank	100 mm OD x 120 mm H	Pyrex glass
2	Tubing inlet	L shape 1/4” x 100mm	Glass
3	Tubing outlet	L shape 1/4” x 50 mm	Glass

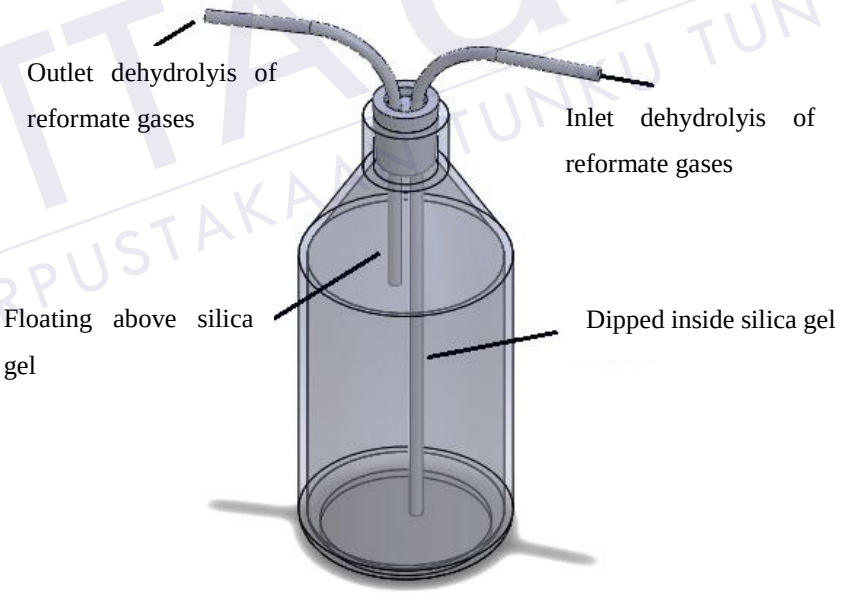

Figure 3.12 : Illustration of dryer

3.4.5 Flare – Reformat Purifier

The flare unit functionally acts as a combustor of the reformat gaseous to comply with the purifier concept of winning over a toxic compound to environmentally friendly. The flare unit functions as a combustor of the reformat gases. It is essential in order to comply with the purifier concept of converting the toxic compounds to environmentally friendly emission. Table 3.5 shows the physical properties and technical drawing as in Appendix D.12, meanwhile Figure 3.13 shows a illustration of flare system. The flare is developed based on the basic concept of single input and two outputs. For reformat analysis, the sample is collected at collector valve. Once completed, it will be fully closed. The flaring valve is operated at fully open and just only close during sample collection.

Table 3.5 : Flare system physical properties

No.	Part	Dimension	Material
1	Tubing tower	12.7 mm OD x 500 mm H	Galvanized steel
2	Tubing inlet	¼” 500 mm	Stainless steel

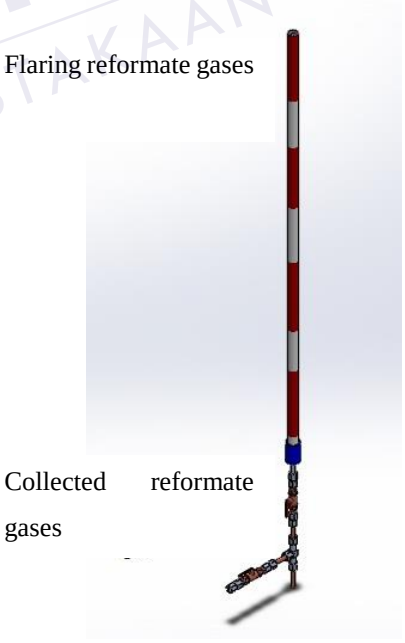

Figure 3.13 : Illustration of Flare system

3.5 Conceptual Design of Micro reactor system

The design, fabrication and development of the micro reactor system, the usage of appropriate hardware configuration is important for framing and shaping. The micro reactor system is made of stainless steel cubes. In parliamentary procedure for implementing this project, a numeral of methods and steps are used up. The accompanying guidelines are utilized to pack out this operation. The primary intent of these conventions and procedures is purposely to ascertain that this product can be dispatched according to the plan with minimal problems. The identified methods are listed as follows:

i. Research is performed on the designed aspect.
ii. Parts of the equipment used are identified.
iii. A survey on existing micro reactor is made.

Fundamentally, the micro channel reactor conceptual design is the beginning stage of conception, in which drawings or solid models are used as the dominant tools and wares. The conceptual design phase provides a description of the proposed system in terms of a set of integrated ideas and concepts about what it should do, behave, and look like. That will be understandable by the users in the manner intended (Morris, 2016).

Towards to the generation concept, requirements are need to be assigned in order to fulfill the micro channel reactor design concept. So that, the design identifies a necessary attribute, capability, characteristic, or quality of a system. The micro channel reactor is a critical path of upstream stage. Since the SMR is an endothermic reaction, therefore for this project, the upstream stage is taking place inside a box furnace. For this project, the micro reactor conceptual design is limited to the usage of box furnace brand Barnsstead Thmolyte 1500 with capacity of operating temperature 1300°C. The box furnace inner chamber space is 200mm length x 100mm width x 120mm height, therefore the designed micro channel system must comply with box furnace specification.

Several requirements are needed in order to ensure that the micro scale reformer system has been complied to the size limitation of box furnace. Hence, it is divided into two major parts; one is superheated steam converter coil and the other part is the micro channel reactor module.

3.5.1 Superheated Steam Converter Coils

For this segment, the requirement for design builds as below:

i. The material chooses should have high temperature resistance and high latent heat.
ii. The superheated steam converter coils has been made of 1/4 inch 316 stainless steel tubing.
iii. The outer diameter coil is 90 mm to ensure fit into box furnace chamber.
iv. There are 10 numbers of repeating coil of length 282.78 mm each coil.
v. Inlet fitting for reactant feed of 1/4 inch 316 stainless steel tubing.
vi. Outlet fitting into a micro channel of 1/4 inch 316 stainless steel tubing.
vii. The fabrication method should be easy as possible and inexpensive.

3.5.2 Micro Channel Reactor Module

At this stage, three major components have been involved, called as cylindrical housing body, inner body and substrate plate. For this segment, the requirement for design builds for each major has been briefly described as infra:

i. Cylindrical housing body:
    a. The material chooses should have high temperature resistance and high latent heat which is stainless steel 304.
    b. Outer module of cylindrical shape with a diameter of 42 mm x 50 mm length.
    c. The flange come in 16mm width x 10mm high x 8mm threaded screw.
    d. The fabrication method should be easy and inexpensive.
    e. The place consists single inlet and outlet stream for reactants and products of 1/4 inch 316 stainless steel tubing.
ii. Inner cylindrical body as below:

a. The material should have high temperature resistance and high latent heat which is stainless steel 304.

b. The multi micro channel module is the cylindrical shape with 33.4 mm outer diameter x 50mm length.

c. The multi micro channel module consists six insert module slots with 15mm x 0.5mm x 50mm.

d. The micro channel passage way of reactants is 200μm.

e. The fabrication method should be gentle and low cost.

iii. Substrate plate as below

a. The material should have high temperature resistance and high latent heat which is stainless steel 304

b. Substrate plate of 15mm x 0.5mm x 60mm

c. Coated areas only laid on 15mm x 0.5mm x 50mm.

d. The fabrication method should be easy and inexpensive

For the process of fabricating, three machines had been used and suited to the requirement and specification that have been assigned during the design stage.

i. CNC turning machine.
ii. CNC milling machine.
iii. CNC electrical discharge wire cut machine.

3.5.3 Cold Commissioning of Micro reactor system

Cold commissioning test is basically used to test the physical properties of the fabricated micro reactor system. It covers several test such as vacuum, hydrostatic and static pressure.

i. The vacuum test has been carried on to detect leakage in a vacuum state inside the micro reactor system. Essentially, this vacuum test is depressurized the micro reactor system in parliamentary procedure to detect any pressure build up in parliamentary procedure to experience any leakage. A manifold pressure gauge has been installed to the vacuum pump and being connected to micro reactor system's inlet and outlet streamlines. Then, the vacuum pump is working on for 3 minutes. After 3 minutes, the

vacuum was shut down to see any changes on the manifold pressure gauge. The schematic diagram of vacuum test is shown as in Figure 3.14 and actual photo of complete apparatus setup as in Appendix E.14.

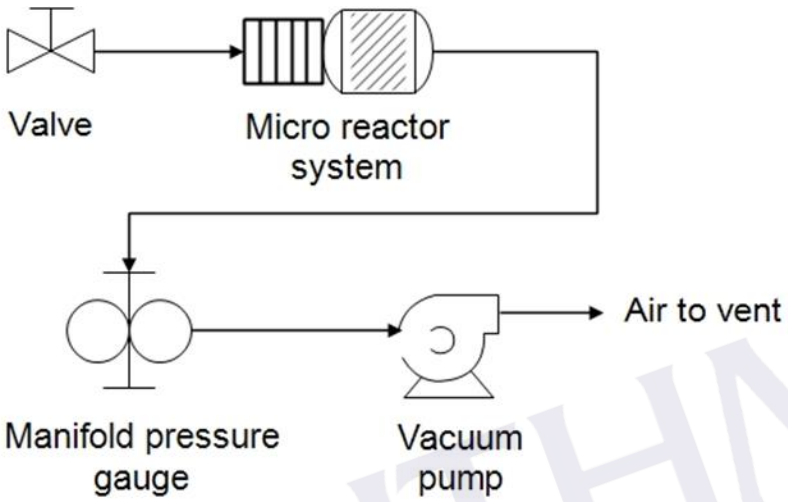

Figure 3.14 : Schematic diagram of vacuum test

ii. The hydrostatic pressure is done to test the pressure drop different inside the micro reactor system. The micro reactor system has been pressurized with compressed natural gas (CNG) at specified test pressure. The main equipment used for this test is an electronic manometer. The electronic manometer is connected to both inlet and outlet stream line by using a Tee fitting. The manometer electronic device is used to record the incoming CNG and the pressure drop different inside the micro reactor system. The schematic diagram of hydrostatic pressure test is shown as in Figure 3.15 and actual photo of complete apparatus setup as in Appendix E.15.

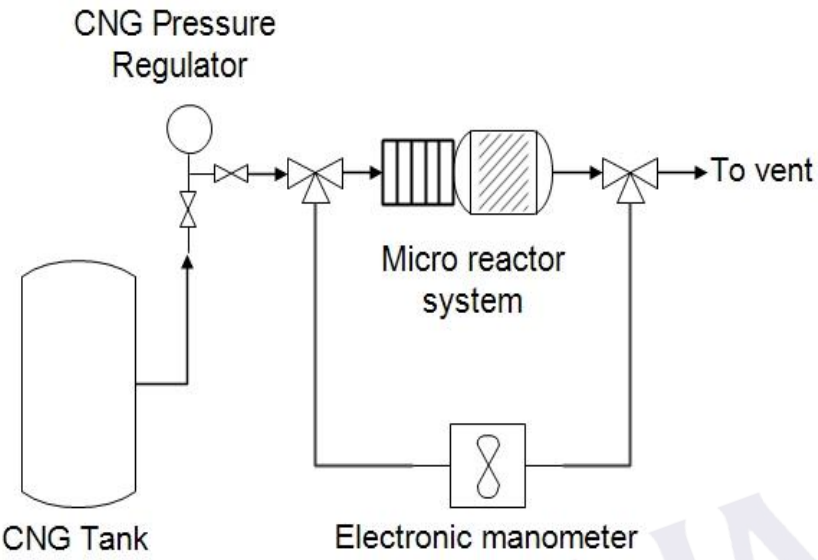

Figure 3.15 : Schematic diagram of hydrostatic pressure test

iii. The static pressure test is conducted to identify the maximum pressure can withstand until any leak occurred. This procedure is required for safety reasons and operating condition during the SMR conversion process. The procedure has been set off by plugging the inlet streamline to the CNG pressure regulator and the outlet stream is connected with a fully closed ball valve. After that, the CNG pressure has been regulated with an interval of 0.5bars to the maximum point until leaking is detected. The schematic diagram of static pressure test is shown as in Figure 3.16 and actual photo of complete apparatus setup as in Appendix E.16.

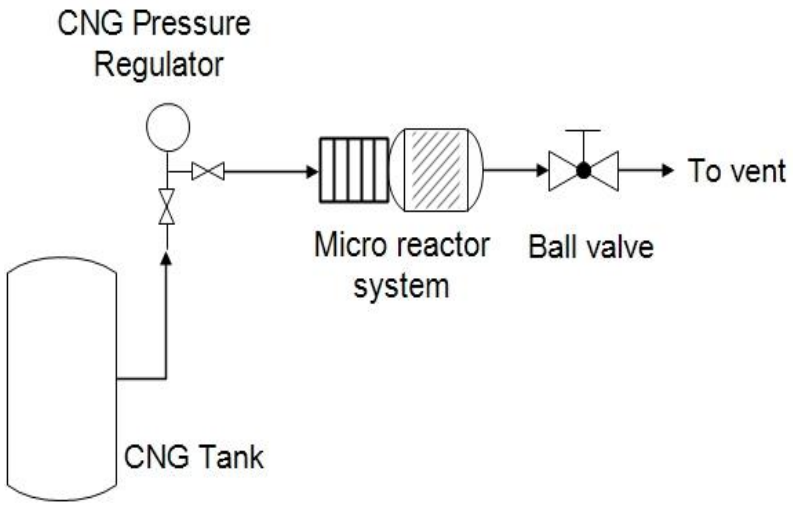

Figure 3.16 : Schematic diagram of static pressure test

3.6 SMR Test Rig Bench and Micro Reactor System Function Test

The micro reactor systems had been installed into the SMR test rig bench and a function test is conducted accordingly to the specification and requirement based on literatures. The functional test also known as a hot commissioning, which is conducted to validate the correlation between SMR test rig bench and micro channel reactor functional properties such as heat transfer, in order to ensure it is ready for conversion process. The micro channel reactor systems are placed in box furnace as the heat supply source. Tested parameter and operating condition have been set as in Table 3.6. The operating condition indicator is reflecting to the overall view of process and instrumentation diagram of SMR test rig bench as shown in Figure 3.3.

Table 3.6: Hot commissioning parameter.

No.	Operating condition	Indicator
1	Temperature	500 to 700°C
2	Steam to carbon ratio	1 to 5
3	Parameter	TI 101, TI 102, TI 103, TI 104, TI 105 TI 106, PI 101, PI 102, PI 103, PI 104, FIC 101, FIC 102, furnace PV

3.7 Catalytic Behavior Analysis

The catalytic behavior analysis has been conducted to validate the performance of catalyst onto methane conversion, SMR yields and reaction rate (methane disappearing rate). This stage is conducted inside the micro reactor system of the SMR test rig bench. The reformat gaseous are analyzed by using gas chromatography (GC) and a multi gas detector. The obtained experimental data has been further analyzed through the mole balance equation of product streamline.

3.7.1 Catalyst Precursor

The catalyst precursors are obtained from the works done by Sarwani (2017). The substrate plat has been deposited with catalyst through preparation method of impregnation via Dip Coating. The dip coating method basically can be defined as a processes of dipping a substrate plate into a reservoir of sol-gel solution for some interval time until the substrate is completely wetted. It is followed by withdrawing the substrate out from the sol-gel solution bath. Next the substrate plate is undergoing calcination and activation process. The main product of dip coating is a thin layer of catalyst precursor, which is coated on top of the substrate plate surface area and ready to be used as catalyst in SMR. Thus, this research is used three different type of catalyst with weight % basis of total precursors, as outlined below:

i. Nickel aluminide (10 wt%)
ii. Ruthenium aluminide (0.1 wt%)
iii. Rhodium aluminide (0.1 wt%)

3.7.2 Catalyst Activation

The coated catalyst substrate plate is pursued for activation stage. Basically, catalyst activation can be defined as a preparation of active site on top of deposit catalyst by removing the oxidation agent such as Oxygen. In this segment, the Ellingham Diagram as in Figure 3.17 is used as based line prediction for activation parameter. The Ellingham diagram has been applied to predict the equilibrium temperature between a

metal, its oxide, and oxygen. From the diagram, the needed parameter such as temperature, partial pressure and activation medium are obtained as marked in red line in Figure 3.17. Table 3.7 shows the activation parameter, which has been used for temperature programmed reduction (TPR) method. This activation parameter has been used also as the baseline for the other type of catalyst loading.

Table 3.7: Catalyst activation parameter.

No.	Operating condition	Indicator
1	Temperature	700°C
2	Pressure	0.5×10^{-5} atm partial pressure
3	Reduction agent	Purified hydrogen
4	Reducing agent flowrate	300ml/min
5	Retention time	90 minutes

3.7.3 Catalyst Test Analysis

The coated catalyst is laid within the multi micro channel module. The microreactor set itself has been installed in Barnstead/Thermolyne Compact Benchtop Muffle Furnace (Type 1500). The temperature of the box furnace is controlled and measured by programmable controller and K-type sheathed thermocouple. The SMR test analysis is conducted at the desired parameters at atmospheric pressure. Before the reaction test, the catalyst has been reduced in situ by a 300 ml/min of purified hydrogen flow rate at 700°C for about 90 minutes. A gas flow meter NBDC_LZB 3 is used to control and measure the desired gas during activation and SMR test run analysis. Meanwhile, for the steam is controlled and measured by NBDC_LZB 10 flow meter. All gaseous and steam flow rates are normalized.

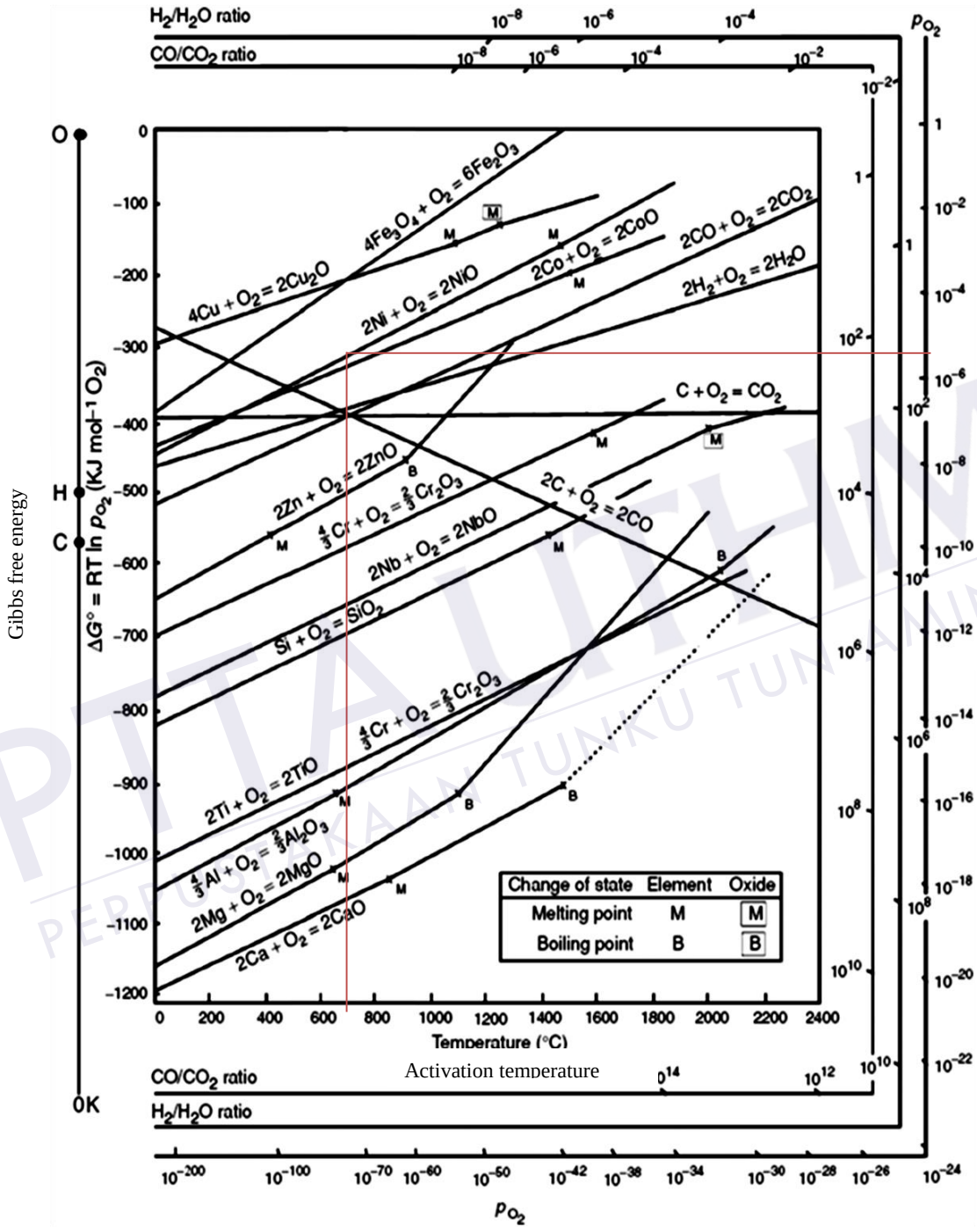

Figure 3.17 : Ellingham diagram for catalyst activation (Oar-Arteta et. al., 2017).

The deposited catalyst has been undergoing several operating conditions in order to define somehow that the catalyst is working. For this study, the reactants used are Methane gas (99.995%), Hydrogen gas (99.9998%), Nitrogen gas (99.9995%) and superheated steam (distilled water based). The critical parameter has been tested as below:

i. Reaction temperature
ii. Steam to carbon ratio
iii. Multiple type of catalyst loading

The Table 3.8 shows the summary of design of experimental works for this study. The catalyst test operates at the proposed operating condition with three-time data acquisitions repetition. In order to ensure that this experiment works run smoothly, a few assumptions have been done.

i. Plug flow conditions, significant axial mass and heat dispersion with negligible radial gradients.
ii. Resistances to external mass and heat transport are taken explicitly into account.
iii. Uniform particle size, constant bed porosity.
iv. Only gas phase reactions considered, which consist of five reactive species (CH_4, CO_2, H_2O, CO, H_2) in the model.

In order to define the catalyst working traits and to check the catalyst stability, all experiments have been conducted at 300 minutes at elevating of 60 minutes for reaction temperature and steam carbon ratio effect. Meanwhile, for multiple catalyst loading, the experiment have been conducted for 300 minutes at elevating of 30 minutes interval. According to the previous researcher works, the working catalyst will show stability less than 500 minutes.

Table 3.8 : Catalyst test parameter.

Test	Parameter	Indicator
1	Reaction temperature:-	
	1.1 Operating temperature	500°C, 550°C, 600°C, 650°C and 700°C
	1.2 Operating pressure	1 bar
	1.3 Steam to carbon ratio	3
	1.4 Retention time	300 minutes (60 minutes interval)
	1.5 Catalyst precursor	Nickel aluminide (10%wt)
2	Steam to carbon ratio:	
	2.1 Operating temperature	Obtained from optimum (1.1)
	2.2 Operating pressure	1 bar
	2.3 Steam to carbon ratio	2,3 and 4
	2.4 Retention time	300 minutes (60 minutes interval)
	2.5 Catalyst precursor	Nickel aluminide (10%wt)
3	Multiple type of catalyst loading	
	3.1 Operating temperature	Obtained from optimum (1.1)
	3.2 Operating pressure	1 bar
	3.3 Steam to carbon ratio	Obtained from optimum (2.3)
	3.4 Retention time	300 minutes (30 minutes interval)
	3.5 Catalyst precursor	Nickel aluminide (10%wt)
		Ruthenium aluminide (0.1wt%)
		Rhodium aluminide (0.1wt%)

3.7.3.1 SMR Yields Characterization

From the Figure 3.18, the collected reformat gas from SMR reaction has been further examined by using gas chromatography (GC) Perkin Elmer Clarus 500 unit and Dräger MSI EM200. The reformat gaseous is collected by using Tedlar Sampling Bag 1L and injected into the GC by using Gastight 250 µL Syringe. Meanwhile, the carbon monoxide is analyzed by using Dräger MSI EM200. The experimental procedure, including all important parameters have been further discussed in Standard Operating Procedure as in sub-chapter 4.1.2.

The installation between column, injector and detector has been done according to the standard operating procedure by Perkin Elmer. These injectors are programmed to split/splitless method and adjusted to the optimum operating pressure of 4-6 bar. Visual inspection for any leak at column connectivity has been done by using leak detector spray with a circulation of Nitrogen gas. The conditioning test which involve oven temperature setting, initially 50°C and elevated 5°C/min till 200°C for 4 hours. This is to ensure that the C1-C5 hydrocarbon column is complied and worked according to the GC setting parameter.

The sample is collected by using the Tedlar Sampling Bag and manually injected into the GC system by using 250 µl gastight needle syringe. This syringe is cleaned and rinsed by Nitrogen gas for each time of sample injection. The appropriate settings for all basic parameters, a summary of the “in house” configuration of Agilent’s C1-C5 hydrocarbon column has been successfully established as shown in Table 3.9.

SMR Test Rig Bench

Tedlar Bag

Gas Chromatography
Perkin Elmer Clarus 500

Dräger MSI EM200

Figure 3.18 : Flow diagram of characterization for SMR yield.

Table 3.9 : “In house” configuration based on ASTMD1945.

	Parameters	Setting
i.	Oven temperature	40°C, 3°C/min, 170°C
ii.	Split ratio	1:15
iii.	Flow rate	2.5 ml/min
iv.	Injector temperature	250°C
v.	Detector temperature	275°C
vi.	Volume	200µl
vii.	Carrier gas	Hydrogen

The proper use of Tedlar bag as in Figure 3.19 is described as below:

i. All gaseous inside Tedlar bag have been eliminated and rinsed by using Nitrogen gas. This is done by using vacuum compressor.
ii. The standard rinse procedure is performed within three rounds.
iii. The inlet valve connects to the SMR product streamline.
iv. The sample gas is only fill 90% of Tedlar bag capacity.

Figure 3.19 : Tedlar Sampling Bag 1L.

The proper use of gastight syringe as in Figure 3.20 is described as below:

i. The needle syringe is pinned into Tedlar bag
ii. This syringe has been rinsed by using Nitrogen gas for three cycles by applying the concept of the suction and delivered to environmental.
iii. The sample is injected into the GC by using Gastight Syringe for 200µL.

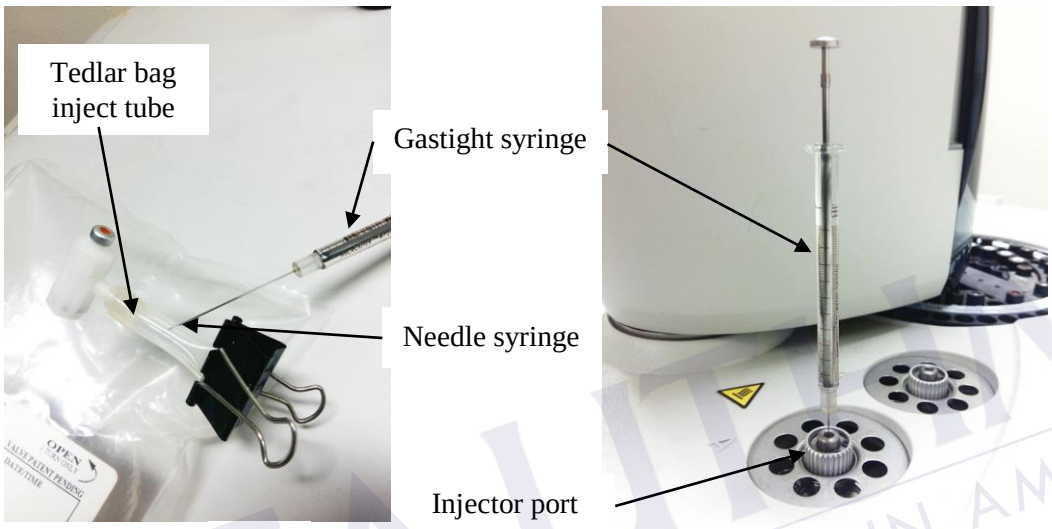

Figure 3.20 : a) Inject sample out of Tedlar bag b) Inject sample into GC.

Meanwhile the Dräger MSI EM200 as in Figure 3.21 works as a multi gas detector to determine the carbon monoxide conversion content in the undiluted outlet stream. Helpful instrument settings guide safely through typical measurement tasks such as:

i. This Dräger MSI EM200 has been connected at V-114 by using silicone rubber tube.
ii. The reformate gas is flown into the receiver channel.
iii. The analysis is simple as plug and analyzes. It provides result of CO.

Figure 3.21 : Dräger MSI EM200.

3.7.3.2 Methane Conversion and Mole Balance Equation for Flow Reactors

The obtained data of reformate gas at outlet stream data obtained from GC has been further analyzed through Equation 3.7 in order to define the methane conversion.

$$X_{CH_4} = \left[\frac{CH_4 \text{ moles reacted}}{CH_4 \text{ moles feed}}\right] = \frac{F^{o}_{CH_4} - F_{CH_4}}{F^{o}_{CH_4}} \tag{3.7}$$

Where:

$F^{o}_{CH_4}$: molar flow of CH_4 in feed

F_{CH_4} : molar flow of CH_4 at output of the chromatograph

X_{CH_4} : CH_4 conversion in products stream

Hence, from basic fundamental of the mole balance equation for the gas phase reaction, especially in this SMR, the chemical reaction stoichiometry formulation is used to solve the yield of the mole flow rate at output stream. Hence, by rearranging the main equation which of 3.1 and 3.2, become as below:

$$CH_4 + H_2O \leftrightarrow CO + 3H_2 = \dot{\xi}_1 \tag{3.8}$$

$$CO + H_2O \leftrightarrow CO_2 + H_2 = \dot{\xi}_2 \tag{3.9}$$

Where:

$\dot{\xi}_1$: the extent of reaction for SMR eqn (mol/s)

$\dot{\xi}_2$: the extent of reaction for WGS eqn (mol/s)

Then, by integrating every element within the main equation with extent of reaction and chemical reaction stoichiometry, obtained equations as below:

$$CH_4 \;:\; \dot{n}CH_4 = \dot{n}_o CH_4 - \dot{\xi}_1 \tag{3.10}$$

$$H_2O \;:\; \dot{n}H_2O = \dot{n}_o H_2O - \dot{\xi}_1 - \dot{\xi}_2 \tag{3.11}$$

$$CO \;:\; \dot{n}CO = \dot{n}_o CO + \dot{\xi}_1 - \dot{\xi}_2 \tag{3.12}$$

$$CO_2 \;:\; \dot{n}CO_2 = \dot{n}_o CO_2 + \dot{\xi}_2 \tag{3.13}$$

$$H_2 \;:\; \dot{n}H_2 = \dot{n}_o H_2 + 3\dot{\xi}_1 + \dot{\xi}_2 \tag{3.14}$$

Where :

$\dot{n}CH_4$: the mole flow rate of methane exit the reactor

$\dot{n}_o CH_4$: the mole flow rate of methane into the reactor

$\dot{n}H_2O$: the mole flow rate of steam exit the reactor

$\dot{n}_o H_2O$: the mole flow rate of steam into the reactor

$\dot{n}CO$: the mole flow rate of carbon monoxide exit the reactor

$\dot{n}_o CO$: the mole flow rate of carbon monoxide into the reactor

$\dot{n}CO_2$: the mole flow rate of carbon dioxide exit the reactor

$\dot{n}_o CO_2$: the mole flow rate of carbon dioxide into the reactor

$\dot{n}H_2$: the mole flow rate of hydrogen exit the reactor

$\dot{n}_o H_2$: the mole flow rate of hydrogen into the reactor

3.7.3.3 Design of Rate of Reaction (Methane disappearing rate)

Basically the rate of reaction for catalytic can be modeled by using Langmuir isotherm, which mainly consists of three assumptions:

i. The adsorption of reactant on top of the catalyst surface active area
ii. Catalyst active area as a reaction platform to cast products
iii. Desorption of the products from the catalyst active area.

By rearranging Eqn. 3.5, hence:

$$\left[F^{o}_{CH_4}\right] - \left[F^{o}_{CH_4}X\right] = \left[F_{CH_4}\right] \tag{3.15}$$

Where:

$\left[F^{o}_{CH_4}\right]$: molar flowrate at which CH_4 is fed into system

$\left[F^{o}_{CH_4}X\right]$: molar rate at which CH_4 is consumed within the system.

$\left[F_{CH_4}\right]$: molar fow rate at which CH_4 leaves the system.

By rearranging the Equation 3.15 gives :

$$F_{CH_4} = F^{o}_{CH_4}(1-X) \tag{3.16}$$

Where :

$F^{o}_{CH_4}$: the entering molar flow rate of CH_4 (mol/s)

F_{CH_4} : the product of the entering of CH_4 (mol/s)

X : the conversion of reactant CH_4 to become product (% fraction)

The micro channel reactor, as having the fluid flowing in plug flow in the example, zero radial gradients in concentration, isothermal and adiabatic. As the reactant enters and flows axially down the reactor, it has been used up and the conversion increases along the distance of the reactor. The main objective of the design equation is to define the rate of reaction CH_4 for PBR $-r'_{CH_4}$ (mol CH_4 /g catalyst. s). In order to develop the PBR design equation, fundamental of the PFR design equation has been used, where by for both sides of the PFR design equation as in 3.17 is multiplied with (-ve) hence becomes Equation 3.18.

$$r_{CH_4} = \frac{dF_{CH_4}}{dV} \tag{3.17}$$

$$-r_{CH_4} = \frac{-dF_{CH_4}}{dV} \tag{3.18}$$

For a flow of CH_4 previously been given in terms of the entering molar flow rate, product of entering and the conversion of X as in Equation 3.16, and differentiating becomes Eqn. 3.19. Then from Eqn. 3.19, substituting it into Equation 3.18 gives the differential form of the design equation for a plug flow reactor (PFR) as in Equation 3.20.

$$dF_{CH_4} = -F^{o}_{CH_4} dX \tag{3.19}$$

$$-r_{CH_4} = F^{o}_{CH_4} \frac{dX}{dV} \tag{3.20}$$

Meanwhile, for the packed bed reactors derivation of the different forms of the design equations for PBR are analogous to those for a PFR as in Equation 3.16. Hence, it becomes as in Equation 3.21.

$$-r'_{CH_4} = F^{o}_{CH_4} \frac{dX}{dW} \tag{3.21}$$

Where :

$-r_{CH_4}$: the mol CH_4 / dm^3.s

$-r'_{CH_4}$: the mol CH_4 / g catalyst.s

dX : the differential of reaction conversion

dV : the differential of reactor volume

dW : the differential of embedded catalyst weight inside reactor

CHAPTER 4

RESULTS AND DISCUSSION

4.0 Introduction

This chapter describes the results and discussions for this research project. Basically, this project has been divided into three major phases. The first phase covers the design, fabrication, development and commissioning of steam methane reforming test rig bench system. The second phase is the stage to build up an interchangeable micro scale reformer. Lastly, for the third phase is the process to affirm and prove that correlation of first and second phase manages to generate the methane conversion accordingly to the theory based on material catalyst used. The new designs had shown a significant improvements in these areas, relative to existing practice and briefly discussed in the succeeding sub-sections.

4.1 Development of SMR Test Rig Bench

This subsection describes the outcome of Phase 1 which is the development of SMR test rig bench as methane conversion platform analysis and also validation of design work according to the SMR operation theory and improvements concerning the test rig bench systems operation including control strategy.

4.1.1 Steam Methane Reforming Test Rig Bench Function Test

The completion of the test rig means that the phase 1 of conceptual design is finished. Then, the test rig is undergoing hot commissioned to ensure all units are functioning according to the theory and application principle. The completed test rig bench is shown in Figure 4.1.

Figure 4.1 (a) shows the complete test rig bench chassis. The primary target of this chassis is the placement support for all unit operations. The chassis body is made of mild steel, which consists of 2 inch hollow bar, 1 inch and 2 inch plat bar, 1/2 inch tubing and 1/2 inch angle bar. The rubber wheels are installed to ensure that this chassis become portable for mobile capability.

Figure 4.1 (b) shows the overall assembly of unit operation on the chassis. The arrangement of unit operation was depends on their stage of pretreatment upstream and downstream. Figure 4.1 (c) shows the arrangement of pretreatment stage is positioned relatively lower to the upstream stage position. This is due to the steam properties which flows upside to avoid condensation. The mixing point position is purposely designed to be parallel to the upstream. After the conversion takes place, the reformat gases flow down towards the downstream stage. The purpose of making the condenser at lower position is to assist the gravity drive flow. As additional, the separator is located at the lowest place to assure the liquid-gas separating works at optimal condition. The dryer is located higher than separator is to ensure the gas flows upward, while heavy molecule such as water vapor left behind inside dryer plus with the support of hydrophilic force from silica gels.

From Figure 4.1, the desired parameter has been tested and presented as in Table 4.1. The table shows the hot commissioning trial run for unit functional test. The hot commissioning is conducted at condition of steam to carbon ratio of 3 and reaction temperature varies from 500°C to 700°C. According to Table 4.1, the test rig is functioning according to the theory and literature. All gained parameter represent the input and output value for each unit operation. Finally the process flow of assembling SMR test rig is shown as in Figure 4.2. Meanwhile, the Figure 4.3 shows photo of completed mobile SMR test rig bench.

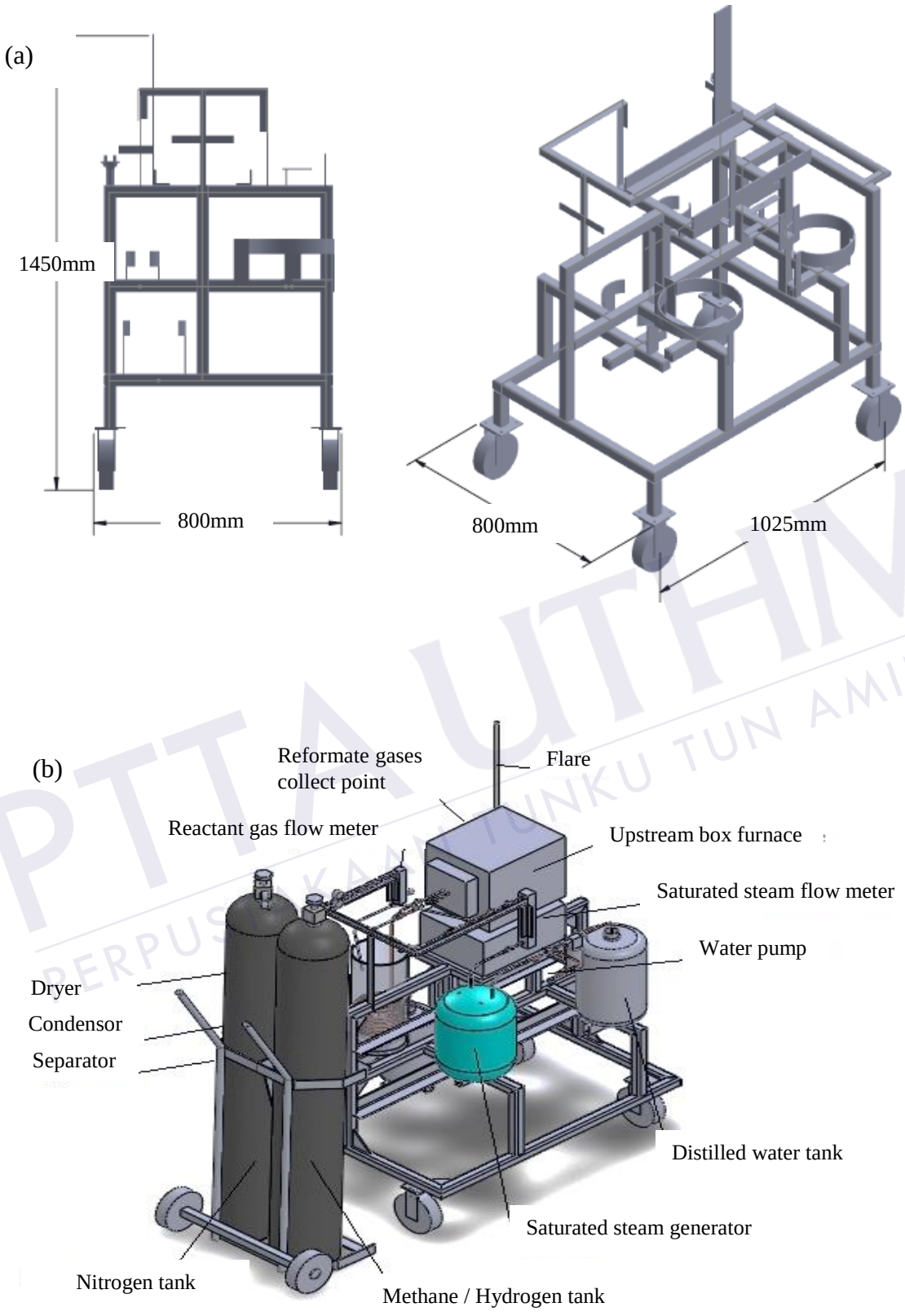

Figure 4.1 : (a) Completed chasis test rig, (b) Isometric view schematic diagram of assemble SMR test rig bench, (continued)

(c)

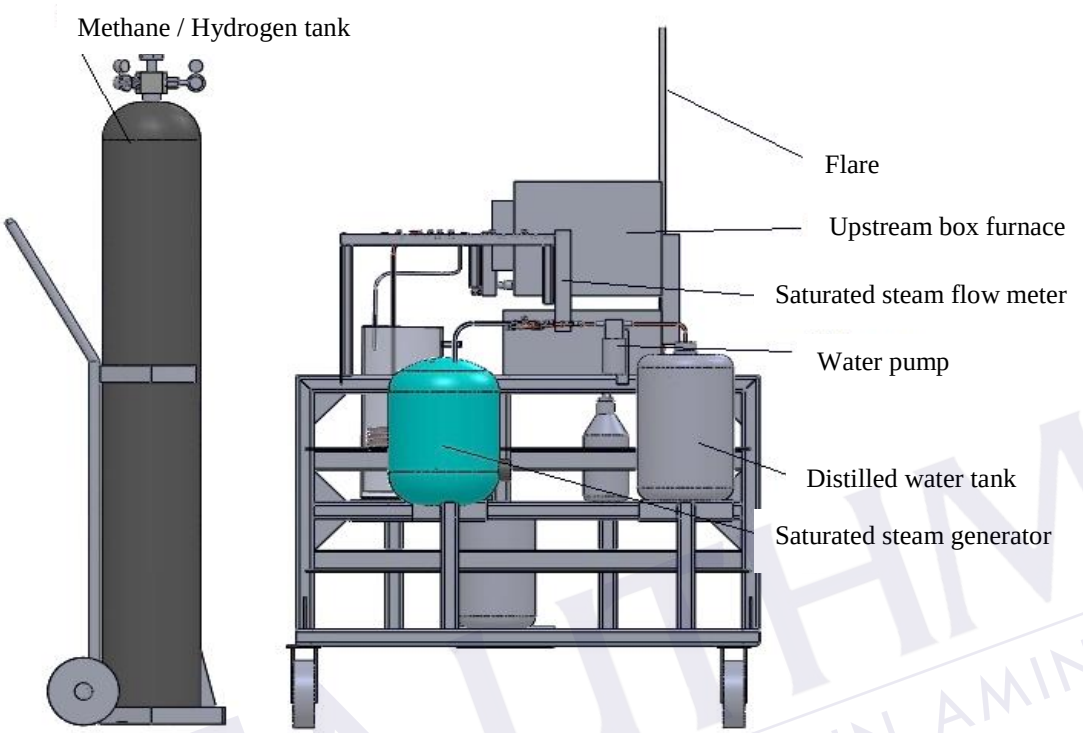

(d)

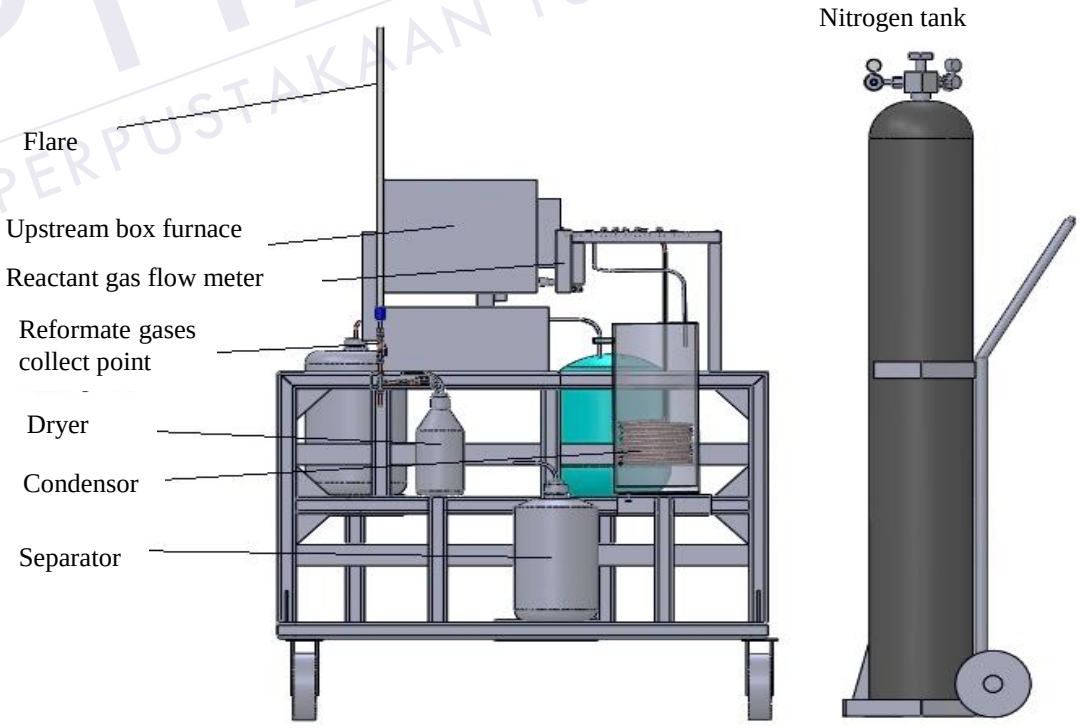

Figure 4.1 : (c) Left view schematic diagram of assemble SMR test rig bench, (d) Right view schematic diagram of assemble SMR test rig bench.

Table 4.1 : SMR test bench hot commissioning

Test	TI 101	TI 102	PI 101	FIC101		TI 103	PI 102	FIC 102	TI 104	P1103	TI105	PI104	furnace	TI106
	°C	°C	bar	lph	lpm	°C	bar	ml/min	°C	bar	°C	bar	°C	°C
1	124	137	1	40.00	0.67	54	0.9	140	144	0.8	500	0.25	600	37
2	122	136	1	40.00	0.67	53	0.9	140	143	0.8	550	0.30	646	37
3	123	138	0.9	40.00	0.67	55	0.8	140	146	0.8	600	0.30	691	36
4	122	138	1	40.00	0.67	54	0.8	140	145	0.8	650	0.30	720	35
5	125	145	1.1	40.00	0.67	62	1.1	140	154	1	700	0.3	787	36

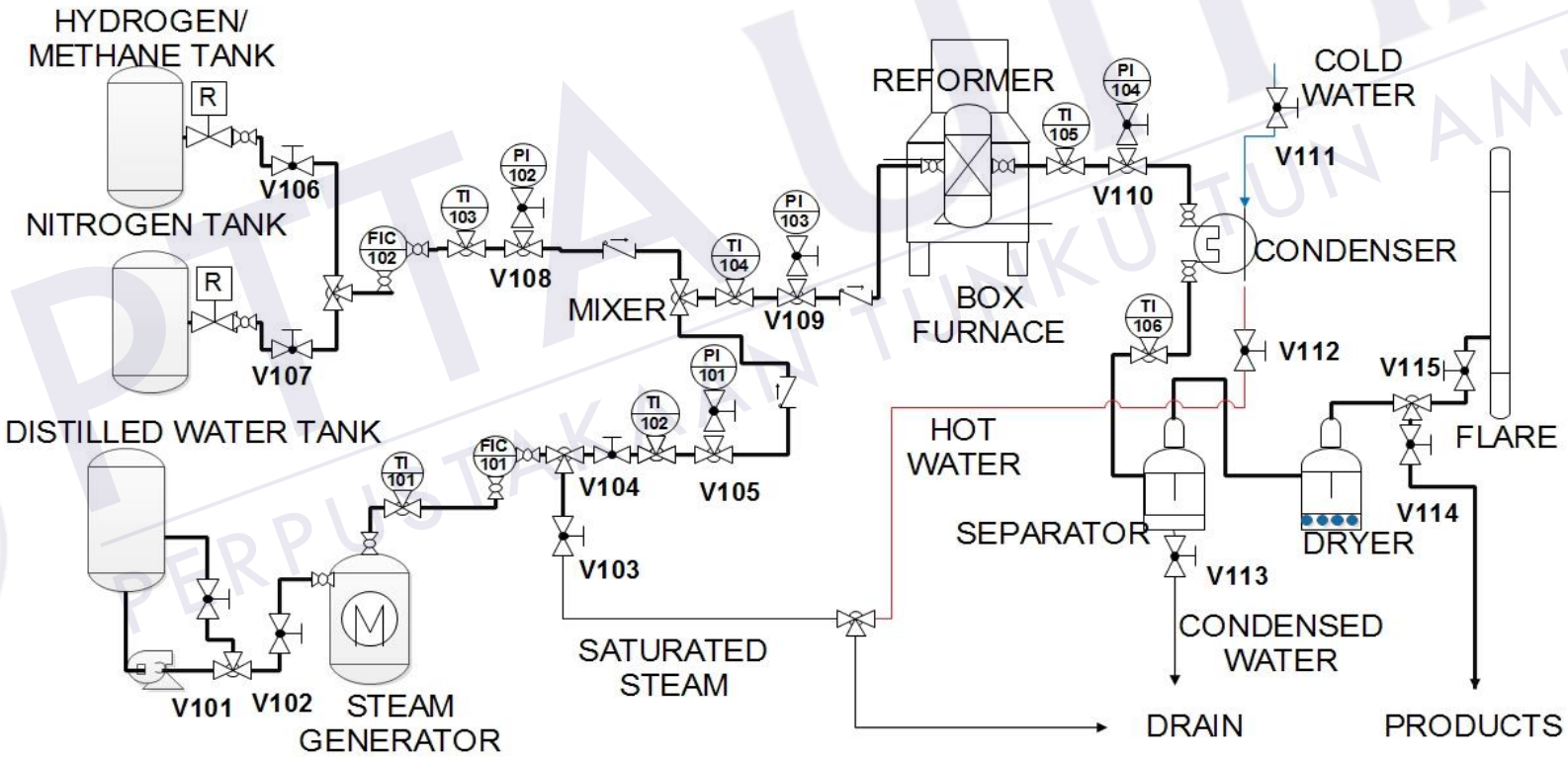

Figure 4.2: Process flow of assembling test rig

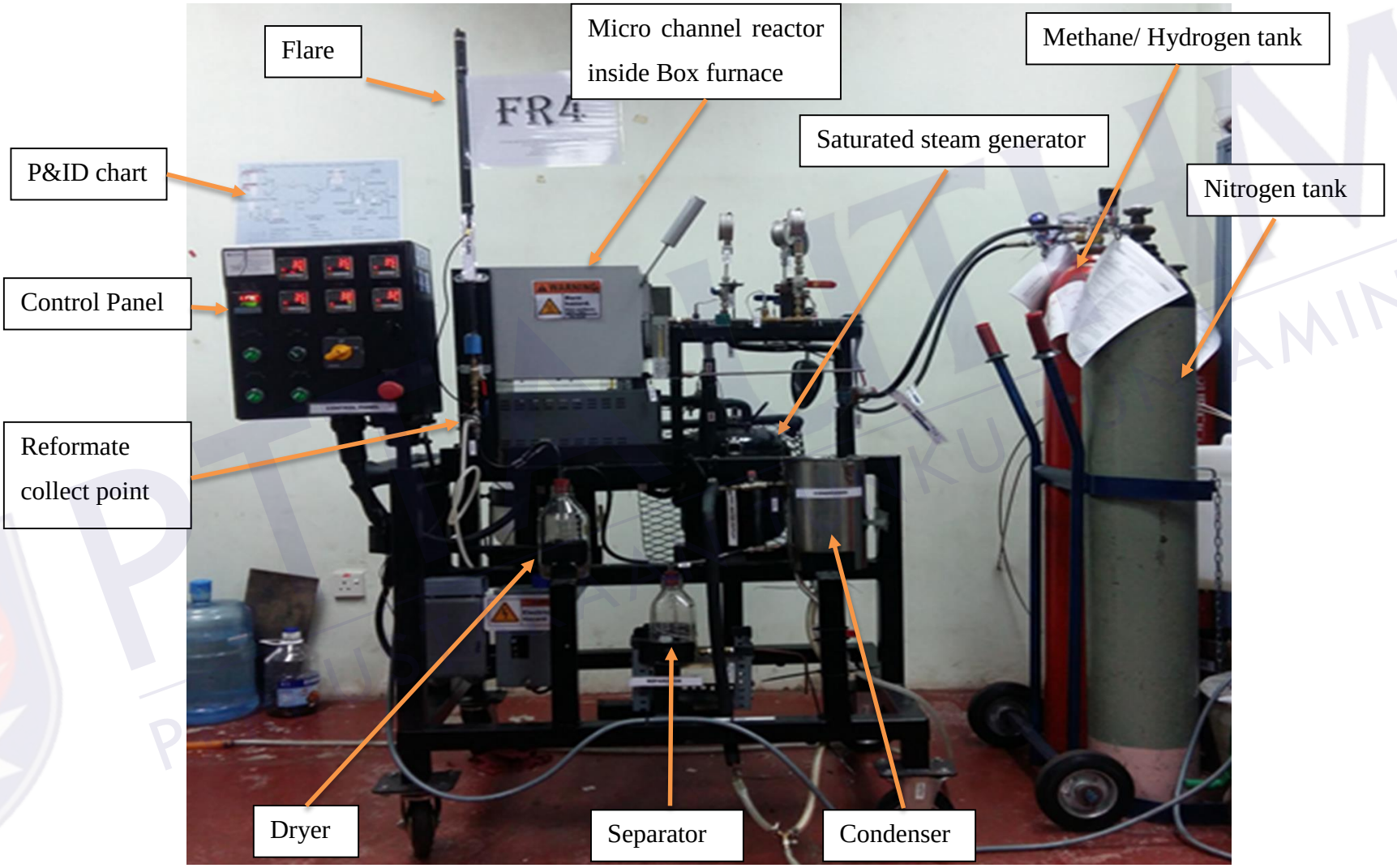

Figure 4.3 : Photo of complete mobile SMR test rig bench.

4.1.2 Standard Operating Procedure of Steam Methane Reforming Test Rig

In order to ensure the safety, reliability and repeatability of this prototype SMR test rig, a Standard Operating Procedure (SOP) has been developed, tested and verified. The following information in the form of the SOP is considered as a part of the outcome of this project. This SOP is an integrated and complied with the Asian Industrial Gas Association (AIGA) SOP. The SOP mainly consist as itemized below:

i. General safety
ii. Operator safety
iii. Emergency response
iv. Process safety
v. Communication
vi. Recommended operating procedure
vii. Material and equipment
viii. Box furnace inspection
ix. Start up procedure
x. Pretreatment stage – saturated steam generator
xi. Pretreatment stage –superheated steam converter
xii. Upstream stage – micro channel reactor
xiii. Downstream stage
xiv. Catalyst activation stage
xv. Shutdown procedure

As a precaution to operate this lab scale test rig bench, the operator should read and understand this general operating procedure. This procedure is covered of start-up and shut down profile, a pretreatment stage, up and down stream process and safety profile matter. Furthermore, the operator must comply and bond to Laboratory General Regulation. This SOP is developed based on the Asia Industrial Gasses Association (AIGA) requirement for Safe Startup and Shutdown Practices for Steam Reformers.

4.1.2.1 General Safety

This general safety operating procedure is well known and command at reforming industries. The primary role is covering parameters such as below:

i. Operator safety cut out
ii. Emergency response system
iii. Process safety and risk assessment
iv. Communication
v. Recommended operating procedure
vi. Materials and equipments
vii. Box furnace routine check

4.1.2.2 Operator Safety

All operators present in the SMR Test Rig Bench training, during startup or shutdown shall be obliged wear personal protective equipment (PPE) as called for by the rules. PPE be required to adhere to applicable regulatory criteria. PPE should include:

i. Lab coat required.
ii. Wear safety glasses.
iii. Hard hats required.
iv. Safety shoes and boots.
v. High temperature resistance gloves.
vi. Portable personal gas monitors.

All operators should have a proper hazard awareness including familiarity with material safety data sheets (MSDS) for methane, hydrogen, nitrogen and other chemicals and catalysts present in the area. All operators present during startup or shut down operations have to be prepared in accordance with experiment procedures.
Extra considerations for unit shutdowns:

i. Catalysts containing nickel should not be exposed to gases containing carbon monoxide at temperatures below 200 °C to avoid the formation of nickel carbonyl. During shutdown, the nickel-containing catalyst should be purged with steam or nitrogen gas prior reaching the nickel carbonyl critical formation temperature. If this does not occur, precautions should be taken to avoid exposure risk of the operator. SMR Trainer specific procedures have to be built up for the prevention of nickel carbonyl formation in steam reformer shutdowns.
ii. Some catalysts in the process are pyrophoric (e.g., pre-reformer, shift reactors); hence, air exposure must be kept off. The risk of an exothermic reaction and temperature increase is greatest during an SMR Trainer shutdown, when plant pressure can be near or at atmospheric pressure. Active temperature monitoring is essential during these periods. The operator has to be knowledgeable of this hazard and should abide by the safety instructions provided by the catalyst vendor.

4.1.2.3 Emergency Response

Prior to the startup or shutdown of the unit, the following emergency response requirements should be satisfied:

i. Availability of site-specific emergency response operations.
ii. Adequate training of operator in emergency response operations.
iii. Availability of firefighting equipment that has been tested and confirmed ready for use (e.g., hydrants, monitors, and extinguishers).

4.1.2.4 Process Safety

For a startup or shutdown, the following process safety factors must be considered:

i. Training and competency of SMR Trainer operators to perform the startup or shutdown procedures.
ii. Staffing levels adequate to insure a safe startup or shutdown.

iii. Limiting the number of individuals present in the SMR working area of essential personnel.
iv. Accuracy of startup or shutdown procedures.
v. Compliance with applicable work processes and rules.
vi. Accuracy of process documentation such PFD and P&ID.
vii. Effective execution processes prior to the plant start-up or shutdown.

4.1.2.5 Communication

Prior to the startup or shutdown of the unit, the following communication should take place:

i. Notify the Head of Laboratory or in charge person that the unit will start or stop generating product.
ii. Notify the Head of Laboratory or in charge person that the unit will start or stop drawing utilities.
iii. Notify the Head of Laboratory or in charge person the unit will be in startup or shutdown mode.

4.1.2.6 Recommended Operating Procedure

Site-specific operating procedures should exist to address applicable utility and auxiliary systems, including the following:

i. Process analyzers
ii. Critical local process instrumentation
iii. Proper testing and operation of safety devices
iv. Temporary connection management
v. Mechanical equipment handling
vi. Steam feed water systems
vii. Cooling water system preparation
viii. Piping and equipment lineup
ix. Routing of syngas
x. Process piping and vessels purge requirements

xi. Fuel system preparation
xii. Nitrogen
xiii. Flare
xiv. Drain of excess water
xv. Demineralized water supply;
xvi. Electric power
xvii. Heater management system preparation

4.1.2.7 Materials and Equipment

The following supplies should be available prior to startup and shutdown:

i. Portable analytical equipment and accessories
ii. Certified hoses
iii. Task-specific tools
iv. Safety equipment such as PTFE tape
v. Breathing air equipment
vi. Shower and hand washer
vii. Clear and brighter light

4.1.2.8 Box Furnace Routine Check

Throughout startup and shutdown periods, frequent visual observations of the furnace interior should be made through the inspection ports. Routine checklist is provided for furnace conditioning before and after SMR operating.

4.1.2.9 Start-up Procedure

This is the preliminary stage of SMR Test Rig Bench startup procedure routine check to ensure that it is function according to the P&ID format.

i. Plug and connect the 415Volt point supply. The plug is tight and fit closed between male and female connector before turning the switch ON.

ii. The EMERGENCY BUTTON should be in released condition. This can be checked by pushing out clockwise the button, if CAN'T PUSH means that the switch is OFF mode, and if CAN PUSH means that the switch is ON mode.
iii. Turn ON the yellow MAIN SWITCH of 60 Amp.
iv. Turn ON the TEMP. DISP. switch, make sure all temp displays are showing a digital temperature reading at range of 27°C till 30°C.
v. Fill in the DISTILLED WATER TANK until it reaches the 10 liter level.
vi. Hack in the Pressure Regulator of Methane and Nitrogen gases and make sure the pressure supply is 2 bar gauge.

4.1.2.10 Pretreatment Stage -Saturated Steam Generator

The pretreatment stage consists reactant feed supply of steam and methane, reactant mixture point and superheated steam converter. Established in the Figure 4.3, the details process flow for this level as below:

i. Turn ON the HEATER switch. This can be checked through TEMP. CTRL. STEAM. GEN is displaying temperature reading at a range of 27°C - 30°C.
ii. Change the Temperature Set Value at TEMP. CTRL. STEAM. GEN to 170°C.
iii. The V-101 is half closed.
iv. The V-102 is quarter opened.
v. The V-103 is fully opened.
vi. Confirm the V104 is fully closed.
vii. Once the Set Value at TEMP. CTRL. STEAM. GEN achieved 170°C, turn ON the PUMP switch.
viii. The saturated steam produced can be seen in side view glass of FIC101 and controlled according to the desired value. (This particular experimental work is kept constant at 40 lph).
ix. This saturated steam temperature is monitored through TI-101.
x. Visually check the saturated steam at the drain of stream 3.
xi. The TI-101 range should regulate at the range 120 till 127^{o}C.

xii. The saturated steam is kept running until FIC-101 reading become quite stable at 40 lph (+/- 2).
xiii. Once the FIC-101 is stable, the saturated steam is kept to produce for a minimum of 15 minutes.

4.1.2.11 Pretreatment Stage – Superheated Steam Converter

The process of producing superheated steam converter, which was covers superheated steam converter coil SSC-101, has been installed inside box furnace F-101 as shown in Figure 4.3. The details of process flow at this stage as below:

i. Turn ON the FURNACE switch. This can be checked through Furnace Temp Ctrl is displaying temperature reading at a range of 27°C - 30°C
ii. The Nitrogen is activated in streamline 6 at V-107 with 300ml/min at FIC-102.
iii. Change the Temperature Set Value at Furnace Temp Ctrl to the desired value as shown in Table 4.6 at a range of 600 till 850°C.
iv. Once the Process Value is achieved 380°C, immediately V-104 is fully open while V-103 is fully closed.
v. The Nitrogen and Saturated Steam is mixed and monitor at TI 104 and PI-103.
vi. This mixture is directed flow into the preheated coil inside the furnace to become superheated steam.

4.1.2.12 Upstream Stage– Micro channel reactor

The Steam Methane Reforming and Water Gas Shift reaction is taking position at this point. This point is likewise known as reactant conversion to desired product.

i. Continue from previous section (4.5.11).
ii. Once the Temperature Set Value at Furnace Temp Ctrl achieves the desired value as shown in Table 4.6 at a range of 600 till 850°C.
iii. Fully closed the V-107.

iv. Fully open the V-106 for Methane flow.
v. The Methane mass flow rate is controlled at FIC-102 according to the desired steam to methane ratio desired as in Table 4.7.
vi. The reaction is take placed at condition of 500 till 700°C, steam to carbon ratio of 2,3,4 and operate at reaction time of 300 minutes.

4.1.2.13 Steam to Carbon Ratio Analysis

This part is the most important in order to determine the precise quantity of methane flow rate as a sequence to the desired steam to carbon ratio. Essentially, this steam to carbon ratio is specified as the number of mole steam over mole of methane according to the stoichiometry equation as in Equation 3.1. From the Equation 3.1, number of stoichiometry is 1 for methane and 1 for steam. Thus, for other steam to carbon ratio cases, the exact mole value for both reactant is needed to be fixed. The SMR test rig is only capable to measure volumetric flow, therefore the stream temperature and pressure for both reactant are desired.

i. Referring to a standard Steam Table, value from TI-I02 and PI-101 are used as a standard to evaluate the mass flow rate in order to validate the Steam to Carbon ratio.
ii. Meanwhile, for methane mass flow rate, the critical value is obtained from TI-103 and PI-102.
iii. At the start, the mole of superheated steam at condition TI-102 and PI-101 is defined.
iv. Then the mole of methane is determined based on the steam to carbon ratio. The number of mole methane is equal to the number of moles superheated steam over ratio.
v. Once the mole of methane has been defined, the volume flow rate is established based on condition TI-103 and PI-102.
vi. Since the SMR test rig bench is fitted out with a general air flow meter, so it has been calibrated at a correction factor of 0.75. Therefor the air value is equal to methane flow times 0.75 (Mathesontrigas, 2010).
vii. All information gathered are recorded in Table 4.7.

Table 4.2 : Steam to carbon ratio

Saturated steam										
Ratio	TI102 °C	PI101 Bar gauge	density kg/m^3	V lph	V m^3/min	mass kg/min	mass g/min	mass g/s	MW of H_2O	mol (m/MW)
2										
3										
4										
Methane										
Ratio	TI103 °C	PI102 Bar gauge	density kg/m^3	mol (m/MW)	MW of CH_4	mass kg/min	mass g/min	mass g/s	V m^3/min	V lph
2										
3										
4										

4.1.2.14 Downstream Stage

At this point, the reformat gas output from reformer undergoes Condenser, Separation, Drying and Purifying proses.

i. As sequence of Upstream stage proses.
ii. The Condenser is function to cool down reformate gases. The V-111 is 30° opened while V-112 is set fully opened. The output is flown into the separator.
iii. The Separator acts to separate condensed steam and reformate gases. The condensed water level is assessed every 30 minutes at V-113.
iv. The reformate gases are then flown into a Dryer to eliminate any (water) moisture content.
v. The reformate gas sample is collected at V-114 at every 30 or 60 minutes depends on the test parameter.
vi. Once complete refilling Tedlar sampling bag at 1000ml, the V-114 is fully closed while V-115 is fully opened.
vii. The V-115 is remained fully open at any condition except during reformat gas collecting progress.
viii. The reformed gas is flared off as purifying process.
ix. All information collected are recorded as in Table 4.8.

Table 4.3 : SMR Data sheet

STEAM						METHANE				MIXING			REFORMER				CONDENSER	
	TI 101 °C	TI 102 °C	PI 101 bar	FIC101 lph	lpm		TI 103 °C	PI 102 bar	FIC 102 lpm		TI 104 °C	P1103 bar		TI105 °C	PI104 bar	Furnace °C		TI106 °C

4.1.2.15 Catalyst Activation Stage

This stage is necessary for activation of the deposited catalyst. The deposited catalyst is mainly composed of Nickel Oxide instead of desired Nickel. The Nickel Oxide has been going along with the reduction process to get rid of the element of Oxygen.

iv. Turn ON the FURNACE switch. This can be checked through Furnace Temp Ctrl, which is displaying temperature reading at a range of 27°C - 30°C
v. Change the Temperature Set Value at Furnace Temp Ctrl to 700°C.
vi. V107 is fully open and Nitrogen is supplied at 306 ml/min (air flow meter = 300 ml/min).
vii. The V-106 is fully closed.
viii. At that place should be ZERO STEAM flow.
ix. Once TI-105 is achieved 700°C, switch the Nitrogen to Hydrogen stream by employing the valve V-106 (open) and V-107 (close).
x. Control the Hydrogen flow at 300ml/min (air flow meter= 78ml/min).
xi. The activation process is pursued for a duration of 90minutes.

4.1.2.16 Shutdown Procedure

Basically, the shutdown procedure was reverted to the start up procedure. Whereby implementing the principle of 'the first item opened is the last item to be closed". The brief procedure was listed under:

i. Turn OFF the water pump switch.
ii. Change the Temperature Set Value at Heater Ctrl to 40°C. Once the Set Value has shown a decrease trend of temperature until 100°C, then immediately turn OFF the HEATER switch.
iii. Change the Temperature Set Value at Furnace Temp Ctrl to 40°C. Once the Set Value has shwon a decrease trend of temperature until 300°C, then immediately turn OFF the FURNACE switch.
iv. Turn OFF the TEMP DISP switch.

v. Turn OFF the yellow MAIN SWITCH
vi. Turn OFF the 415Volt point supply and unplug the input Plug.
vii. Fully close the V106 and V107.
viii. Fully close the pressure regulator for all gas cylinders.
ix. Fully close all valves accordingly to the numbering as in the P&ID.

4.2 The Art of Micro Reactor System

This subsection describes the outcome of Phase 2 which is the development of a new interchangeable micro scale reformer. This micro reactor system has a unique art trait of changeability usage for multiple type of catalyst. Through this Phase 2, main outcomes were designed, fabricate and develop a fix rigid micro scale reformer with an insert slot module which compatible for any catalyst test.

4.2.1 Micro Reactor Systems

This phase consists of design, fabrication, development and commissioning of an interchangeable micro scale reformer. The micro reactor system used for this work has been filed for patent with a reference number of IP2017300009. The accompanying information is an extract from the filed patent document.

The present invention is a Steam Methane Micro Channel Reactor that efficiently enables the endothermic energy for reforming process to be uniform and continuously supply by the Methane and steam during the response. The Methane gas and saturated steam are supplied at once into the superheated steam converter coils stream, whereby the saturated steam is heated up to become superheated steam. The Methane gas/superheated steam mixture is also known as reactant mixture which is directed into a multi micro channel module inside a cylindrical housing reformer. This reactant mixture is flown into the multi micro channel module with a gap space of

200μm each. The coated catalyst on the substrate plate, installed inside the micro channel module, is at once contacted and the reaction took place continuously among the reactant mixture and catalyst embedded.

Meanwhile, the outer cylindrical housing reformer, is continuously heated inside the box furnace. The reactant mixture produces a desired yield i.e. H_2 and also byproducts compound such CO, CO_2, unreacted CH4 and steam. Table 4.4 shows the summary of the designed and fabricated micro reactor systems physical properties.

Table 4.4 : Micro reactor system physical properties

No.	Part	Dimension	Material
1	Cylindrical housing body	42 mm OD x 50 mm L	Stainless steel
2	Superheated steam converter coils	90 mm OD x 10 coils x 1/4" tubing	Stainless steel
3	Micro channel module	33.4mm OD x 50mm L	Stainless steel
4.	Multi micro channel passage	6 slot x 15mm 50mm x 0.5 mm	Stainless steel
5.	Substrate plate	15mm x 0.5mm x 60mm	Stainless steel
6	Flange	80mm OD x 16mm L	Stainless steel

Figure 4.4 illustrates a schematic diagram of exploded isometric view of micro reactor system's component. Meanwhile, for Figure 4.5 is showing an installation view between coated substrate plate into multi micro channel passage.

The selection of materials for the micro reactor system is determined based on the requirements and operating conditions of the SMR process up to 900°C. This is due to the whole parts need to be able to resist high temperatures and should not be oxidized or interrupt the operation of steam methane reforming. The method of the invention serves to manufacture micro-structured of multi micro channel module and micro channel passage. It consists of micro -structured component (reactor) layers, more specifically of stainless steel 304 blocks and comprising passageways, channels in particular, which are loaded with catalyst.

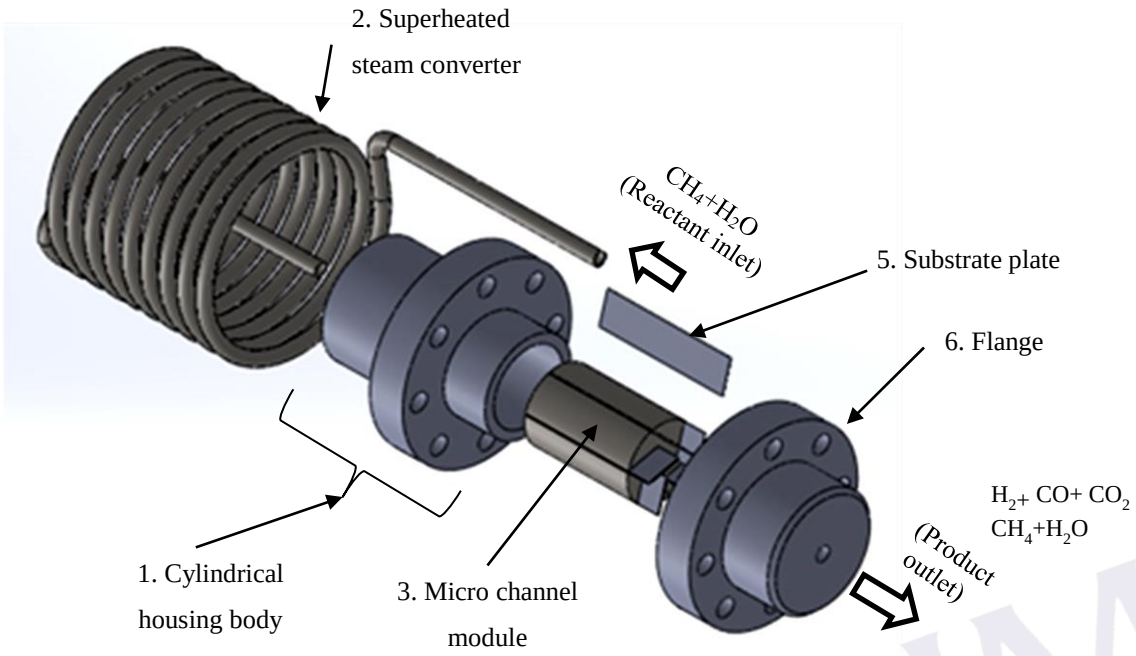

Figure 4.4 : An exploded isometric view of micro reactor system

Saturated steam (H_2O) and Methane gas (CH_4) function as reactant mixture and the Steam to Carbon ratio (S:C) is regulated according to the desired setting value. This reactant mixture is feed directed into superheated steam converter coils at the inlet point tubing of 16.4mm^2 flow areas. Essentially, the superheated steam converter coils acts as a heat exchanger for converting saturated steam to become superheated steam. The Methane gas (CH_4) is fully in vapor state and started to react with the superheated steam. This superheated steam converter coils is made of stainless steel 316 tubing of inner area 16.2mm^2 and is integrated along inside the box furnace. The superheated steam converter coils is designed as a one way flow circular coil shape which manage to improve heat transfer and secure the strong endothermic requirement of steam phase changes. This superheated steam converter coils is heated, up to 900°C and operated at 1 bar gauge.

Then the reactant mixture is fed into the micro channel passage and react with the catalyst on a coated substrate plate and straightly produces reformat gases as in Equation 3.1 and Equation 3.2. All parts were actively heated inside a box furnace at a certain operating temperature, in order to provide the energy needed to maintain the endothermic reaction. This SMR processing system has been heated, up to 900°C and operate at 1 bar gauge.

Referring to Figure 4.5, the concept generation of the multi micro channel module is selected for multiple pathways which synchronized the reactant mixture flow rates. It is very important to avoid flow rate choking phenomenon. The coated substrate plat covered up to 1300mm^2 coating area. It uses catalyst from a group of material consisting of Nickel, Ruthenium, Rhodium and supported by aluminide. Once the coated substrate plate is installed into a micro channel passage, the depth structure of the micro channel should have 200 μm depth and area of 5.2 mm^2 in order to increase potential contact surface area between coated catalyst and reactant mixture.

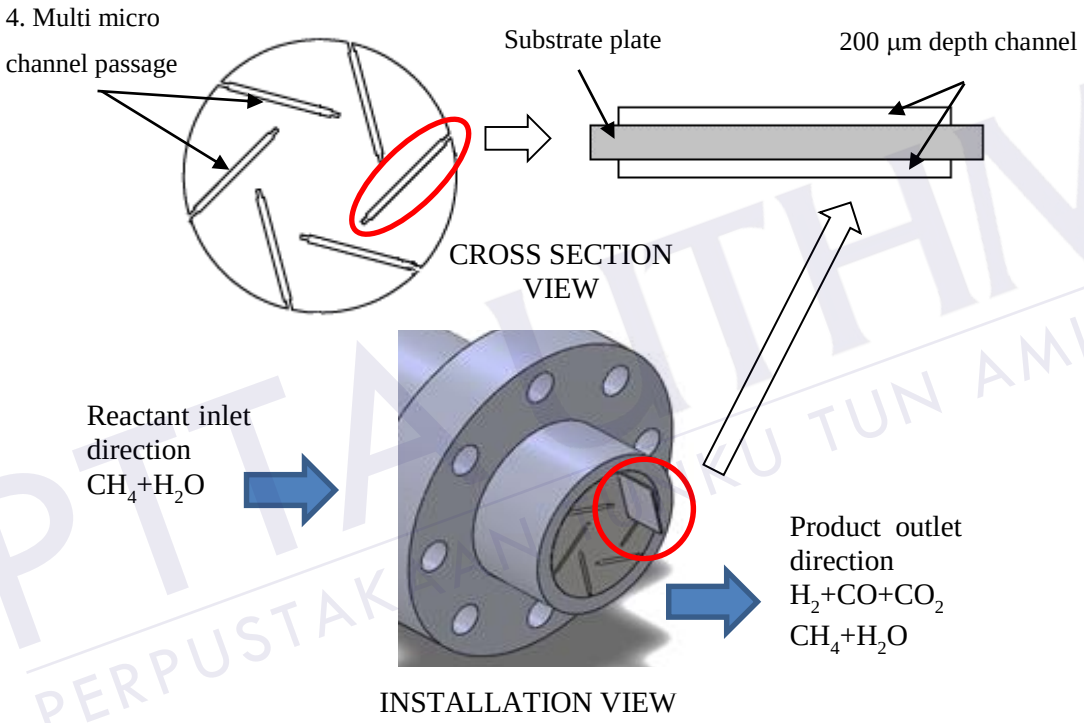

Figure 4.5 : Installation of coated substrate plate inside micro reactor system

As the reactant mixture flows in the gap space of 200 μm, this narrow compartment leads to improve the heat absorbing efficiencies. It is possible to improve Methane cracking and reforming process reaction. This improvement is due to the catalyst on the coated substrate plat subwall, inside the multi micro channel module was directly in contact. Thus the reaction occurs simultaneously and continuously among the reactant mixture and the catalyst embedded. Figure 4.6 shows a photo of the completed micro reactor system.

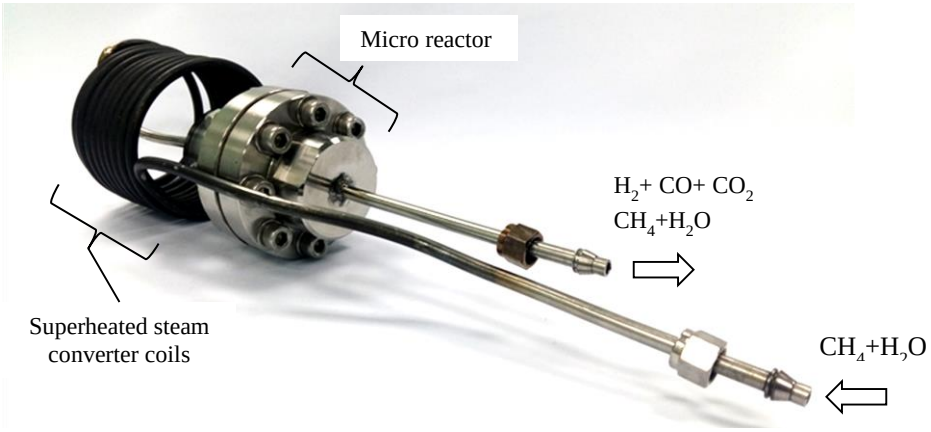

Figure 4.6 : Photo of complete micro reactor system

4.2.2 Micro Reactor Cold Commissioning

The designed, invented and developed micro reactor is undergoing several function tests to ensure the reactor is working according to the theory and withstand the actual reaction condition. Several tests have been executed such as vacuum, hydrostatic pressure, static pressure and reactant flow of the steam carbon ratio test.

4.2.2.1 Vacuum Test

Vacuum test is a procedure for detecting any leak in vacuum state by evaluating through pressure differences. From Table 4.5, it is clearly established that there is no pressure difference occurred, which means zero leak. The elongation of holding time is a more standard process which is employed. Hence, it is acceptable that the micro reactor is depressurized and managed to withstand up to one hour projection with zero leaking potential.

Table 4.5 : Vacuum test

No.	Holding time (s)	Vacuum state (bar)	Static state (bar)	Pressure difference (bar)
1	180	-25	-25	0
2	360	-25	-25	0
3	540	-25	-25	0
4	720	-25	-25	0
5	900	-25	-25	0

4.2.2.2 Hydrostatic Pressure Test

A hydrostatic pressure test is a manner in which pressure vessel such as the micro reactor is trying out for strength, leaks and pressure drop. Hydrostatic test is required to determine whether the pressure drop occurred at the micro reactor is proportional to applied pressure. The determination of the pressure drop test has been just to observe the deviation in force per unit area between two levels of network carrying fluid. Pressure drops occur when frictional forces, which is induced by the resistance to flow, act on a fluid as it falls through the micro reactor. The hydrostatic pressure test is taken in two conditions, namely with or without loading plates. The previous one means that the existence of the micro channel plates in the micro reactor while the latter means no micro channel plate was inserted into the micro reactor.

Table 4.6 shows that the pressure drop for loading plate and unloading plate condition is directly proportional to the input pressure. Relatively, this result shows that the loading pressure drop is slightly larger than the without load condition. This is due to the open area of micro channel path narrowed and pressure drops build up somewhat. Yet, both of the pressure drops for loading and without loading plates are considered to be minimum and both pressure drop does not exceed the operating pressure of 1 bar for the micro reactor.

Table 4.6 : Hydrostatic pressure test for load and without load plate condition

No	Input pressure (bar) gauge	Holding time (s)	Pressure drop (bar) – Load	Pressure drop (bar) Without load
1	0.2068	30	0.024	0.011
2	0.3447	30	0.0504	0.042
3	0.4826	30	0.076	0.0593
4	0.6895	30	0.1602	0.0901
5	1.0342	30	0.1538	0.1355

4.2.2.3 Static Pressure Test

A static pressure test is conducted to determine the maximum withstand the pressure of the micro reactor. It is served as a judge of the micro reactor's ability to accommodate the highest pressure before any leak occurred. Table 4.7 depicts the result of the static pressure test at pressures starting from 0.5 bar - 5.0 bar with a holding time of 600 seconds at each pressure. PASS judgment in based on zero leaking, vice versa to the FAIL judgment. Unfortunately, at 2.5 bar input pressure, the leakage occurs in micro reactor during holding time of 212.4 seconds. Even though it is a FAIL judgment, this micro reactor system is considered as successful since the intended operating pressure is below 1 bar gauge.

Table 4.7 : Static pressure test

No	Input pressure (bar) gauge	Holding time (s)	Remarks
1	0.5	600	PASS
2	1.0	600	PASS
3	1.5	600	PASS
4	2.0	600	PASS
5	2.5	212.4	FAIL

4.2.2.4 Steam to Carbon ratio

The functionaries test for the overall test rig are made out. A subtest, the vital path for reactant feed is performed. The steam to carbon ratio is specified as the reactant feed according to the number of Mole based on the SMR stoichiometry equation. The steam flow rate had been tuned at a constant value of 666.67 milliliter per minutes and operating condition used as in Table 4.1 (Test no.5). Granting to the literature, optimum steam to carbon ratio is laid on a range of 1.8 to 3.3. The steam to carbon ratio analysis is shown as in Figure 4.7. The outcome of this test verifies that this test rig is able to perform a bigger range of steam to carbon ratio experiments.

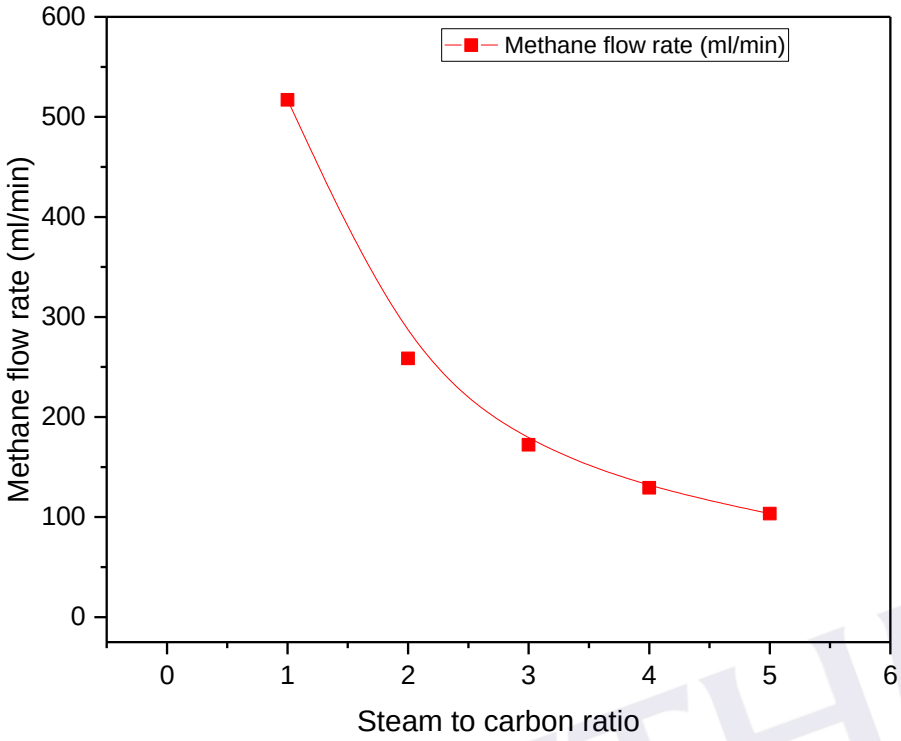

Figure 4.7 : Methane flow rate based on steam to carbon ratio.

4.3 Reforming Catalytic Analysis

This subsection describes the outcome of Phase 3 which is affirm and prove that correlation of first and second phase manages to generate the methane conversion according to the theory based on material catalyst used. The SMR test rig bench is potentially able to provide evaluation of SMR experimental tests, such as catalyst performance, conversion rate and products at output stream.

4.3.1 Catalytic Behavior Effect on Steam Methane Reforming Yields

Steam methane reforming is a ubiquitous industrial process which involves thermal integration due to its high energy requirement of reaction temperature (400-900 °C). Basically the SMR yields a mixture of hydrogen (H_2) and carbon monoxide (CO) is likewise known as synthetic gas. The CO at output stream is further reacted with excess steam (H_2O) to bring about carbon dioxide (CO_2) and increase H_2 yield. The exact composition of the reformed gas leaving the reactor depends upon the feedstock composition, operating conditions such as temperature and pressure. Hence, an

increased temperature favors the conversion of hydrocarbons, but result in a higher concentration of CO. Meanwhile, a low reforming temperature has resulted in a mixture containing relatively high amounts of methane (CH_4) and CO_2. The steam reforming and water-gas shift reaction are equilibrium reactions, which add limitations to these processes.

As mentioned before, the aim of this project is to create a low-temperature reformer, capable of intensified CH_4 conversion, H_2 yield and get down the carbon formation at 700°C or lower. Thus, this chapter is the Phase 3 and consequently to affirm and prove that correlation of first and second phase manages to generate the methane conversion according to the theory based on material catalyst used. Furthermore, the interchangeable catalyst traits of reformer and also be able to process different feedstock such as natural gas and alcohols.

4.3.2 Effect of Reaction Temperature on SMR

The catalytic experiment of SMR has been successfully performed according to the process operating conditions as in Chapter 3 (Table 3.8). This subchapter discusses further the reaction temperature effect on SMR yields. It is significant to set the optimal reaction temperature for SMR since each newly developed catalyst has their own peculiar traits of endothermic reaction, which only optimally works at a certain temperature. Therefore, in order to study the influence of reaction temperature on catalytic behavior, experiment are conducted for five different reaction temperatures such as 500°C, 550°C, 600°C, 650°C and 700°C at steam to carbon ratio of 3 (S:C 3) with elevating 300 minutes reaction time at an interval of 60 minutes and using 10wt% loading of Nickel aluminide as the catalyst. The experiments only involve a fresh catalyst each.

The Figure 4.8, it shows the results of the reaction temperature effect on Methane conversion which is plotted in the form of error bars. This result is clearly shown that for every mean value is placed well within the corresponding confidence interval and straightly proved that the value has a very good reproducibility of the repeated experiment.

Figure 4.8 shows the methane conversion rises proportionally to the reaction temperature except at 700°C. At reaction temperature 700°C, methane conversion is inversely proportional to reaction time. At the beginning methane conversion already occurs and rises, simply due to the possible effect of bigger heat flux at this period. Methane cracking is rapidly occurred which lead to drastically carbon formation and deposited on top of the active catalyst surface area. Thusly, the catalyst at the 700°C starts to deactivate because of carbon clogging. Among these reaction temperatures, temperature at 650°C yields the maximum methane conversion of 52.75%, follows by 600°C, 700°C, 550°C and lastly 500°C. It is founded along the catalytic behavior of the Nickel aluminide (10wt % loading) inside the micro channel reactor, 500°C points has become the lower limit due to zero reaction activity and 700°C is the upper limit due to the catalyst deactivation activity, for this reaction temperature.

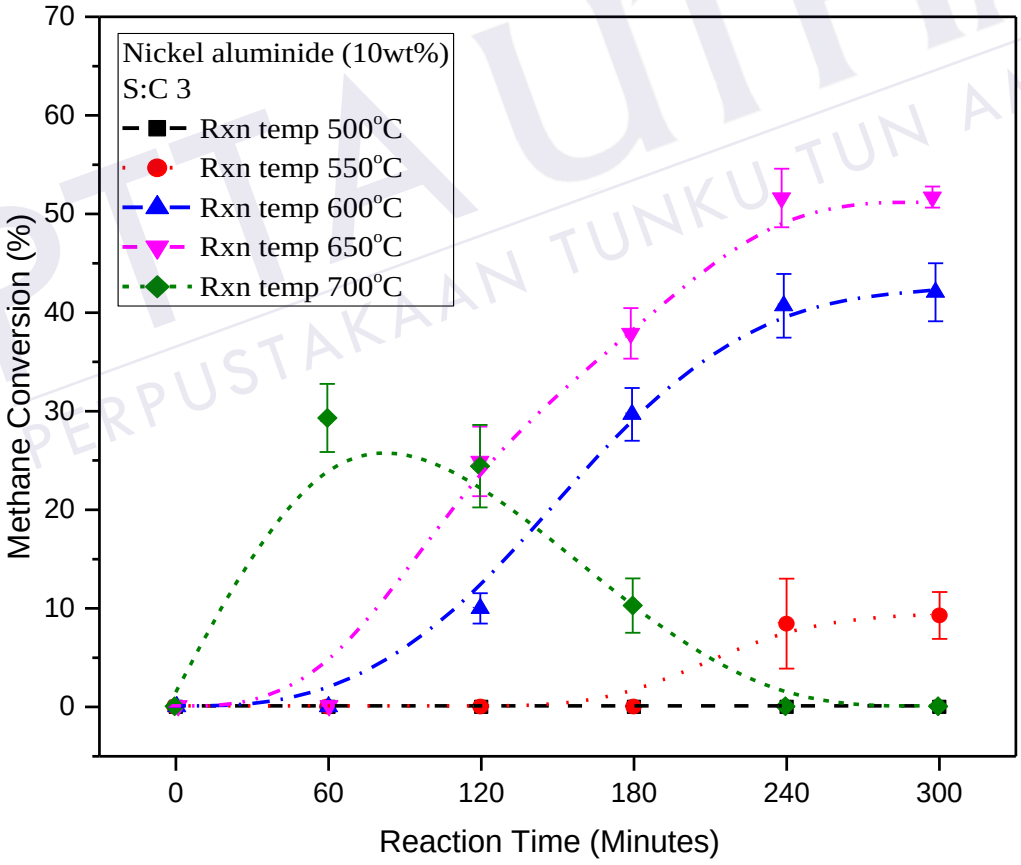

Figure 4.8 : Effect of reaction temperature on methane conversion (error bars of 95% confident interval mean value statistic).

These limits prove that the SMR endothermic reaction is sensitive to the reaction temperature. In conditions of stability, only 600°C and 650°C show a trend of heterogeneous catalytic traits, which is lagged from 0 to 60 minutes (pre-conversion), logarithm from 60 to 240 minutes (rapidly increasing conversion) and stationary stage from 240 to 300 minutes (stable remained unchanged of the transition). Results exhibit similar trend as work done by Bej et al., (2013); Cheng et al., (2011); Jeon et al., (2017); Maluf & Assaf, (2009); and Simsek et al., (2013).

Figure 4.9 shows a summary of the reaction temperature effect on SMR yield. As the reactant for SMR and WGS reaction, methane and steam at outlet stream decrease proportionally to the reaction temperature. This trend proves that the reactant is consumed and converted during the reaction stage. But yet only at 500°C and 700°C have shown increasing due to the low conversion during the reaction. Both reactant remain in the outlet stream due to developed catalyst efficiency is not 100%. This loop has become a potential future work study either to achieve full conversion or at least enhance the valet.

The hydrogen, 650°C yields the upper limit at 41.34%, follows by 600°C, 700°C, 550°C and lastly 500°C. During these works, only 600°C and 650°C demonstrate a stability trend of hydrogen production, since the heat flux is supplied at most optimum performance for SMR and WGS reaction. The noted trend is quite alike to the methane conversion of heterogeneous catalytic traits. For 650°C, the hydrogen formation is dominated at a value of 41.34% at outlet stream compare to the unreacted methane 9.35%, unreacted steam 38.87%, carbon monoxide 0.4% and carbon dioxide at a value of 10.04%. It is summarized that 650°C has become the optimal reaction temperature of the developer catalyst.

Figure 4.9 shows that the carbon monoxide and carbon dioxide are inversely proportional to each other, due to the mass balancing at output stream. However, at 600°C and 650°C, results show a stability trend of carbon monoxide and carbon dioxide production. For 650°C, the rate of carbon dioxide formation grows much faster compare to the one of carbon monoxide at a CO_2/CO ratio of 25.29. This implies that the WGS reaction took place inside reformer. This is similar to the works done by Howe et. al., (2001). For 650°C, a major parameter for syngas production (H_2 + CO)

by the SMR, the ratio of hydrogen to carbon monoxide yields a maximum ratio value of 109.66, which it indicate that the WGS reaction dominantly converts carbon monoxide in SMR to produce hydrogen and carbon dioxide. Moreover, the carbon monoxide formation rate decreases to the reaction temperature and straightly help to procure from any solid carbon formation which may lead to catalyst clogging. By comparing both yield, it is proven that the developed catalyst on a substrate plate is functionally worked inside a micro channel reactor.

The Figure 4.10, methane disappearing rate ($-r'_A$) is introduced, which exhibits the similar pattern in Figure 4.8. The obtained result for 650°C shows the highest conversion number of mol for methane for every weight of catalyst at reaction time (seconds) 1.32. The $-r'_A$ value becomes a critical point for the SMR scaling up stage, especially in reformer sizing and reactant mass flow rate.

As the summary of effect reaction temperature on SMR yields, it can be determined that the optimal point is 650°C with maximum conversion of 52.75%. It is discovered that 500°C and 700°C become the lower and upper bound. Results prove the developed catalyst inside micro channel reactors is successful to work between ranges of 500°C and 700°C, reaction temperature of steam to carbon ratio of 3, reaction time of 300 minutes at intervals of 60 minutes and using 10wt% loading of Nickel aluminium as the catalyst.

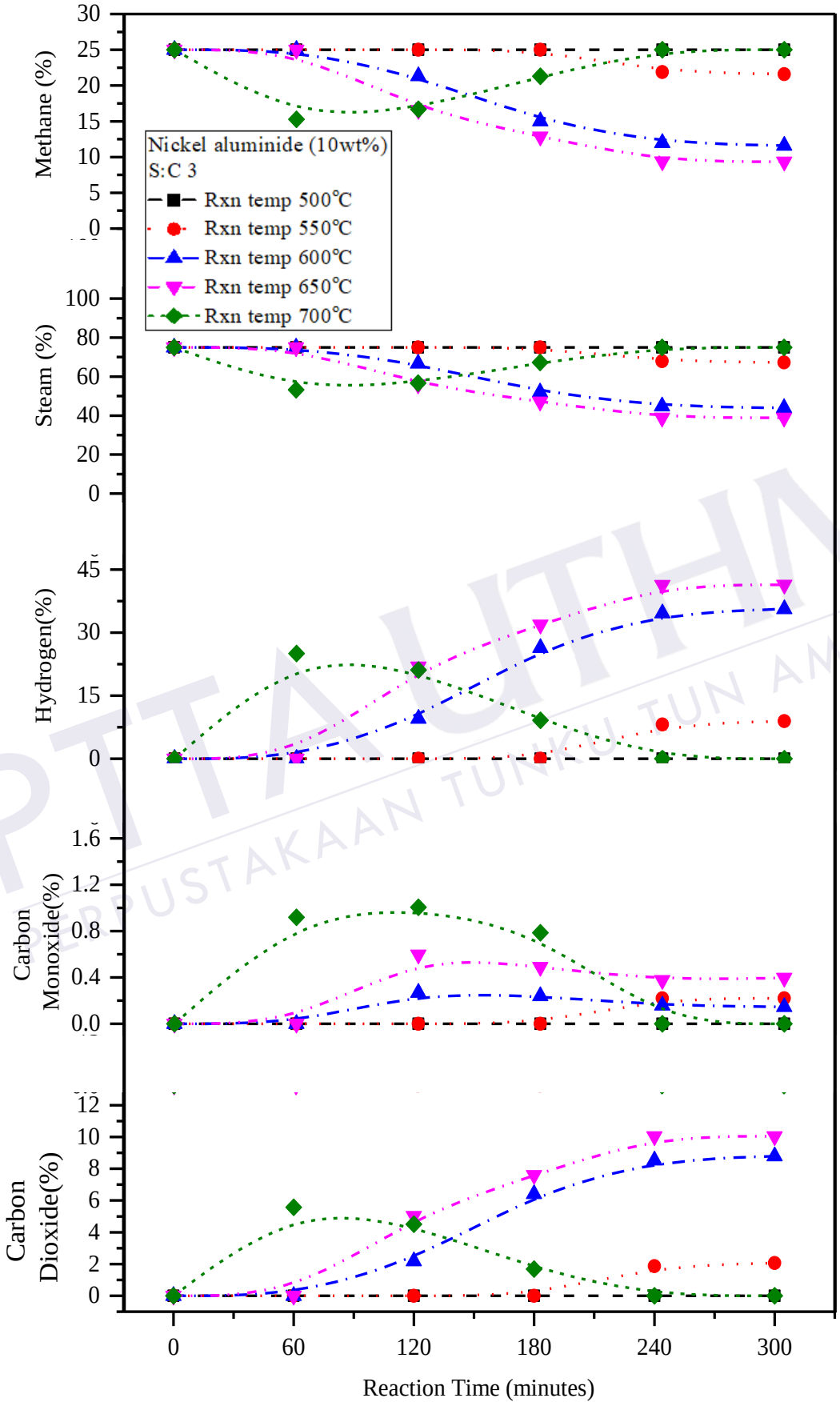

Figure 4.9 : Effect of reaction temperature on SMR yield.

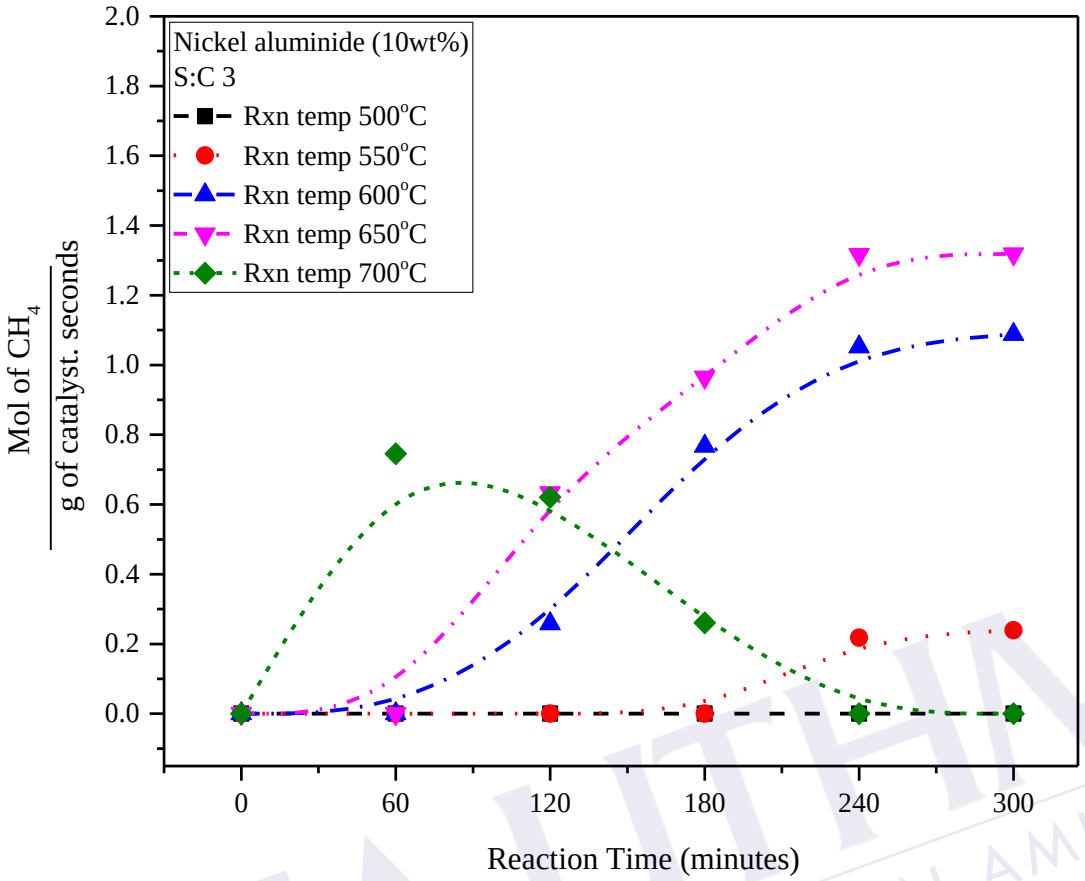

Figure 4.10 : Effect of reaction temperature on methane disappearing rate.

4.3.3 Effect of Steam to Carbon Ratio on Steam Methane Reforming Yields

The catalytic experiment of SMR successfully undergoes according to the process status. This subchapter is discussed further the effect of steam to carbon ratio on SMR yields. There are three steam to carbon ratio that have been tested, S:C 2, S:C 3 and S:C 4. All the steam to carbon ratio reaction took place by applying the same reaction operating condition of reaction temperature 650°C from subchapter 4.3.2, reaction time of 300 minutes at intervals of 60minutes and using 10wt% loading of Nickel aluminide as the catalyst. The 650°C becomes the optimal reaction temperature of this developed catalyst. It is proven that this point produces the maximum methane conversion at stable condition of heterogeneous catalyst fundamental.

Figure 4.11 shows the results of steam to carbon ratio effect on Methane conversion which is plotted in the form of error bars. This result clearly shows that every mean value is laid well within the corresponding 95% confidence interval and straightly proved that the value has a very good reproducibility of the repeated experiment.

Figure 4.11 also shows a variation of steam to carbon ratio effect on methane conversion. It is distinctly established that methane conversion is proportional to the steam to carbon ratio. The S:C 2 gives minimum conversion of 30.14%, as compared to the maximum 65.56% obtained in S:C 4. This outcome follows the principal of steam methane reforming reaction at multiple steam carbon ratio. The methane conversion increases as the steam to carbon ratio increases. This finding is similar to the work done by Maluf et. al., (2009), Bej et. al., (2103), Cheng et. al., (2011), Ayabe et. al., (2003), and Mbodji et. al., (2012). This phase took place due to the excess steam at reactant stream, which enhances the methane cracking reaction to make high yield at the product end stream. For this SMR reaction, methane is the limiting reactant whereby it is finished first, then with enough or excess steam, the methane conversion rate can be increased.

The Figure 4.11, only S:C 2 and S:C 3, exhibit trends of heterogeneous catalytic traits between 0 and 300 minutes, which are lag (pre-conversion)), logarithm (rapidly increasing conversion) and stationary stage (stable remained unchanged of the conversion). Meanwhile, for the S:C 4, even though methane conversion is high and towards stability, it already exceeds the defined reaction time range of 300 minutes. For comparison between S:C 2 and S:C 3, the S:C 2 has faster and smoother trend line of stability, which start the stationary stage as early 180 minutes. However, the S:C 3 yields the highest methane conversion compared with S:C 2. It is inferred that S:C 3 had become optimum steam to carbon ratio for the developed catalyst.

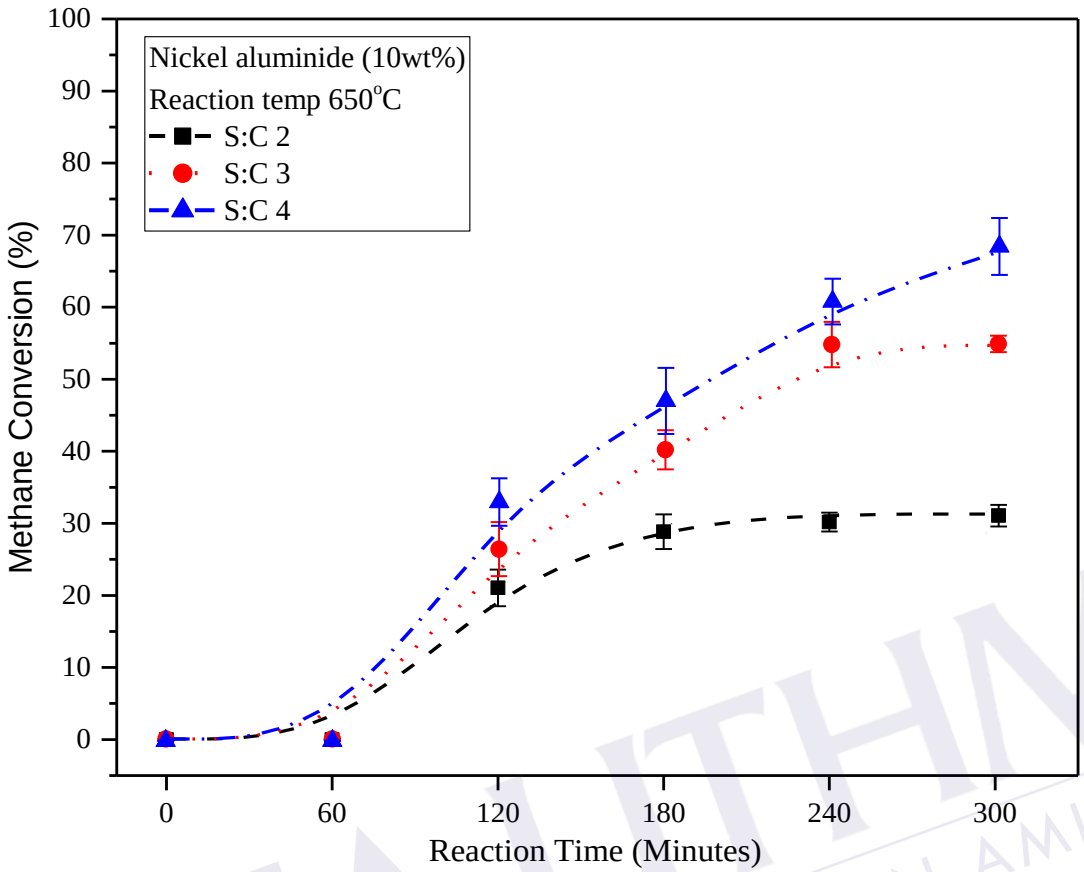

Figure 4.11 : Steam to carbon ratio effect on methane conversion (error bars of 95% confident interval mean value statistic).

According to the Figure 4.12, the methane and steam at outlet stream decrease proportionally to the steam to carbon ratio. This is due to the consumption during SMR and WGS reaction. Unfortunately, the steam mass flow rate for S:C 4 has the biggest amount compare to the S:C 2 and S:C 3. It is due to supply excess steam and mostly becomes waste due to WGS requires only desired certain mass flow rate of steam to react with the carbon monoxide.

The hydrogen formation demonstrates the same style and rule with the methane conversion. The maximum hydrogen formation is achieved at S:C 3 with a value of 41.34% and the minimum 33.29% is obtained by S:C 2. As reported by Simsek et. al., (2011), according to Le Chatelier's principle, excess steam in the product direction converts the generated carbon monoxide by SMR into hydrogen and carbon dioxide, which leads to the highest H_2/CO ratios as observed at S:C 3 in this work. Even though the S:C 4 yields the maximum value of methane conversion, simply due to WGS

reaction dominantly laid on the S:C 3, the hydrogen formation of S:C 3 slightly becomes greater as compared to the S:C 4. For S:C 4, only 20% methane is supplied to react with excess steam as compared to S:C 3 which obtained 25% of methane. It is straightly increased the hydrogen formation at outlet stream. In the other hands, carbon monoxide is limiting reactant in WGS, thus, it is unable to win over 100% while the conversion reaches unity.

Figure 4.12 also proves that the carbon monoxide formation impact by SMR and WGS reaction, is inversely proportional to the carbon dioxide formed from the mass balancing between desired and undesired product in the output flow. It demonstrates that the carbon dioxide formation ratio of CO_2/CO (WGS reaction converts carbon monoxide in SMR to produce hydrogen and carbon dioxide), for S:C 2, 3 and 4 are 23.54, 25.30 and 49.2 respectively. Thus, it proves that the carbon monoxide formation decrease proportionally to the steam carbon ratio, which prevents the solid carbon to build up on top of the developed catalyst. This finding was similar to the reported works by Graf et al., (2007), Radfarnia & Iliuta, (2014), Simsek et al., (2011) Wang F. et al., (2013), Wang H. et al., (2012).

The methane disappearing rate ($-r'_A$) for steam to carbon ratio is recorded as in Figure 4.13. It shows $-r'_A$ is proportional to the steam to carbon ratio. But due to the variation of the methane mass flow rate supplied for each steam to carbon ratio, this has been influenced the $-r'_A$ values. This S:C 3 slightly crosses over the S: C 4 at the point of 180 minutes onwards until it achieves an almost similar point to each other at 300minutes. The S:C 3 has already achieve the stationary stage of heterogeneous catalyst at 240 minutes. Compared to S:C 4, the projected trend is continuously raised and exceed the specified reaction time range of 300 minutes. The maximum $-r'_A$ at optimum stability trend is laid on S:C 3 at valued of 1.32 .

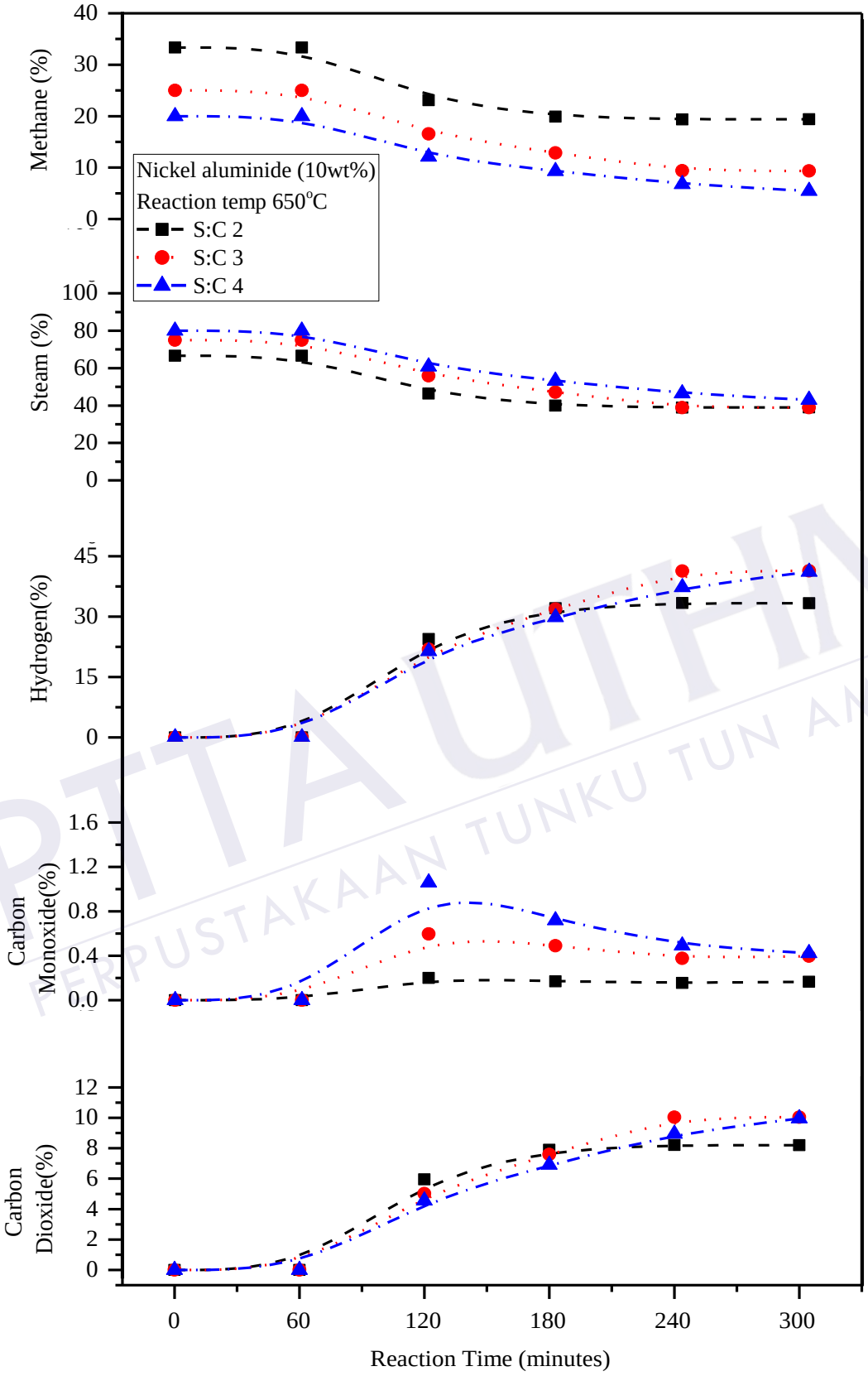

Figure 4.12: Summary effect steam to carbon ratio on SMR yield.

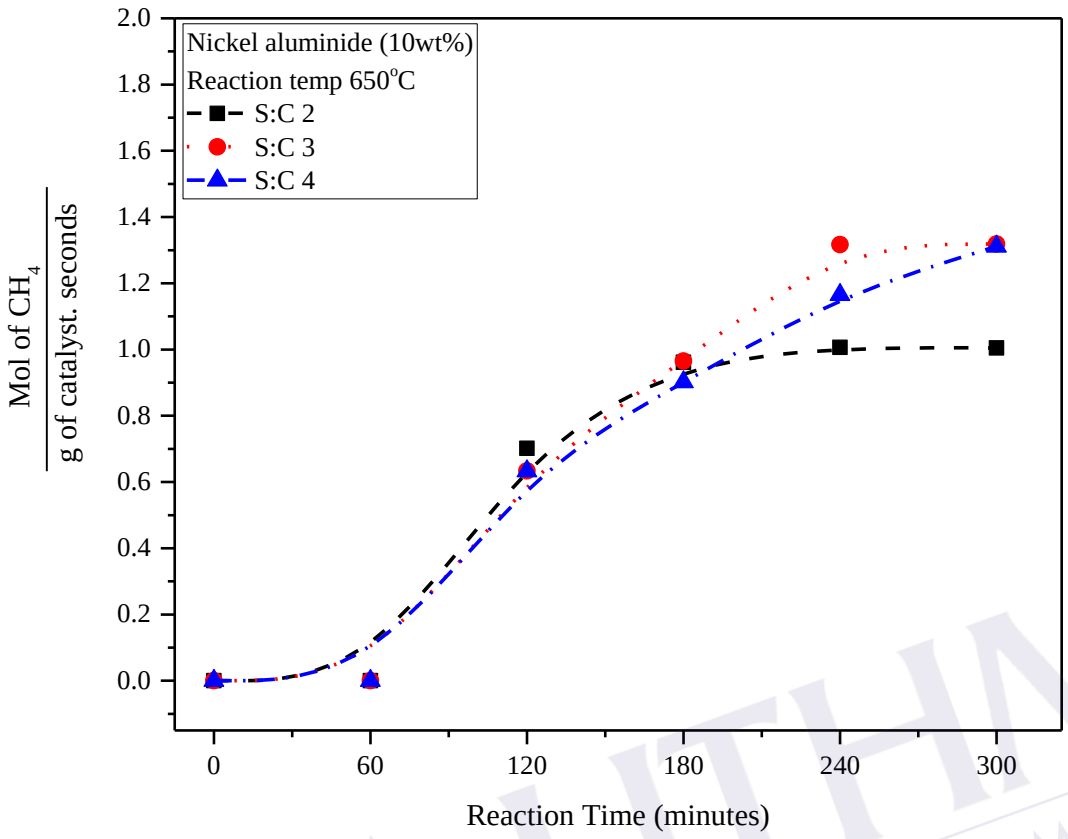

Figure 4.13 : Effect of reaction steam to carbon ratio on methane disappearing rate

As the summary of effect steam to carbon ratio on SMR yields, it is found that the most optimum point is S:C 3 with a methane conversion of 52.75%, the maximum hydrogen yield of 41.34% and the maximum $-r'_A$ of 1.32. The developed Nickel aluminide by using substrate plat inside a micro channel reactor assists to augment the SMR reaction process. For the succeeding level, this steam to carbon ratio is employed as a constant parameter for the next tested parameter.

4.3.4 Effect of Multiple Type Catalyst Loading on SMR

This subchapter is discussed about the effect of multiple type of catalyst on the SMR yields. Three types of catalyst loading have been tested, which are Nickel aluminide (10wt%), Ruthenium aluminide (0.1wt%) and Rhodium aluminide (0.1wt%). All catalyst loaded are tested by using optimum condition setting process yield, as described in subchapter 4.3.2 and 4.3.3, which are a reaction temperature of 650°C and steam to carbon ratio of 3. The test is conducted in reaction time of 300 minutes at an

interval of 30 minute measurement points. This reaction measurement time interval has been set half of the previous experiment since Ruthenium aluminide and Rhodium aluminide are expected to show faster reaction rate compared to the Nickel aluminide. For this test, Nickel aluminide (10wt%) is classified as the conventional catalyst, while the Ruthenium aluminide (0.1wt%) and Rhodium aluminide (0.1wt%) are noble metal based catalyst.

In order to validate the data, a 95% confidence interval of the mean value is analyzed. By adverting to the Figure 4.14, showed the results of the multiple catalyst effect on Methane conversion which was plotted in the form of error bars. This results is clearly shown that every mean value is plotted within the corresponding 95% confidence interval. It is straightly proved that the value has a very good reproducibility of the repeated experiment.

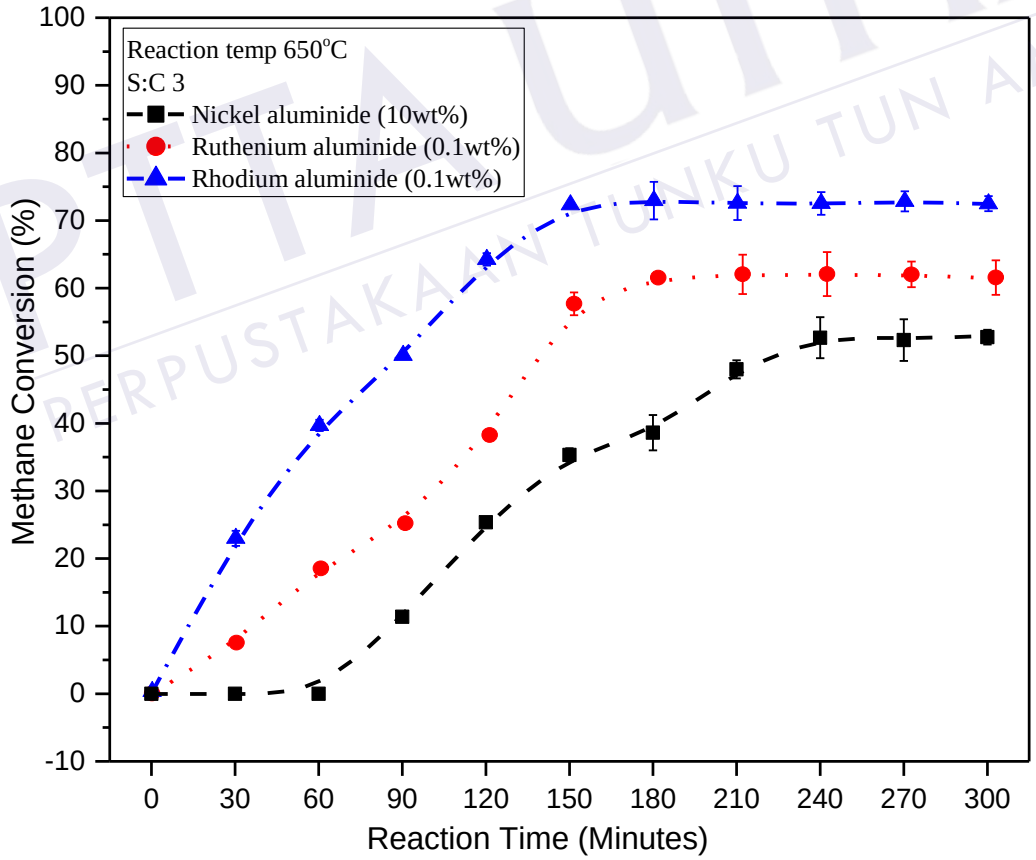

Figure 4.14: Multiple type of catalyst effect on methane conversion (error bars of 95% confident interval mean value statistic).

Figure 4.14 shows the methane conversion is proportional to the type of catalyst used. Rhodium aluminide yields the highest conversion of 72.63%, follows by Ruthenium aluminide with 61.75% and lastly Nickel aluminide of 52.75%. From this study, it infers noble metal had a faster reaction rate as early after 0 minutes reaction time and higher methane conversion, compare to the conventional catalyst which only start having a conversion after 60 minutes reaction time. The gas chromatography analysis of output stream gas is conducted gradually by batch at interval 30minutes, therefore the transition which occurs in the middle of 0 to 30 minute period is unable to be identified.

The figure also shows the Nickel aluminide achieves the stationary stage at 240 minutes, Ruthenium aluminide at 180 minutes and Rhodium aluminide at 150 minutes. It is demonstrated that the role of noble metal as catalyst for SMR has high potential to speed up reaction rate and enhance conversion. This claim is supported by Beurden, (2004), Rajagopal (2007), Stefanidis & Vlachos (2010) and Yang et al., (2014). It is highlighted that the noble metal is used as catalyst to improvise the metal surface area by increasing the number of active sites for reactant conversion. This sites functionally acts as a point of chemisorption of atoms in reactant and reduce activation energy for conversion, which help to secure the C–H bonds cracking become more effective.

Figure 4.15 summarize the effect of multiple type of catalyst loading on SMR yield. The lowest unreacted methane is at 5% and steam of <30% laid on Rhodium aluminide. This proves that the reactant has been consumed and converted effectively during the reaction stage. Considering the unreacted steam shows a quite bit of redundancy, therefore potential loop study of correlation steam to carbon ratio with catalyst parameter is remarked.

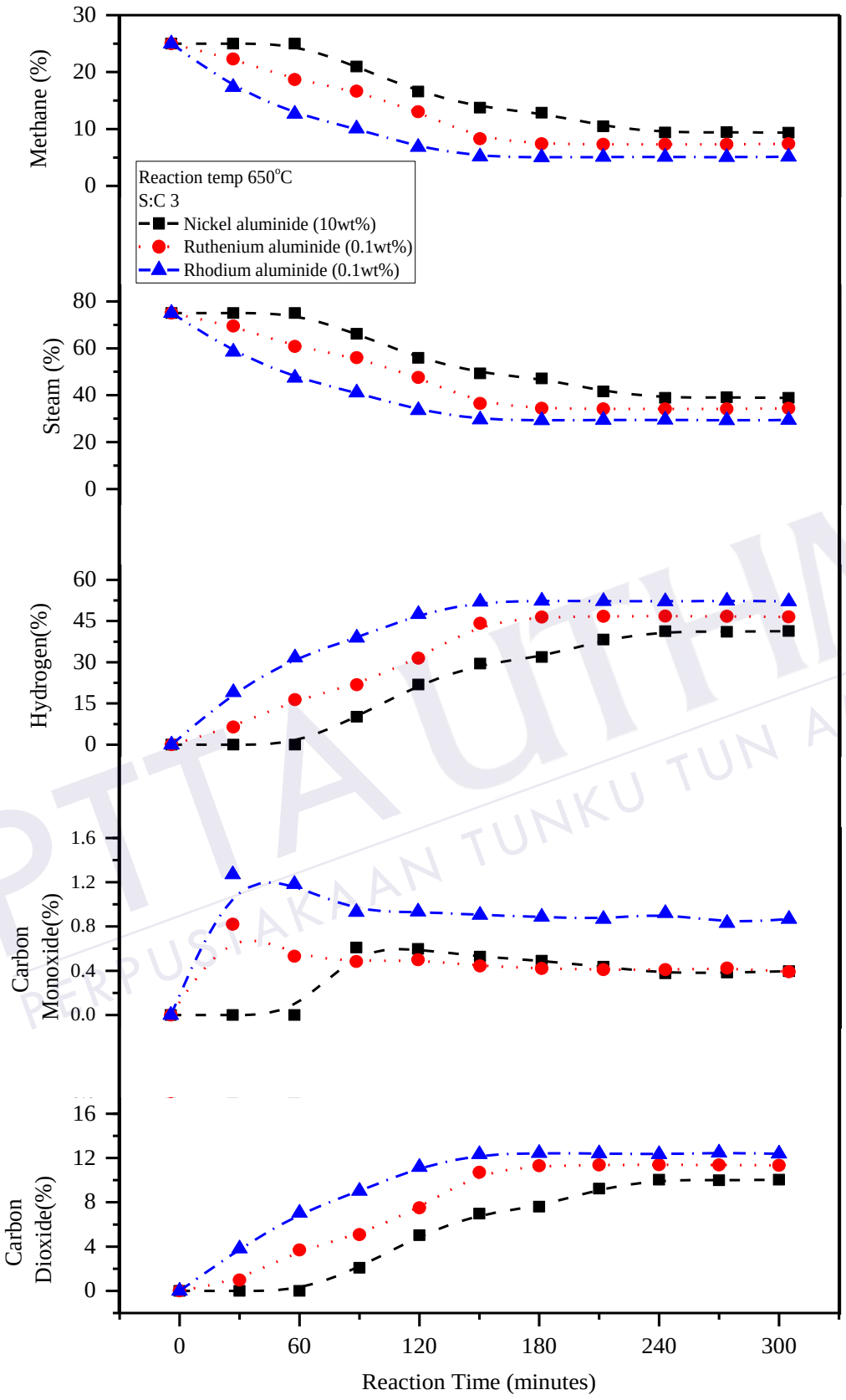

Figure 4.15 : Multiple catalyst loading effect on SMR yield.

The hydrogen formation, Rhodium aluminide yields the upper limit at 52.39%, follows by Ruthenium aluminide and Nickel aluminide. The results then is compared to the work done by Delparish & Avci, (2016). It is highlighted that rising methane conversion of Rhodium aluminide allowed maximize hydrogen concentration at the effluent flow. Meanwhile, for the H_2/CO ratio, Rhodium aluminide yield the upper limit. This is the important metric to quantify the quality of sync gas as fuels for Fischer-Tropsch synthesis.

Figure 4.15 shows that the carbon dioxide formation ratio of CO_2/CO (WGS reaction converts carbon monoxide in SMR to produce hydrogen and carbon dioxide), for Rhodium aluminide yields 14.3 lower compare to the Nickel aluminide at 25.3. This noble catalyst slightly has not impacting the WGS reaction instead of SMR reaction, which manages to increase methane conversion. This is due to Rhodium aluminide itself only favors active site for chemisorption of atom hydrocarbon instead of carbon monoxide. This noble catalyst yields more amount of both hydrogen and carbon monoxide compare to the conventional catalyst. However, this conventional catalyst produced at most CO_2/CO ratio. It infers that conventional catalyst has much higher catalytic activity for WGS and this finding is supported according to the works done by Cao et al., (2015) and Cao, Zhang, & Cheng, (2016).

Referring to the Figure 4.16, showed the methane disappearing rate ($-r'_A$) for multiple type of catalyst loading. The $-r'_A$ ratio of noble metal to the conventional catalyst is 116 times greater for Ruthenium aluminide and 138 times greater for Rhodium aluminide. The $-r'_A$ for both noble metal catalyst favor the methane conversion rate for the developed catalyst tested inside the micro channel reactor.

By comparing these results to the most similar works, done by Simsek et. al., (2011), it is indicated that this study is successfully demonstrated a few critical parameters for the enhancement of methane conversion and SMR yields, particularly for newly developed catalyst combination with micro channel properties. Adverting to the Table 4.8, obtained result from this study are successfully enhance the methane conversion for Ruthenium at almost 32 times greater of conversion over the weight of used catalyst from the literature. Moreover, for the Rhodium uses only 0.1wt%, which

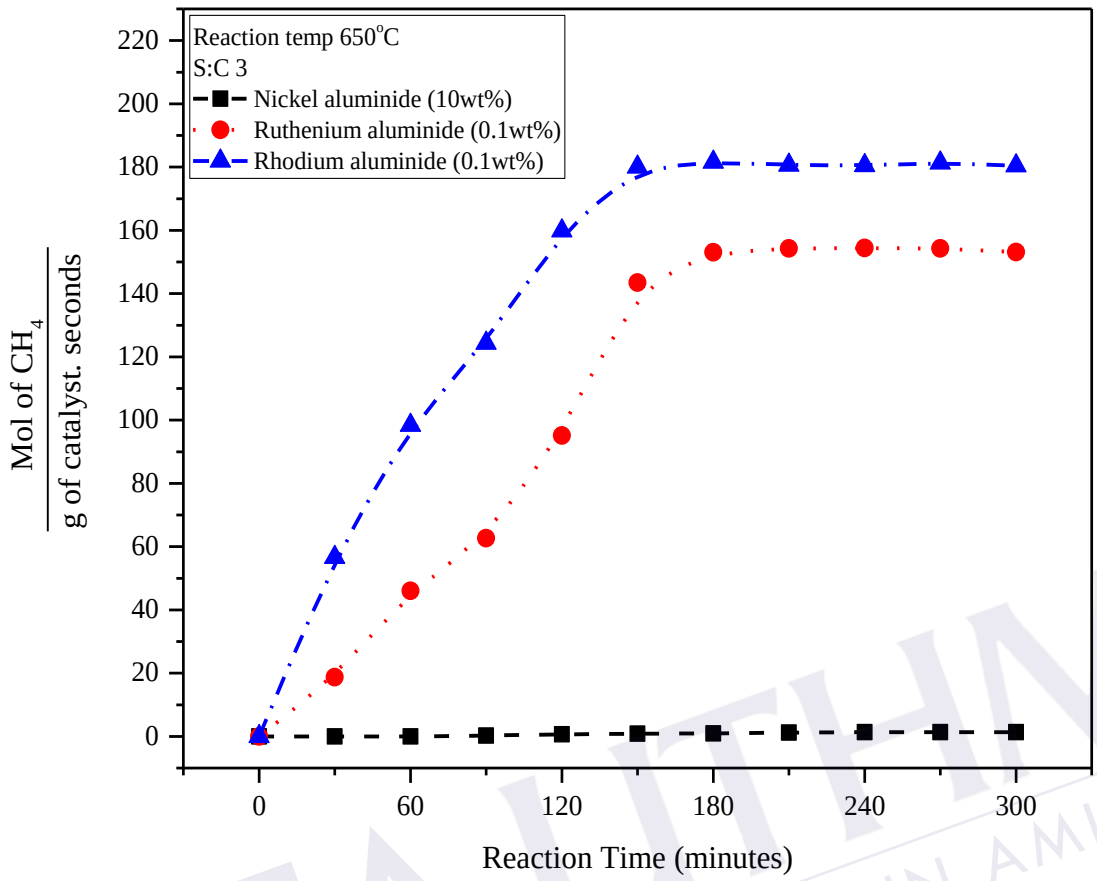

Figure 4.16 : Effect of multiple type catalyst on methane disappearing rate

is compare to literature 2% but still achieves almost similar methane conversion. This indicates that Rhodium used in this works has increased the reaction up to 19 times quicker. Meanwhile, for Nickel catalyst, compared to the literature, exhibits almostsimilar value for methane conversion at different reaction temperature which is 13% lower. The enhancements are obtained at the lower reaction temperature of 650°C, which differ with the literature. In the literature, the reaction temperature used is 750°C. This accomplishment is due to the improvise of micro channel depth from 500 µm to 200 µm. This claimed is supported by Chen et al., (2016), Haynes & Johnston, (2011), Stefanidis & Vlachos, (2010) and Tonkovich et al., (2004), which is emphasized that micro scale is useful to secure desired heat flux as the main endothermic SMR traits.

As the summary of the multiple type of catalyst loading effect on SMR yields, the results shows that Rhodium aluminide (0.1%wt) yields the optimum methane conversion and SMR yield analysis. The developed conventional and noble metal

catalyst by using substrate plat inside the micro channel reactor are functionally worked according to the SMR reaction process. The correlation of Rhodium aluminide used within the micro channel reactor proves that it is managed to intensify the methane conversion and hydrogen yield at multiple time greater compare to conventional catalyst.

Table 4.8 : Comparison works between previous researcher and current analysis

No.	Parameters	Simsek et. al., (2011)	Current analysis
1.	Catalyst deposition	Substrate plate coating	Substrate plate coating
2.	Reaction temp	750°C	650°C
3.	Steam to carbon	3	3
4.	Catalyst (weight) (CH_4 conversion)	Nickel (10%) (53.9%)	Nickel (10%) (52.75%)
		Ruthenium (2%) (37.6%)	Ruthenium (0.1%) (61.75%)
		Rhodium (2%) (71.6%)	Rhodium (0.1%) (72.63%)
5.	Micro channel depth	500 µm	200 µm

4.4 Summary of Findings

This subsection is summarizing all findings related to the all phases involved and briefly discussed in the succeeding sub-sections.

4.4.1 Mobile Steam Methane Reforming Test Rig

The mobile SMR Test Rig is most crucial parts to undergo all reaction process for reforming, straightly become the conversion platform. From the present research outcome, it is concluded several findings such as below:

i. A working prototype of small scale mobile steam methane reformer has been developed which can operate from 500°C to 700°C of operating reaction temperature.
ii. This mobile SMR test rig is featured by simplifying operation for pretreatment, upstream and downstream stage.

iii. The SMR test rig bench is regarded as an economic breakpoint technology scale property due to containing a novel portable small scale of syngas generator.
iv. The saturated steam generator for the test rig had the ability to produced 40 liter per hour saturated steam at a operating condition of 120°C to 127°C and 1 bar gauge.
v. The *in-situ* superheated steam converter coils manages to produced superheated steam temperature ranging 500°C to 700°C and 0.2 to 0.4 bar gauge pressure.
vi. The test rig bench is capable to obtain liquid/gas sample during a downstream stage in liquid and gas separator unit.
vii. The process control and data acquisition for temperature is used a PLC controller merge with SSR relay, which is capable to serve real time monitoring and digital user interface.
viii. The bench scale unit has the ability to be operated on a continuous basis with minimum single operator for the whole system.
ix. The bench scale unit is able to work in continuous steady state operating mode up to 10 hours.
x. To ascertain the safety, reliability and repeatability of this prototype SMR test rig, a Standard Operating Procedure (SOP) is produced, tested and verified. This SOP is a configuration to Asian Industrial Gas Association (AIGA) regulations.

4.4.2 Micro Channel Reactor

The micro channel reactor system denotes a few interesting findings and are concluded as below.

i. The designed, invented and developed micro channel reactor for this work has been filed for patent to the Intellectual Property Corporation of Malaysia with a reference number of IP2017300009.
ii. The micro channel reactor passage for substrate placement was successfully fabricated through computer numerical control (CNC) machining with 200 μm depth space for reactant conversion.

iii. The fabricated micro channel reactor only can withstand the static pressure test below 2.5 bar gauge. This reactor is considered as satisfactory since the intended operating pressure is approximately 1 bar gauge.

iv. The micro channel reactor is capable to resist high temperatures up to 800°C inside box furnace during upstream stage without any failure of physical deformation or reactant leaked.

v. The micro channel reactor system manages to operate at steam to carbon ratio from 1 until 5. It was established that this micro channel reactor is able to perform a broad range of steam to carbon ratio compare with the literature.

4.4.3 Catalytic Behavior Effect on SMR Yield

In order to validate the performance of an SMR test rig bench and the micro channel reactor, an experimental work for catalytic behavior through multiple type of catalyst has been conducted. From this present research outcome, it is concluded several findings such as:

i. The temperature of 650°C yields the maximum methane conversion and hydrogen formation and becomes the optimal reaction temperature of the developed catalyst Nickel aluminide with 10wt% loading.

ii. It was discovered that 500°C and 700°C become the lower and upper bound for the Nickel aluminide catalyst 10wt% loading.

iii. The S:C 4, yields the highest methane conversion and continuously rise towards heterogeneous catalyst stability stage. However, it exceeds the defined reaction time range. Thus, this S:C 4 is considered as non-primary ingredient in the SMR execution analysis.

iv. The S:C 2 exhibits faster and smoother trend line of heterogeneous catalyst stability stage compares to S:C 3 and S:C 4. But due to the methane conversion is slightly low compared to the others, this S:C 2 impact has been dismissed from primary SMR's yield factor.

v. The highest H_2/CO ratios for quantifying syngas formation is determined at S:C 3.

vi. For the carbon dioxide formation ratio of CO_2/CO, this S:C 4 provides the highest value.

vii. Steam to carbon ratio 3 effects on SMR yield, denotes the optimum methane conversion and hydrogen formation at most stable reaction within the defined reaction time range.

viii. For the succeeding level, the combination 650°C and S:C 3 are utilized as constant parameters for the multiple type of catalyst psychoanalysis.

ix. The methane conversion is proportional to the type of catalyst used, whereby Rhodium aluminide yields the highest value, follows by Ruthenium aluminide and lastly Nickel aluminide. Consequently, the fabricated micro channel reactor is capable to take over the interchangeable catalyst modules.

x. For the hydrogen formation, Rhodium aluminide yields the upper limit of 52.39%, follows by Ruthenium aluminide and Nickel aluminide.

xi. The noble metal has a lot faster reaction rate as early after 0 minutes reaction time compared to the conventional catalyst which only start having a conversion after 60 minutes reaction time.

xii. The $-r'_A$ ratio of noble metal to the conventional catalyst are 116 times greater for Ruthenium aluminide and 138 times greater for Rhodium aluminide.

xiii. This works manages to discover that micro reactor geometry improves the methane conversion of Nickel aluminide. Although a temperature difference of 13% lower compared to previous researcher, it has successfully achieved almost similar methane conversion.

CHAPTER 5

CONCLUSIONS AND RECOMMENDATIONS

5.1 Conclusions

In order to enhance the SMR yield, a baseline system for the reaction has been developed and tested according to the condition such as reaction temperature, steam to carbon ratio and multiple type of catalyst used, especially due to unique catalyst characteristics experimented in this field. Thus, parameters such as catalyst characteristics, methane conversion rate, and rate of reaction has been successful fundamentally studied. From this research, a small scale SMR test bench was successfully designed, fabricated and developed. A novel micro channel reactor with the substrate plate insert module was introduced that capable to operate with an interchangeable catalyst material mechanism in the SMR process. The main findings from this work are concluded as below:

i. The new steam methane reforming mobile plant is capable to operate up to 700°C of operating reaction temperature and 0.2 bar to 0.4 bar gauge operating pressure with controlled operating condition of steam to carbon ratio up to 5:1.
ii. Using Nickel aluminide catalyst, reaction temperature 650°C and steam to carbon ratio 3:1 were found to yield the optimum methane conversion at 52.75% and hydrogen formation at 41.34%.
iii. Catalyst of Rhodium aluminide yields the highest value of methane conversion and hydrogen formation followed by Ruthenium aluminide and

Nickel aluminide, where the rate of reaction (methane disappearing rate) of $-r'_{CH_4}$ (mol CH_4 / g catalyst.s) are 181.58, 154.39 and 1.32 respectively.

The outcomes of this work has the potential to be scaled up for hydrogen production supply chain system of future fuel-cell electric vehicle transportation sector especially in any region with affordable natural gas price.

5.2 Recommendations

Although the mobile SMR test rig bench with micro channel reactor has been successfully developed and trial run, which conduce to the several interesting findings in catalytic behavior effect on SMR yields, it has been recognized that this maturation is more a beginning point than a termination. For this reason, several gap analysis areas for future research have been distinguished. An exploration and investigation in these areas are essential to gain more knowledge and understanding. In order to improve and to provide continuity of this research, few steps have been proposed and projected.

i. Facility of online GC monitoring at reformat gas collecting points is needed in order to identify conversion for every instant of reaction time. It is advised to use GC which equipped with TCD and FID detector.
ii. Depth analysis of the unreacted reactant in the outlet stream due to developed catalyst efficiency is not 100%, this loop has become a potential future works study either to achieve full conversion or at least enhance the valet.
iii. The unreacted steam shows a quite bit of redundancy, therefore potential loop study of correlation steam to carbon ratio with catalyst parameter is remarked.
iv. Introduction and configuration of noble metal as promoter in Nickel catalyst loading.
v. Wider the variety of feedstock for reactant either from natural gas or alcohol.
vi. All related parties such industry, government and especially community people need to identify and prioritize specific issues facing for small scale

reformer, especially newly developed SMR mobile plant for producing hydrogen for given application and resources.

vii. The market assessment and system should be further analyzed in order to evaluate this SMR mobile plant technology for both distributed and centralized hydrogen production, and for refueling station design.

viii. The developed SMR mobile plant is suggested to be further analyzed in terms of scaling up for hydrogen production supply chain system to the transportation sector especially in region with affordable natural gas prices.

REFERENCES

Aaltonen, T., Ritala, M., & Leskelä, M. (2005). ALD of Rhodium Thin Films from Rh(acac)[sub 3] and Oxygen. *Electrochemical and Solid-State Letters*, *8*(8), C99.

Abeden, Z. bin Z. (2016). Eksperimen Untuk Kolum Hidrokarbon C1-C5 Bagi Analisis Gas Kromatografi. *Universiti Tun Hussein Onn Malaysia. Undergraduates Thesis*.

Aloisi, I., Giuliano, A. Di, Carlo, A. Di, Foscolo, P. U., Courson, C., & Gallucci, K. (2017). Sorption enhanced catalytic Steam Methane Reforming : Experimental data and simulations describing the behaviour of bi-functional particles. *Journal of Chemical Engineering*. *314*, 570–582.

Anwar Ul-Hamid, Abdul Quddusa, Huseyin Saricimen, & Hatim Dafalla. (2015). Corrosion Behavior of Coarse- and Fine-Grain Ni Coatings Incorporating NaH2PO4.H2O Inhibitor Treated Substrates. *Materials Research*, *18*(1), 20–26.

Armor, J. N. (1999). The multiple roles for catalysis in the production of H2. *Applied Catalysis A: General*, *176*(2), 159–176.

Barelli, L., Bidini, G., Gallorini, F., & Servili, S. (2008). Hydrogen production through sorption-enhanced steam methane reforming and membrane technology: A review. *Energy*, *33*(4), 554–570.

Bartels, J. R., Pate, M. B., & Olson, N. K. (2010). An economic survey of hydrogen production from conventional and alternative energy sources. *International Journal of Hydrogen Energy*, *35*(16), 8371–8384.

Bej, B., Pradhan, N. C., & Neogi, S. (2013). Production of hydrogen by steam reforming of methane over alumina supported nano-NiO/SiO2 catalyst. *Catalysis Today*, *207*, 28–35.

Beurden, P. Van. (2004). *On the catalytic aspects of steam methane reforming : A Literature Survey*. *Energy Centre Netherland* (Vol. 04).

British Petroleum. (2017). *BP Statistical Review of World Energy 2017*. *British Petroleum*. London. economics/statistical-review-2017/bp-statistical-review-of-

Butcher, H., Quenzel, C. J. E., Breziner, L., Mettes, J., Wilhite, B. a., & Bossard, P.

(2014). Design of an annular microchannel reactor (AMR) for hydrogen and/or syngas production via methane steam reforming. *International Journal of Hydrogen Energy*, 1–12.

C.M. Ward-Close, R.Minor, P. J. D. (1996). Intermetallic-matrix composites-a Review. *Intermetallics 4*, *9795*(95), 217–229.

Cao, C., Zhang, N., Chen, X., & Cheng, Y. (2015). A comparative study of Rh and Ni coated microchannel reactor for steam methane reforming using CFD with detailed chemistry. *Chemical Engineering Science*, *137*, 276–286.

Cao, C., Zhang, N., & Cheng, Y. (2016). Numerical analysis on steam methane reforming in a plate microchannel reactor: Effect of washcoat properties. *International Journal of Hydrogen Energy*, *41*(42), 18921–18941.

Charisiou, N. D., Siakavelas, G., Papageridis, K. N., Baklavaridis, A., Tzounis, L., Avraam, D. G., & Goula, M. A. (2016). Syngas production via the biogas dry reforming reaction over nickel supported on modi fi ed with CeO 2 and / or La 2 O 3 alumina catalysts, *31*, 164–183.

Chen, J., Yan, L., Song, W., & Xu, D. (2016). Operating strategies for thermally coupled combustion-decomposition catalytic microreactors for hydrogen production. *International Journal of Hydrogen Energy*, *41*(46), 21532–21547.

Cheng, Y., Zhai, X., Cheng, Y., Zhang, Z., & Jin, Y. (2011). Steam reforming of methane over Ni catalyst in micro-channel reactor. *International Journal of Hydrogen Energy*, *36*, 7105–7113.

Chibane, L., & Djellouli, B. (2011). Methane Steam Reforming Reaction Behaviour in a Packed Bed Membrane Reactor. *International Journal of Chemical Engineering and Applications*, *2*(3), 147–156.

Cohron, J. W., George, E. P., Heatherly, L., Liu, C. T., & Zeeb, R. H. (1996). Effect of low-pressure hydrogen on the room-temperature tensile ductility and fracture behavior of N & Al, *9795*(96), 497–502.

Czernik, S., Evans, R., & French, R. (2007). Hydrogen from biomass-production by steam reforming of biomass pyrolysis oil☆. *Catalysis Today*, *129*, 265–268.

Czernik, S., French, R., Feik, C., & Chornet, E. (2002). Production of hydrogen from biomass by pyrolysis steam reforming. *Advances in Hydrogen Energy*, 87–91.

Daud, W. R. W. (2006). Hydrogen Economy:Perspective From Malaysia. In W. R. W. Daud (Ed.), *International Seminar on the Hydrogen Economy for Sustainable Development* (p. 30). Reykjavik, Iceland.

de Smet, C. R. H., de Croon, M. H. J. M., Berger, R. J., Marin, G. B., & Schouten, J. C. (2001). Design of adiabatic fixed-bed reactors for the partial oxidation of methane to synthesis gas. Application to production of methanol and hydrogen-for-fuel-cells. *Chemical Engineering Science*, *56*, 4849–4861.

Delparish, A., & Avci, A. K. (2016). Intensified catalytic reactors for Fischer-Tropsch synthesis and for reforming of renewable fuels to hydrogen and synthesis gas. *Fuel Processing Technology*, *151*, 72–100.

Deutschmann, O., Maier, L. ., Riedel, U., Stroemman, A. ., & Dibble, R. . (2000). Hydrogen assisted catalytic combustion of methane on platinum. *Catalysis Today*, *59*(1), 141–150.

Doma, M. M.-, Jó, P., Jankiewicz, B. J., & Bartosewicz, B. (2016). Study of cyclic Ni 3 Al catalyst pretreatment process for uniform carbon nanotubes formation and improved hydrogen yield in methanol decomposition, 171–177.

Douglas, J. M. (1988). Conceptual Design of Chemical Processes. (B. J. C. and J. W.Bradley, Ed.) (1st Editio). Singapore: McGraw Hill Book Company.

Dupont, V., Ross, A. B., Knight, E., Hanley, I., & Twigg, M. V. (2008). Production of hydrogen by unmixed steam reforming of methane, *63*, 2966–2979.

Dybkjær, I., Ovesen, C. V, Schjødt, N. C., Sehested, J., & Thomsen, S. G. (2011). Journal of Natural Gas Science and Engineering Natural gas to synthesis gas e Catalysts and catalytic processes, *3*.

Eduardo, L., Oliveira, G., & Carlos, A. (2009). Steam Methane Reforming in a Ni/Al2O3 Catalyst: Kinetic and Diffusional Limitations in Extrudates. *The Canadian Journal of Chemical Engineering*, *87*(6), 945–956.

Eswaramoorthi, I., & Dalai, A. K. (2009). A comparative study on the performance of mesoporous SBA-15 supported Pd-Zn catalysts in partial oxidation and steam reforming of methanol for hydrogen production. *International Journal of Hydrogen Energy*, *34*(6), 2580–2590.

Fabas, A., Put, A. R., Doublet, S., Domergue, D., Salem, M., & Monceau, D. (2017). Metal dusting corrosion of austenitic alloys at low and high pressure with the e ff ects of Cr , Al , Nb and Cu, *123*(September 2016), 310–318.

Florin, N. H., & Harris, A. T. (2007). Hydrogen production from biomass coupled with carbon dioxide capture: The implications of thermodynamic equilibrium. *International Journal of Hydrogen Energy*, *32*, 4119–4134.

Gangadharan, P., Kanchi, K. C., & Lou, H. H. (2012). Evaluation of the economic and

environmental impact of combining dry reforming with steam reforming of methane. *Chemical Engineering Research and Design*, *90*(March), 1956–1968.

Ghorbanzadeh, A. M., Lotfalipour, R., & Rezaei, S. (2009). Carbon dioxide reforming of methane at near room temperature in low energy pulsed plasma. *International Journal of Hydrogen Energy*, *34*(1), 293–298.

Graf, P. O., Mojet, B. L., van Ommen, J. G., & Lefferts, L. (2007). Comparative study of steam reforming of methane, ethane and ethylene on Pt, Rh and Pd supported on yttrium-stabilized zirconia. *Applied Catalysis A: General*, *332*, 310–317.

Group, T. F. (2013). World Hydrogen Market. *Freedonia*, 331 pages. Retrieved from http://www.reportlinker.com/p0944103-summary/World-Hydrogen-Industry.html

Halabi, M. H., De Croon, M. H. J. M., Van Der Schaaf, J., Cobden, P. D., & Schouten, J. C. (2010). Low temperature catalytic methane steam reforming over ceria-zirconia supported rhodium. *Applied Catalysis A: General*, *389*, 68–79.

Haynes, B. S., & Johnston, A. M. (2011). Process design and performance of a microstructured convective steam – methane reformer, *178*, 34–41.

Hoang, D. L., Chan, S. H., & Ding, O. L. (2005). Methane in an Oxygen Permeable. *ICHeme Journal*, (83(A2)), 177–186.

Holladay, J. D., Hu, J., King, D. L., & Wang, Y. (2009). An overview of hydrogen production technologies. *Catalysis Today*, *139*, 244–260.

Hou, K., & Hughes, R. (2001). The kinetics of methane steam reforming over a Ni/α-Al2O catalyst. *Chemical Engineering Journal*, *82*(1–3), 311–328.

Hwang, S. M., Kwon, O. J., & Kim, J. J. (2007). Method of catalyst coating in micro-reactors for methanol steam reforming. *Applied Catalysis A: General*, *316*(1), 83–89.

Inayat, A., Ahmad, M. M., Mutalib, M. I. A., & Yusup, S. (2012). Process modeling for parametric study on oil palm empty fruit bunch steam gasification for hydrogen production. *Fuel Processing Technology*, *93*(1), 26–34.

Izquierdo, U., Barrio, V. L., Cambra, J. F., Requies, J., Güemez, M. B., Arias, P. L., … Arraibi, J. R. (2012). Hydrogen production from methane and natural gas steam reforming in conventional and microreactor reaction systems. *International Journal of Hydrogen Energy*, *37*, 7026–7033.

Jeon, Y., Kim, H., Lee, C., Lee, S., Song, S., & Shul, Y. gun. (2017). Efficient methane reforming at proper reaction environment for the highly active and stable fibrous

perovskite catalyst. *Fuel*, *207*, 493–502.

Jianguo Xu, Froment, G. F. (1989). Methane Steam Reforming , Methanation and Water-Gas Shift : I . Intrinsic Kinetics. *AIChE Journal*, *35*(1), 88–96.

Jin, M. H., Lee, C. B., Lee, D. W., Lee, S. W., Park, J. W., Oh, D., Park, J. S. (2016). Microchannel methane steam reformers with improved heat transfer efficiency and their long-term stability. *Fuel*, *176*, 86–92.

Kamarudin, S. K., Daud, W. R. W., Yaakub, Z., Misron, Z., Anuar, W., & Yusuf, N. N. a N. (2009). Synthesis and optimization of future hydrogen energy infrastructure planning in Peninsular Malaysia. *International Journal of Hydrogen Energy*, *34*(5), 2077–2088.

Karagiannidis, S., Mantzaras, J., & Boulouchos, K. (2011). Stability of hetero-/homogeneous combustion in propane- and methane-fueled catalytic microreactors: Channel confinement and molecular transport effects. *Proceedings of the Combustion Institute*, *33*(2), 3241–3249.

Karim, A., Bravo, J., Gorm, D., Conant, T., & Datye, A. (2005). Comparison of wall-coated and packed-bed reactors for steam reforming of methanol. *Catalysis Today*, *110*(1–2), 86–91.

Khan, Z., Yusup, S., Ahmad, M. M., Chok, V. S., Uemura, Y., & Sabil, K. M. (2010). Review on hydrogen production technologies in Malaysia. *International Journal of Engineering*, *10*(02), 111–118.

Kim, H. Y., Chung, D. S., & Hong, S. H. (2005). Reaction synthesis and microstructures of NiAl / Ni micro-laminated composites, *396*, 376–384.

Kolb, G., & Hessel, V. (2004). Micro-structured reactors for gas phase reactions. *Chemical Engineering Journal*, *98*(1–2), 1–38.

Kook, S., Keun, S., Ok, J., Seong, J., & Chul, Y. (2013). Numerical study of effect of operating and design parameters for design of steam reforming reactor. *Energy*, *61*, 410–418.

Kr, M., Chandra, P., & Kr, P. (2015). Journal of Environmental Chemical Engineering A review on the fuel gas cleaning technologies in gasi fi cation process, *3*, 689–702.

Kuba, M., Havlik, F., Kirnbauer, F., & Hofbauer, H. (2016). Biomass and Bioenergy In fl uence of bed material coatings on the water-gas-shift reaction and steam reforming of toluene as tar model compound of biomass gasi fi cation, *89*, 40–49.

Langé, S., & Pellegrini, L. a. (2013). Sustainable combined production of hydrogen

and energy from biomass in Malaysia. *Chemical Engineering Transactions*, *32*, 607–612.

Liu, J. a. (2006). Kinetics , catalysis and mechanism of methane steam reforming. *Worcester Polytechnic Institute*, *Master The*, 118. Retrieved from http://scholar.google.com/scholar?hl=en&btnG=Search&q=intitle:Kinetics,+catalysis+and+mechanism+of+methane+steam+reforming#0

Liu, Z., Chu, B., Zhai, X., Jin, Y., & Cheng, Y. (2012). Total methanation of syngas to synthetic natural gas over Ni catalyst in a micro-channel reactor. *Fuel*, *95*, 599–605.

Lutz, A. E., Bradshaw, R. W., Bromberg, L., & Rabinovich, A. (2004). Thermodynamic analysis of hydrogen production by partial oxidation reforming. *International Journal of Hydrogen Energy*, *29*(8), 809–816.

Madon, R. H., Fawzi, M., Osman, S. A., Alimin, A. J., Razali, A., Khairul, M., Abeden, Z. Z. (2018). Gas Chromatography Analysis of a C1-C5 Hydrocarbon Column. *International Journal of Integrated Engineering*, *10*(1), 85–91.

Madon, R. H., Mustaffa, N., Fawzi, M., & Osman, S. A. (2015). Review of Yield Intensification on Steam Methane Reforming through Micro Reactor and Rare Earth Catalyst. *Journal of Advanced Review on Scientific Research*, *7*(2289–7887), 32–37.

Madon, R. H., Sarwani, M. K. I., & Fawzi, M. (2016). Effect of substrate surface roughness on morphological and topography of nickel-alumina thin film. *ARPN Journal of Engineering and Applied Sciences*, *11*(8), 5304–5308.

Maluf, S. S., & Assaf, E. M. (2009). Ni catalysts with Mo promoter for methane steam reforming. *Fuel*, *88*(9), 1547–1553.

Marshall, D. W. (2002). *Bench-Scale Design and Testing*. *INEEL/EXT-0201018*.

Martin, S., Kraaij, G., Ascher, T., & Wails, D. (2015). An experimental investigation of biodiesel steam reforming. *International Journal of Hydrogen Energy*, *40*, 95–105.

Mathesontrigas. (2010). Basic Flowmeter Principles. Retrieved from www.mathesontrigas.com

Mbodji, M., Commenge, J. M., & Falk, L. (2014). Preliminary design and simulation of a microstructured reactor for production of synthesis gas by steam methane reforming. *Chemical Engineering Research and Design*, *92*(9), 1728–1739.

Mbodji, M., Commenge, J. M., Falk, L., Di Marco, D., Rossignol, F., Prost, L., Del-

Gallo, P. (2012). Steam methane reforming reaction process intensification by using a millistructured reactor: Experimental setup and model validation for global kinetic reaction rate estimation. *Chemical Engineering Journal*, *207–208*, 871–884.

Moghtaderi, B. (2007). Effects of controlling parameters on production of hydrogen by catalytic steam gasification of biomass at low temperatures. *Fuel*, *86*, 2422–2430.

Molburg, J. C., & Doctor, R. D. (2003). Hydrogen from Steam-Methane Reforming with CO 2 Capture. *20th Annual International Pittsburgh Coal Conference*, 20.

Mondal, T., Pant, K. K., & Dalai, A. K. (2015). ScienceDirect Catalytic oxidative steam reforming of bio-ethanol for hydrogen production over Rh promoted Ni / CeO 2 e ZrO 2 catalyst. *International Journal of Hydrogen Energy*, *40*(6), 2529–2544.

Monzon, A., Latorre, N., Ubieto, T., Royo, C., Romeo, E., Villacampa, J. I., Montioux, M. (2006). Improvement of activity and stability of Ni-Mg-Al catalysts by Cu addition during hydrogen production by catalytic decomposition of methane. *Catalysis Today*, *116*(3), 264–270.

Morris, C. C. (2016). Development of A Multi Microchannel Reactor for Steam Methane Reforming Process. *Universiti Tun Hussein Onn Malaysia. Undergraduates Thesis*, (May).

Murphy, D. M., Manerbino, A., Parker, M., Blasi, J., Kee, R. J., & Sullivan, N. P. (2013). Methane steam reforming in a novel ceramic microchannel reactor. *International Journal of Hydrogen Energy*, *38*, 8741–8750.

Nexant Inc. (2006). Equipment Design and Cost Estimation for Small Modular Biomass Systems , Synthesis Gas Cleanup , and Oxygen Separation Equipment. Task 1: Cost Estimates of Small Modular Systems. *Subcontract Report NREL/SR-510-39943*, (May). Retrieved from http://www.nrel.gov/docs/fy06osti/39943.pdf

Oar-Arteta, L., Wezendonk, T., Sun, X., Kapteijn, F., & Gascon, J. (2017). Metal organic frameworks as precursors for the manufacture of advanced catalytic materials. *Mater. Chem. Front.*, *1*, 1709–1745.

Ogden, J. M. (2001). Review of Small Stationary Reformers for Hydrogen Production. *Environmental Studies*, (609), 63.

Palma, V., Martino, M., Meloni, E., & Ricca, A. (2017). Novel structured catalysts configuration for intensification of steam reforming of methane. *International*

Journal of Hydrogen Energy, *42*(3), 1629–1638.

Park, S., Jung, I., Lee, Y., Kshetrimayum, K. S., Na, J., Park, S., Han, C. (2016). Design of microchannel Fischer – Tropsch reactor using cell-coupling method : Effect of fl ow con fi gurations and distribution, *143*, 63–75.

Park, S., Yoo, J., Han, S. J., Song, J. H., Lee, E. J., & Song, I. K. (2017). Steam reforming of liquefied natural gas (LNG) for hydrogen production over nickel–boron–alumina xerogel catalyst. *International Journal of Hydrogen Energy*, *42*(22), 15096–15106.

Perez-Moreno, Soler, Herguido, & Menendez. (2013). Stable hydrogen production by methane steam reforming in a two zone fluidized bed reactor: Experimental assessment. *Journal of Power Sources*, *243*, 233–241.

Pirez, C., Fang, W., Capron, M., Paul, S., Jobic, H., Dumeignil, F., & Jalowiecki-Duhamel, L. (2016). Steam reforming, partial oxidation and oxidative steam reforming for hydrogen production from ethanol over cerium nickel based oxyhydride catalyst. *Applied Catalysis A: General*, *518*, 78–86.

Platinum, O., & Catalytic, I. N. (2016). Hetero- / Homogeneous Combustion and Flame Stability of Fuel-Lean Propane – Air Mixtures, *100*, 932–943.

Pudukudy, M., & Yaakob, Z. (2015). Methane decomposition over Ni, Co and Fe based monometallic catalysts supported on sol gel derived SiO2 microflakes. *Chemical Engineering Journal*, *262*, 1009–1021.

Pudukudy, M., Yaakob, Z., & Akmal, Z. S. (2015). Direct decomposition of methane over SBA-15 supported Ni, Co and Fe based bimetallic catalysts. *Applied Surface Science*, *330*, 418–430.

Radfarnia, H. R., & Iliuta, M. C. (2014). Development of Al-stabilized CaO-nickel hybrid sorbent-catalyst for sorption-enhanced steam methane reforming. *Chemical Engineering Science*, *109*, 212–219.

Rafiq, M. H., & Hustad, J. E. (2011). Synthesis gas from methane by using a plasma-assisted gliding arc catalytic partial oxidation reactor. *Industrial and Engineering Chemistry Research*, *50*(9), 5428–5439.

Rais Hanizam Madon, Mas Fawzi, MZahar, K. I. (2017). *IP2017300009*. Malaysia: MyIPO.

Rajagopal, A. (2007). *Preparation And Characterization Of Ni/Rh/Al2O2 Catalyst And catalytic Methane-Steam Reforming*. *Master of Applied Science in Chemical Engineering Thesis*. Royal Military College of Canada :

Raju, A. S. K., Park, C. S., & Norbeck, J. M. (2009). Synthesis gas production using steam hydrogasification and steam reforming. *Fuel Processing Technology*, *90*(2), 330–336.

Rashad, M., Pan, F., Tang, A., & Asif, M. (2014). Effect of Graphene Nanoplatelets addition on mechanical properties of pure aluminum using a semi-powder method. *Progress in Natural Science: Materials International*, *24*(2), 101–108.

Reinke, M., Mantzaras, J., Bombach, R., Schenker, S., & Inauen, A. (2005). Gas phase chemistry in catalytic combustion of methane/air mixtures over platinum at pressures of 1 to 16 bar. *Combustion and Flame*, *141*(4), 448–468.

Roh, H.-S., Eum, I.-H., & Jeong, D.-W. (2012). Low temperature steam reforming of methane over Ni–Ce(1−x)Zr(x)O2 catalysts under severe conditions. *Renewable Energy*, *42*, 212–216.

Saadi, S., Hinnemann, B., Appel, C. C., Helveg, S., Abild-pedersen, F., & Nørskov, J. K. (2011). Surface Science First-principles investigations of Ni 3 Al (111) and NiAl (110) surfaces at metal dusting conditions, *605*, 582–592.

Salhi, Boulahouache, Petit, Kiennemann, & Rabia. (2011). Steam reforming of methane to syngas over NiAl2O4 spinel catalysts. *International Journal of Hydrogen Energy*, *36*, 11433–11439.

Samuel, P. (2003). GTL Technology – Challenge and Opportunities in Catalyst. *Bulletin of The Catalysis Society of India*, *2*, 82–99.

Sarwani, K. I., Madon, R. H., Ibrahim, S. A., & Fawzi, M. (2016). Effect of Calcination Temperature on Morphological and Topography of Nickel-Alumina Thin Film. *MATEC Web of Conferences*, *78*, 4–9.

Sarwani, M. K. I. (2017). Nickel Aluminide Coating as Catalyst in Steam Methane Reforming Microreactor. *Universiti Tun Hussein Onn Malaysia.*, (Master's Thesis).

Schädel, B. T., Duisberg, M., & Deutschmann, O. (2009). Steam reforming of methane, ethane, propane, butane, and natural gas over a rhodium-based catalyst. *Catalysis Today*, *142*, 42–51.

Sciazko, A., Komatsu, Y., Brus, G., Kimijima, S., & Szmyd, J. S. (2014). A novel approach to the experimental study on methane/steam reforming kinetics using the Orthogonal Least Squares method. *Journal of Power Sources*, *262*, 245–254.

Seider, W.D. Seader, J.D. Lewin, D. R. (2003). *Product and Process Design Principles - Synthesis, Analysis, and Evaluation*. (I. John Wiley and Sons, Ed.) (Second Edi).

New Jersey: Wiley International Edition.

Seris E.L.C, A. G. (2006). Demonstration PLant For Distributed Production. *Chemical Engineering Research and Design*, *83 (A6)*(June 2005), 619–625.

Shinagawa, T., Oshima, K., & Sekine, Y. (2013). Steam reforming of methane at low temperature in an electric field. *ACS National Meeting Book of Abstracts*, *8*, 1.

Silversand, F. A. (2003). Fuel processor for small-scale production of hydrogen – Experimental study. *Rapport SGC*, *139*, 1102–7371.

Simsek, E., Avci, A. K., & Önsan, Z. I. (2011). Investigation of catalyst performance and microstructured reactor configuration for syngas production by methane steam reforming. *Catalysis Today*, *178*(1), 157–163.

Simsek, E., Karakaya, M., Avci, A. K., & Onsan, Z. I. (2013). Oxidative steam reforming of methane to synthesis gas in microchannel reactors. *International Journal of Hydrogen Energy*, *38*, 870–878.

Smith, R. (2005). *Chemical Process Design and Integration*. (M. Hill, Ed.) (2nd ed.). John Wiley & Sons, Ltd.

Stefanidis, G. D., & Vlachos, D. G. (2010). Intensification of steam reforming of natural gas: Choosing combustible fuel and reforming catalyst. *Chemical Engineering Science*, *65*(1), 398–404.

Stutz, M. J., Hotz, N., & Poulikakos, D. (2006). Optimization of methane reforming in a microreactor-effects of catalyst loading and geometry. *Chemical Engineering Science*, *61*, 4027–4040.

Sulka, G. D., & Jó, P. (2011). Intermetallics Electrochemical behavior of Ni 3 Al-based intermetallic alloys in NaOH, *19*, 974–981.

Tonkovich, a., Kuhlmann, D., Rogers, a., McDaniel, J., Fitzgerald, S., Arora, R., & Yuschak, T. (2005). Microchannel Technology Scale-up to Commercial Capacity. *Chemical Engineering Research and Design*, *83*(June), 634–639.

Tonkovich, a. Y., Perry, S., Wang, Y., Qiu, D., Laplante, T., & Rogers, W. a. (2004). MicroChannel process technology for compact methane steam reforming. *Chemical Engineering Science*, *59*, 4819–4824.

Tonkovich, A. L. Y., Yang, B., Perry, S. T., Fitzgerald, S. P., & Wang, Y. (2007). From seconds to milliseconds to microseconds through tailored microchannel reactor design of a steam methane reformer. *Catalysis Today*, *120*, 21–29.

Türks, D., Mena, H., Armbruster, U., & Martin, A. (2017). Methanation of CO2 on Ni/Al2O3 in a Structured Fixed-Bed Reactor—A Scale-Up Study. *Catalysts*,

7(5), 152–167.

Udengaard, N. (2004). Hydrogen Production by Steam Reforming of Hydrocarbons. *Preprints of Symposia-American Chemical Society*, , *49*, 906–907.

Vagia, E. C., & Lemonidou, A. A. (2008). Thermodynamic analysis of hydrogen production via autothermal steam reforming of selected components of aqueous bio-oil fraction. *International Journal of Hydrogen Energy*, *33*(10), 2489–2500.

Verykios, & Piga. (2000). *An advanced reactor configuration for the partial oxidation of methane to synthesis gas*. *Catalysis Today* (Vol. 60).

Vidal Vázquez, F., Simell, P., Pennanen, J., & Lehtonen, J. (2016). Reactor design and catalysts testing for hydrogen production by methanol steam reforming for fuel cells applications. *International Journal of Hydrogen Energy*, *41*(2), 924–935.

Wang, F., Qi, B., Wang, G., & Li, L. (2013). Methane steam reforming: Kinetics and modeling over coating catalyst in micro-channel reactor. *International Journal of Hydrogen Energy*, *38*, 5693–5704.

Wang, H., Zhang, L., Yuan, M., Xx, T., & Liu, Y. (2012). Steam reforming of ethanol over Ni/Ce0.7Pr0.3O2 catalyst. *Journal of Rare Earths*, *30*(7), 670–675.

Wang, J., Shen, M., Wang, J., Gao, J., Ma, J., & Liu, S. (2012). Steam effects over Pd/Ce0.67Zr0.33O2-Al2O3 three-way catalyst. *Journal of Rare Earths*, *30*(3), 748–752.

Wang, Y. (2005). Hydrogen production from steam methane reforming coupled with in situ CO capture: Conceptual parametric study. *Fuel*, *84*(14–15), 1778–1789.

Wang, Y., & Chen, W. (2004). Microstructures , properties and high-temperature carburization resistances of HVOF thermal sprayed NiAl intermetallic-based alloy coatings, *183*, 18–28.

Wu, H., La Parola, V., Pantaleo, G., Puleo, F., Venezia, A., & Liotta, L. (2013). Ni-Based Catalysts for Low Temperature Methane Steam Reforming: Recent Results on Ni-Au and Comparison with Other Bi-Metallic Systems. *Catalysts*, *3*, 563–583.

Wu, Z., & Jiang, H. (2015). Efficient palladium and ruthenium nanocatalysts stabilized by phosphine functionalized ionic liquid for selective hydrogenation. *RSC Advances*, *5*(44), 34622–34629.

Xu, J., Yeung, C. M. Y., Ni, J., Meunier, F., Acerbi, N., Fowles, M., & Tsang, S. C. (2008). Methane steam reforming for hydrogen production using low water-ratios without carbon formation over ceria coated Ni catalysts. *Applied Catalysis A:*

General, *345*, 119–127.

Xu, Y., Kameoka, S., Kishida, K., Demura, M., Tsai, A., & Hirano, T. (2005). Catalytic properties of alkali-leached Ni 3 Al for hydrogen production from methanol, *13*, 151–155.

Yamada, O. (2006). Generation of hydrogen gas by reforming biomass with superheated steam, *509*, 207–211.

Yang, H.-C., Lee, M.-W., Hwang, H.-S., Moon, J.-K., & Chung, D.-Y. (2014). Study of cerium-promoted rhodium alumina catalyst as a steam reforming catalyst for treatment of spent solvents. *Journal of Rare Earths*, *32*(9), 831–836.

Ye, G., Xie, D., Qiao, W., Grace, J. R., & Lim, C. J. (2009). Modeling of fluidized bed membrane reactors for hydrogen production from steam methane reforming with Aspen Plus. *International Journal of Hydrogen Energy*, *34*(11), 4755–4762.

Youn, M. H., Seo, J. G., Cho, K. M., Park, S., Park, D. R., Jung, J. C., & Song, I. K. (2008). Hydrogen production by auto-thermal reforming of ethanol over nickel catalysts supported on Ce-modified mesoporous zirconia: Effect of Ce/Zr molar ratio. *International Journal of Hydrogen Energy*, *33*(19), 5052–5059.

Zeppieri, M., Villa, P. L., Verdone, N., Scarsella, M., & De Filippis, P. (2010). Kinetic of methane steam reforming reaction over nickel- and rhodium-based catalysts. *Applied Catalysis A: General*, *387*, 147–154.

Zhai, X., Ding, S., Liu, Z., Jin, Y., & Cheng, Y. (2011). Catalytic performance of Ni catalysts for steam reforming of methane at high space velocity. *International Journal of Hydrogen Energy*, *36*, 482–489.

Zhang, J., Li, X., Chen, H., Qi, M., & Zhang, G. (2017). Hydrogen production by catalytic methane decomposition : Carbon materials as catalysts or catalyst supports. *International Journal of Hydrogen Energy*, *2*, 1–21.

APPENDIX A: LIST OF PUBLISHED PAPERS DURING STUDY

1) R.H. Madon, M.A.M. Zamree, S.H. Aminordin, M. Fawzi (2015). Heating and Cooling of an Aluminium-Cased Parallel Flow Microreactor for Steam-Methane Reforming. Applied Mechanic and Materials. 773-74 : 408-412

2) R.H. Madon, S.A. Osman, N. Mustaffa, M. Fawzi (2015). Review of Yield Intensification on Steam Methane Reforming through Micro Reactor and Rare Earth Catalyst. Journal of Advanced Review on Scientific Reseach. 7 (1) : 32-37.

3) R.H. Madon, M.K.I. Sarwani, M. Fawzi (2016). Effect of Substrate Surface Roughness on Morphological and Topography of Nickel-Alumina Thin Film. ARPN Journal of Engineering and Applied Sciences. 11 (8) : 5304-5308.

4) K.I. Sarwani, R.H. Madon, S.A. Ibrahim, M. Fawzi (2016) Effect of Calcination Temperature on Morphological and Topography of Nickel-Alumina Thin Film. MATEC Web of Conference. 78 (01049)

5) R.H. Madon, M. Fawzi, K.I. Sarwani, S.A. Osman, M.A. Razali, A.W. Mohammad (2018). Effect of Reaction Temperature on Steam Methane Reforming's yield over Coated Nickel Aluminide (Ni_3Al) Catalyst in Micro Reactor. Journal of Advanced Research in Fluid Mechanics and Thermal Sciences. 50 (2) : 170-177.

6) R.H. Madon, M. Fawzi, S.A. Osman, A.J. Alimin, M.A. Razali, M.K.I. Sarwani, Z.Z. Abeden (2018). Gas Chromatography Analysis of a C1-C5 Hydrocarbon Column. International Journal of Integrated Engineering. 10 : 85-91.

VITA

The author was born in February 14, 1985, in Ayer Hitam, Johor. He went to Sek Men Keb Datuk Menteri, Ayer Hitam, Johor for his secondary school. He pursued his bachelor degree at the Universiti Malaysia Pahang (formerly known as Kolej Universiti Kejuruteraan & Teknologi Malaysia) and graduated with the B.Eng in Chemical Engineering (Biotechnology). Upon graduation he worked as a QC/Prod Engineer at Yamauchi (M) Sdn Bhd, Johor. Then, he switched to academician carrier as a Tutor in the Faculty of Mechanical and Manufacturing Engineering at Universiti Tun Hussein Onn Malaysia, Johor. He then enrolled at the Universiti Kebangsaan Malaysia, Selangor in 2011, where he was awarded the M.Eng in Chemical Engineering in 2013. In 2014, Mr Rais pursued into a Ph.D program in Mechanical Engineering at Centre for Graduate Studies in Universiti Tun Hussein Onn Malaysia. His main research interest and expertise are laid on Steam Methane Reforming chemical process, RO membrane for desalination and bioprocess engineering. He is currently a member of the Institute of Engineer Malaysia and Board of Engineer Malaysia. He is also an expert for Malay Art Weapon's theory and practical wise at national level.